

**Synthesis, Recycling, and Modification of Thermoset Silicone Resins via Fluoride
Ion Catalyzed Rearrangement**

by

David James Krug III

A dissertation submitted in partial fulfillment
of the requirements for the degree of
Doctor of Philosophy
(Macromolecular Science and Engineering)
in The University of Michigan
2019

Doctoral Committee:

Professor Richard M. Laine, Chair
Professor Nicholas A. Kotov
Associate Professor Kenichi Kuroda
Professor Richard E. Robertson

David James Krug III

djkrug@umich.edu

ORCID iD: 0000-0003-1584-7872

© David James Krug III 2019

Dedication

This dissertation is dedicated to my parents who made everything possible
and to my wife who made everything worthwhile

Everything I am, I owe to them

Acknowledgements

I could not have embarked on, let alone finished, this dissertation without the help of many wonderful people. First, I would like to thank my advisor, Professor Richard M. Laine, for his guidance, mentorship, and the many opportunities he has given to me over the years. I am also grateful for the support of my committee members Professor Nicholas A. Kotov, Professor Kenichi Kuroda, and Professor Richard E. Robertson.

I would also like to thank all past and present members of the Laine Group. In particular, Dr. Michael Z. Asuncion, Dr. Jose Azurdia, Dr. Julien C. Marchal, and Dr. Santy Sulaiman for their direction and patience when I was an undergraduate researcher. And Dr. Eongyu Yi and Dr. Joseph C. Furgal for their support during graduate school. A special thanks to the Macromolecular Science and Engineering Department and the program coordinators over my tenure: Nonna Hamilton, Adam Mael, and Julie Pollak

I thank Continental Structural Plastics (CSP) for their financial support of this work. Moreover, I thank CSP, especially the entire R&D Department, for their understanding and cooperation that allowed me to pursue my doctorate while working. In particular, I would like to thank Dr. Michael J. Siwajek, Probir K. Guha, Frank E. Macher, Dr. Nicholas A. Kamar, and Dr. Michael Z. Asuncion.

I would like to acknowledge the many influential professors and science teachers that I've been very lucky to have at the University of Michigan, Luke M. Powers High School, and St. John Vianney School. In particular I thank Sharon Cuttitta who connected young students with the Flint Area Science Fair where my interest in science grew exponentially.

I would like to thank Dr. Michael Z. Asuncion a third time for not only being an exceptional mentor, but a great friend who has helped me in so many matters, scientific and otherwise.

Last, but not least, I thank my friends and family for their limitless support. Most of all I thank my parents (Jim and Anita), my sister (Carolyn), and my wife (Kate), for their endless encouragement and unconditional love. All my accomplishments are owed to them.

Table of Contents

Dedication	ii
Acknowledgements	iii
List of Tables	vii
List of Figures	viii
List of Schemes	xv
List of Abbreviations	xvii
List of Appendices	xix
Abstract	xx
Chapter 1 - Introduction	1
1.1 Research Motivation and Objectives	1
1.2 Introduction to Silicones	2
1.2.1 Definition, Structures, and Nomenclature	2
1.2.2 Silicone Polymerization Techniques	3
1.2.3 Types and Properties of Silicones	5
1.3 Introduction to Silsesquioxanes	8
1.4 Introduction to Fluoride Ion Catalyzed Rearrangement Reactions	10
1.5 Overview of Polymer Recycling	12
1.6 References	16
Chapter 2 - Experimental Techniques	23
2.1 Materials	23
2.2 Analytical Procedures	23
2.3 Synthetic Methods	27
2.3.1 Synthesis of Dodecaphenylsilsesquioxane	27
2.3.2 Synthesis of Silicone Resins	27

2.3.3 Recycling of Silicone Resins	29
2.3.4 <i>In situ</i> Modification during Recycling of Silicone Resins	29
2.4 Coating Application	30
2.5 Monolith Casting	31
2.6 References	32
Chapter 3 - Silicone Resin Coatings via Fluoride Ion Catalyzed Rearrangement	34
3.1 Introduction	35
3.2 Experimental Procedures	40
3.3 Results and Discussion	40
3.3.1 FTIR Study	41
3.3.2 Thermal Behavior	42
3.3.3 Wear Resistance	44
3.4 Conclusions	48
3.5 References	50
Chapter 4 - Recycling Silicone Resins	55
4.1 Introduction	56
4.2 Experimental Procedures	62
4.3 Results and Discussion	62
4.3.1 Prime Silicone Resin Properties vs Cure Temperature	63
4.3.2 Effect of Fluoride Ion Concentration on Recycled Silicone Resin Properties	70
4.3.3 Recycling Commercial Silicones under Optimized Conditions	77
4.4 Conclusions	84
4.5 References	86
Chapter 5 - <i>In situ</i> Modification of Recycled Silicone Resins	90
5.1 Introduction	91
5.2 Experimental Procedures	93
5.3 Results and Discussion	93
5.3.1 <i>In situ</i> Modification of Recycled Silicone Resin for Increased Thermal Stability	93

5.3.2 <i>In situ</i> Modification of Recycled Silicone Resin for Increased Flexibility	97
5.3.3 <i>In situ</i> Modification of Recycled Silicone Resin for Increased Hydrophobicity	99
5.3.4 <i>In situ</i> Modification of Recycled Commercial Silicone Resin	101
5.4 Conclusions	106
5.5 References	107
Chapter 6 - Future Work	109
6.1 Discussion	109
6.2 References	118
Appendices	119

List of Tables

Table

1.1	Symbol, formula, and uses of polysiloxane (silicone) structural units	3
3.1	Surface energy of common polymers, aluminum, and glass	37
3.2	Thermal stability of hybrid coatings (T at 5% mass loss via TGA)	43
3.3	WCA versus wear cycles on silicone resin coatings	46
4.1	Cured (250°C) silicone resin dissolution time vs [F ⁻]	71
4.2	Silicone resin thermal stability vs [F ⁻]	76
5.1	Thermal properties of SILRES and the model silicone resin (1 Ph : 1 Me)	101
C.1	Thermal stability of prime and recycled model silicone resin (1 Ph : 1 Me) with increasing cure temperature	130

List of Figures

Figure

1.1	An idealized silicone resin structure, where R = methyl, phenyl, etc.;	
	Orange Si = M unit, Green Si = D unit, Red Si = T unit, Blue Si = Q unit	8
1.2	Silsesquioxane (SQ) structures	9
1.3	Soluble intermediate species during F ⁻ catalyzed rearrangement	
	of T ₈ SQ, spheres represent capped corners	12
1.4	Global rates for recycling, incineration, and discard of all plastic waste	13
1.5	Cumulative global plastic waste generation and disposal, historical data	
	and future projections represented by solid and dashed lines respectively	14
1.6	Schematic of thermoplastic and thermoset polymer behavior upon heating	15
2.1	Linear wear test set up with 2000 grit sandpaper and 100g weight (2kPa)	25
2.2	Coating tape adhesion test scale according to ASTM D3359	26
3.1	Schematic of water contact angles from hydrophilic to superhydrophobic	35
3.2	Water on a lotus leaf (left) and a schematic of the Cassie-Baxter	
	model (right)	36
3.3	Superhydrophobic coating containing silica nanoparticles on glass	36
3.4	Water bounces off superhydrophobic coating on Al substrate due to high	
	WCA (top), but coating is easily worn away with a single finger rub	
	(bottom)	38
3.5	F ⁻ catalyzed rearrangement reaction as a route to silicone resins	39
3.6	Structures of PFS and MAS added to coating systems for	
	multi-functionality	41
3.7	FTIRs of silicone resin coatings with successive incorporation of	
	functionalities	42
3.8	Typical TGAs of silicone resin coatings in N ₂	43
3.9	Typical TGAs of silicone resin coatings in air	44

3.10	WCA of silicone resin coatings cured at 250°C versus wear cycles with 100 g weighted 2000 grit sandpaper	45
3.11	SEM-EDS images with WCA photo insets of coatings before and after 200 wear cycles. (a-d) DDPS + D ₄ , (e-h) DDPS + D ₄ + PFS, (i-l) DDPS + D ₄ + PFS + MAS, (m-p) DDPS + D ₄ + PFS + MAS + SiO ₂ . Magnification 100x, scale bar 300 μm. EDS map colors: Red = Al, Blue = C, Green = Si, Light Blue = F.	46
3.12	SEM-EDS images of a silicone resin coating (DDPS + D ₄ + PFS + MAS) after 200 wear cycles suggests uniform distribution of functional groups: SEM, EDS maps where a) Al = red and b) C = blue, c) Si = green, d) F = light blue. Magnification 100x, scale bar 300 μm.	48
4.1	Structure of PDMS	56
4.2	Three types of thermoset polymer or composite recycling	57
4.3	Aminolysis of silicone rubber yields 20-40% loss in mechanical properties	58
4.4	Alcoholysis of silicone oil/rubber requires a pressure reactor	59
4.5	Thermally reversible cross-links incorporated into silicone	60
4.6	Silicone rubber with disulfide bond containing cross-links that are reversible with sunlight	60
4.7	F ⁻ catalyzed rearrangement as a new method for recycling silicones	62
4.8	Effect of cure temperature on wear resistance of prime silicone resin coatings	64
4.9	SEM-EDS images of prime silicone resin coatings cured at 150°C before and after 200 wear cycles and cross-hatch tape adhesion test. Wear micrograph magnification 100x, scale bar 300 μm. Cross-hatch magnification 35x, scale bar 800 μm, EDS map: yellow = Si, blue = Al.	64
4.10	SEM-EDS images of prime silicone resin coatings cured at 200°C before and after 200 wear cycles and cross-hatch tape adhesion test. Wear micrograph magnification 100x, scale bar 300 μm. Cross-hatch magnification 35x, scale bar 800 μm, EDS map: yellow = Si, blue = Al.	65
4.11	SEM-EDS images of prime silicone resin coatings cured at 250°C before	

	and after 200 wear cycles and cross-hatch tape adhesion test. Wear micrograph magnification 100x, scale bar 300 μm . Cross-hatch magnification 35x, scale bar 800 μm , EDS map: yellow = Si, blue = Al.	65
4.12	Typical TGAs in air of prime silicone resins cured at increasing temperatures	66
4.13	GC-MS of prime silicone resin a) cured at 150°C and tested at 150°C – 200°C, and b) cured at 200°C and tested at 200°C – 250°C to determine volatile content at different cure temperatures.	67
4.14	DMA of the model mixed phenyl/methyl silicone resin	69
4.15	TMA of the model mixed phenyl/methyl silicone resin	70
4.16	WCA vs number of wear cycles at various [F ⁻]	72
4.17	SEM-EDS images of recycled (0.1M TBAF/THF) silicone resin coatings cured at 250°C before and after 200 wear cycles and cross-hatch tape adhesion test. Wear micrograph magnification 100x, scale bar 300 μm . Cross-hatch magnification 35x, scale bar 800 μm , EDS map: yellow = Si, blue = Al.	72
4.18	EDS shows F in silicone resin recycled with 0.1 M TBAF/THF	73
4.19	SEM-EDS images of recycled (0.002M TBAF/THF) silicone resin coatings cured at 250°C before and after 200 wear cycles and cross-hatch tape adhesion test. Wear micrograph magnification 100x, scale bar 300 μm . Cross-hatch magnification 35x, scale bar 800 μm , EDS map: yellow = Si, blue = Al.	74
4.20	SEM-EDS images of recycled (0.01M TBAF/THF) silicone resin coatings cured at 250°C before and after 200 wear cycles and cross-hatch tape adhesion test. Wear micrograph magnification 100x, scale bar 300 μm . Cross-hatch magnification 35x, scale bar 800 μm , EDS map: yellow = Si, blue = Al.	75
4.21	Typical TGAs in air of prime and recycled silicone resins with increasing [F ⁻]	76
4.22	GC-MS of a) prime and b) recycled (0.01 M TBAF/THF) silicone resins cured at 250°C and tested at 250°C – 300°C to determine volatile content	77

4.23	GC-MS of recycled (0.1 M TBAF/THF) silicone resins cured at 250°C and tested at 250°C – 300°C to determine volatile content	77
4.24	DMA of SILRES compared to the model mixed phenyl/methyl silicone resin	78
4.25	SILRES cured at 250°C dissolves in 55 min in presence of F ⁻	79
4.26	WCA versus number of wear cycles for prime and recycled SILRES	80
4.27	SEM-EDS images of prime SILRES coatings cured at 250°C before and after 200 wear cycles and cross-hatch tape adhesion test. Wear micrograph magnification 100x, scale bar 300 μm. Cross-hatch magnification 35x, scale bar 800 μm, EDS map: yellow = Si, blue = Al.	80
4.28	SEM-EDS images of recycled (0.01M TBAF/THF) SILRES coatings cured at 250°C before and after 200 wear cycles and cross-hatch tape adhesion test. Wear micrograph magnification 100x, scale bar 300 μm. Cross-hatch magnification 35x, scale bar 800 μm, EDS map: yellow = Si, blue = Al.	81
4.29	Typical TGAs of prime and recycled SILRES in air	82
4.30	GC-MS of a) prime and b) recycled (0.01 M TBAF/THF) SILRES cured at 250°C and tested at 250°C – 300°C to determine volatile content	82
4.31	DMAs of prime and recycled SILRES silicone resins	83
4.32	Dissolution of RTV silicone ELSATOSIL in the presence of F ⁻ in 15 min	84
5.1	Silicone resin recycling loop and <i>in situ</i> modification after resin dissolution	91
5.2	Increased [F ⁻] (TBAF molarity) is necessary to dissolve extra DDPS required to produce a 2 Ph : 1 Me silicone resin	94
5.3	Typical TGAs in air of prime 1 Ph : 1 Me silicone resin and after recycling and <i>in situ</i> modification to 2 Ph : 1 Me silicone resin with higher thermal stability	95
5.4	WCA vs number of wear cycles before and after recycling and <i>in situ</i> modification of a 1 Ph : 1 Me silicone resin to a 2 Ph : 1 Me silicone resin	96

5.5	Recycled 1 Ph : 1 Me silicone resin after recycling and <i>in situ</i> modification to left) 1 Ph : 4 Me has right) increased flexibility	97
5.6	Typical DSC of recycled 1 Ph : 1 Me silicone resin modified to a 1 Ph : 4 Me silicone resin shows a T_g at -31 °C	98
5.7	Typical TGA of prime 1 Ph : 1 Me silicone resin compared to after recycling and <i>in situ</i> modification to a 1 Ph : 4 Me silicone resin	99
5.8	Typical initial WCA of 1 Ph : 1 Me silicone resin in a) prime condition and b) after recycling and <i>in situ</i> modification to 1 Ph : 4 Me : 1 PFS silicone resin	100
5.9	WCA vs number of wear cycles before and after recycling and <i>in situ</i> modification of a 1 Ph : 1 Me silicone resin to a 1 Ph : 4 Me : 1 PFS silicone resin	100
5.10	Typical TGAs in air of prime SILRES and after recycling and <i>in situ</i> modification to add 10 wt % DDPS for higher thermal stability	102
5.11	TMA of prime SILRES and after recycling and <i>in situ</i> modification to add 10 wt % DDPS for lower CLTE	103
5.12	DMA of prime SILRES and after recycling and <i>in situ</i> modification to add 10 wt % DDPS for higher stiffness	104
5.13	WCA vs number of wear cycles before and after recycling and <i>in situ</i> modification of a SILRES to add 10 wt % DDPS	105
6.1	left) CF_3-D_3 structure, right) initial WCA of coating with CF_3-D_3	109
6.2	Schematic of isocyanate bonding to reactive aluminum oxide surface	110
6.3	Schematics and WCA vs wear cycles with pertinent coatings for comparison of Layered System a-b) 1 and c-d) 2	111
6.4	Structure of octaphenylcyclotetrasiloxane	113
6.5	Examples of octafunctional SQ cages as building blocks for various thermoset polymers susceptible to F^- catalyzed recycling	116
6.6	Cured (250°C) SILRES pattern a) before and b) after selective removal with 0.01M THF/TBAF; magnification 27x, scale bar 1000 μm	117
A.1	SEM of 5 wt % silicone resin coating; magnification 100x, scale bar 500 μm	119

A.2	SEM of 10 wt % silicone resin coating; magnification 100x, scale bar 300 μm	120
A.3	SEM of 15 wt % silicone resin coating; magnification 100x, scale bar 500 μm	120
A.4	SEM of 25 wt % silicone resin coating; magnification 100x, scale bar 500 μm	121
A.5	SEM of patterned SILRES coating; magnification 25x, scale bar 2 mm	121
A.6	SEM of reapplication of SILRES coating over patterned (or “damaged”) coating; magnification 27x, scale bar 2 mm	122
B.1	DSC of model mixed phenyl/methyl silicone resin (1 Ph : 1 Me)	123
B.2	TMA of commercial SILRES silicone resin	124
B.3	DSC of commercial SILRES silicone resin	124
B.4	DSC of 1 Ph : 4 Me silicone resin	125
B.5	DSC of 1 Ph : 4 Me : 0.2 PFS silicone resin	125
B.6	TMA of 1 Ph : 4 Me silicone resin	126
B.7	TMA of ELASTOSIL E10 commercial RTV silicone rubber	126
C.1	WCA vs wear cycles on recycled model silicone resin (1 Ph : 1 Me) cured at increasing temperatures	127
C.2	SEM-EDS images of recycled (0.01M TBAF/THF) model silicone resin coatings cured at 150°C before and after 200 wear cycles and cross-hatch tape adhesion test. Wear micrograph magnification 100x, scale bar 300 μm . Cross-hatch magnification 35x, scale bar 800 μm , EDS map: yellow = Si, blue = Al.	128
C.3	SEM-EDS images of recycled (0.01M TBAF/THF) model silicone resin coatings cured at 200°C before and after 200 wear cycles and cross-hatch tape adhesion test. Wear micrograph magnification 100x, scale bar 300 μm . Cross-hatch magnification 35x, scale bar 800 μm , EDS map: yellow = Si, blue = Al.	128
C.4	SEM-EDS images of recycled (0.01M TBAF/THF) model silicone resin coatings cured at 250°C before and after 200 wear cycles and cross-hatch tape adhesion test. Wear micrograph magnification 100x,	

	scale bar 300 μm . Cross-hatch magnification 35x, scale bar 800 μm , EDS map: yellow = Si, blue = Al.	129
C.5	Typical TGAs in air of prime and recycled model silicone resin with increasing cure temperature	129
D.1	GC-MS of 0.01M TBAF in BHT stabilized THF accounts for decomposition products found in silicone resin systems synthesized via F ⁻ catalyzed rearrangement	131
D.2	GC-MS of D ₄	131
D.3	GC-MS of Al dishes used for casting some samples shows dish coated with grease release agent as a source of potential contamination	132

List of Schemes

Scheme

1.1	The Direct Process to synthesis silicone precursor dichlorodimethylsilane	4
1.2	Formation of octamethylcyclotetrasiloxane (D ₄) via hydrolysis of dimethyldichlorosilane	4
1.3	Formation of hydroxyl-terminated oligomeric dimethylsiloxanes via hydrolysis of dimethyldichlorosilane	4
1.4	Ring opening polymerization of octamethylcyclotetrasiloxane (D ₄) to polydimethylsiloxane	5
1.5	Polycondensation of hydroxyl-terminated oligomeric dimethylsiloxanes to PDMS	5
1.6	Hydroxyl terminated polysiloxane reacting with methyltriacetoxysilane cross-linker to form end blocked intermediate for one component RTV silicone elastomer	6
1.7	Cross-linking of RTV silicone elastomer upon exposure to humidity	7
1.8	Traditional hydrolytic condensation reaction to produce SQs	10
1.9	F ⁻ catalyzed rearrangement of polymeric SQ into T ₁₀ and T ₁₂ SQ cages	11
1.10	F ⁻ catalyzed rearrangement of T ₈ SQ into T ₁₀ and T ₁₂ SQ cages	11
4.1	Free radical sequence of phenyl/methyl silicones at elevated temperature	68
5.1	Modification of model 1 Ph : 1 Me silicone resin with DDPS to increase ratio phenyl/methyl ratio to 2 Ph : 1 Me and increase thermal stability	92
6.1	Pathway to siloxane containing epoxy-amine thermoset susceptible to F ⁻ catalyzed recycling	114
6.2	Pathway to siloxane containing polyurethane thermoset susceptible to F ⁻ catalyzed recycling	114
6.3	Pathway to siloxane containing polyurea thermoset susceptible to F ⁻ catalyzed recycling	115

6.4	Pathway to siloxane containing cross-linked unsaturated polyester thermoset susceptible to F ⁻ catalyzed recycling	115
------------	--	-----

List of Abbreviations

AIBN	azobisisobutyronitrile
ASTM	American Society for Testing and Materials
APS	average particle size
BHT	butylated hydroxytoluene
CLTE	coefficient of linear thermal expansion
D ₃	hexamethylcyclotrisiloxane
D ₄	octamethylcyclotetrasiloxane
D ₅	decamethylcyclopentasiloxane
DDPS	dodecaphenylsilsesquioxane
DMA	dynamic mechanical analysis
DSC	differential scanning calorimetry
EDS	energy dispersive X-ray spectroscopy
FTIR	Fourier transform infrared spectroscopy
GC-MS	gas chromatography-mass spectrometry
MAS	methacryloxypropyltrimethoxysilane
PDMS	polydimethylsiloxane
Ph ₈ D ₄	octaphenylcyclotetrasiloxane
PFS	(tridecafluoro-1,1,2,2-tetrahydrooctyl)triethoxysilane
PTES	phenyltriethoxysilane
RTV	room temperature vulcanized
SEM	scanning electron microscope
SQ	silsesquioxane
TBAF	tetrabutylammonium fluoride
T _{d5%}	five percent thermal decomposition temperature
T _g	glass transition temperature

TGA	thermogravimetric analysis
THF	tetrahydrofuran
TMA	thermomechanical analysis
UV	ultraviolet
VTMS	vinyltrimethoxysilane
WCA	water contact angle

List of Appendices

Appendix A. Supplemental SEM Images	119
Appendix B. Supplemental Thermal Analyses	123
Appendix C. Cure Temperature Effect on Recycled Silicone Resin Properties	127
Appendix D. Supplemental GC-MS	131

Abstract

Silicones are unique polymers with inorganic backbones that, in part, afford properties that cannot be matched by organic polymers. A short list of their many attractive properties includes thermal stability, chemical resistance, hydrophobicity, and physiological inertness. Such an intriguing combination of properties lends itself to an abundant and diverse array of applications ranging from aerospace sealants to automotive molding release agents to marine anti-corrosion/fouling coatings to medical prosthetic devices. Despite, and in some cases because of, their excellent properties there are challenges associated with this important class of polymers. This dissertation aims to explore some of these opportunities and offer new solutions.

First, we focus on using fluoride ion (F^-) catalyzed rearrangement of siloxane and silsesquioxane bonds as a new route to synthesize multi-functional and highly cross-linked silicone resin networks. The resulting monoliths and coatings exhibit high thermal and oxidative stability, up to $>460^\circ C$. Our approach also allows for the typically difficult combination of hydrophobicity and wear resistance.

Thereafter, we employ a mixed phenyl/methyl silicone resin synthesized via F^- catalyzed rearrangement as a model system for our new recycling technique. Silicones, especially resins, are some of the most challenging polymers to recycle. Not only are they cross-linked thermosets, but their high temperature stability and inertness make them even more difficult to degrade by conventional recycling methods, such as pyrolysis. Here, we present the facile recycling of highly cross-linked silicones at ambient temperature and pressure via F^- catalyzed rearrangement in solvent. Rigid virgin silicone resin cured at $250^\circ C$ becomes soluble in less than 24 h in the presence of F^- and can be reapplied or cast easily. The recycled silicones maintain nearly 100% of key properties such as thermal and wear resistance.

We also show this technique works for commercially relevant silicone rubber and resin made by conventional means. In some cases, the properties of the recycled material is higher than the virgin material, which suggests the potential for up-cycling.

Lastly, we explore a discovered opportunity presented by the nature of our recycling process. When the fully cured silicone resin dissolves in the presence of F^- , the ratio of starting materials can be adjusted by the addition of new silicone building blocks. For example, increasing the phenyl content and cross-link density yields a silicone resin with a thermal stability of $>530^\circ\text{C}$. The introduction of wholly new functionalities can modify the virgin silicone such that the recycled material can be used in a different, and possibly more demanding, application. For example, the introduction of 10 wt% of a phenyl functionalized silsesquioxane to a recycled commercial silicone resin via F^- catalyzed rearrangement increased the T_g and thermal stability by 115°C and 30°C , respectively.

Chapter 1

Introduction

This dissertation describes our work on the synthesis, recycling, and modification of silicone resins and the characterization of their properties. This chapter contains background information on objectives, general concepts, and a review of pertinent literature as a foundation for the topics discussed in this dissertation. Section **1.1** provides an overview of the motivation for this research and project objectives. Section **1.2** provides background information on the structure, synthesis, and properties of silicones. Section **1.3** provides a brief overview of silsesquioxanes. Section **1.4** describes the general chemical reactions used throughout this work. Lastly, section **1.5** provides a brief overview on the current status of polymer recycling.

1.1 Research Motivation and Objectives

Silicones or polysiloxanes are unique polymers with inorganic backbones of alternating silicon and oxygen atoms. Their low glass transition temperature, thermal stability, chemical inertness, and low coefficient of friction make silicones useful in many applications in the automotive, aerospace, cookware, and medical industries. Despite their many attractive properties, applications of silicones can be limited by mechanical property demands and environmental consciousness. Filling these gaps is the impetus of the work described in this dissertation.

The primary research objectives were to develop facile routes to synthesize, recycle, modify, and optimize silicone resins. In Chapter **3**, we demonstrate that fluoride ion catalyzed rearrangement reactions of silicone building blocks including silanes, siloxanes, and silsesquioxanes can be used as a new polymerization technique to form silicone resins

and their subsequent application as hydrophobic coatings that also exhibit wear resistance and high thermal and oxidative stabilities. Chapter 4 explores using the same facile route to solubilize and recycle highly cross-linked thermoset silicone resins and the retention of properties in the 2nd generation materials. In Chapter 5, we demonstrate the modification of silicone resins during the recycling dissolution reaction to introduce new functionalities that drastically change the properties of the resin from one generation to the next. Finally, in Chapter 6 we discuss potential future work for designing, synthesizing, recycling, and modifying not only silicone resins, but also other thermoset polymers based on the results of this dissertation.

1.2 Introduction to Silicones

The term silicone was coined by Kipping in 1901, but it is actually a misnomer. Kipping was using an analogy to ketones when describing polydiphenylsiloxane because he first thought there was an O doubled bonded to a Si and called it a silicoketone, which he shortened to silicone. Kipping was a silicon, silane, siloxane chemistry pioneer and the ACS Silicon Chemistry Award is named in his honor. The correct term for polymers with alternating Si and O atoms in their backbone is polyorganosiloxanes or polysiloxanes. However, the much more widely used term, silicone, will be used throughout this dissertation. Silicones have a low glass transition temperature, high thermal stability, chemical inertness, and low coefficient of friction making them useful in many applications in the automotive, aerospace, cookware, and medical industries.

1.2.1 Definition, Structures, and Nomenclature

As stated above polysiloxanes or silicones consist of an O-Si-O or siloxane backbone. Silicones can be in the form of fluids, elastomers (rubbers), or resins depending on their structure (Table 1.1). There are four types of monomer units used to build silicones with the letter designations M (monofunctional), D (difunctional), T (trifunctional), and Q (tetrafunctional), which can be used to define a so called MDTQ formula.

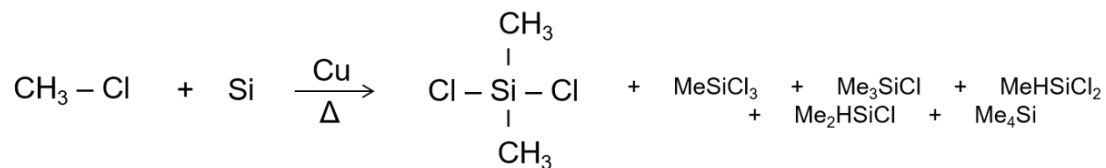
Table 1.1 Symbol, formula, and uses of polysiloxane (silicone) structural units¹

Valency	Symbol	General Formula	Uses
Mono	M	$R_3SiO_{1/2}$	Chain end in silicone fluids
Di	D	$R_2SiO_{2/2}$	Linear polysiloxanes for silicone fluids and elastomers
Tri	T	$RSiO_{3/2}$	Silicone resins
Tetra	Q	$SiO_{4/2}$	Silicone resins

D units can be linked together to form linear polysiloxanes of low to high molecular weight and take the form of silicone fluids. The most industrially important polysiloxane, polydimethylsiloxane (PDMS), is formed when both functional R groups in the linear polymer are methyl groups. If the functional groups in the D unit are cross-linkable then silicone elastomers can be formed. Silicone fluids and elastomers are based on linear polysiloxanes, but silicone resins are highly branched due to large amounts of T and Q units. Silicone resins can also contain D units to add flexibility as well as M units.

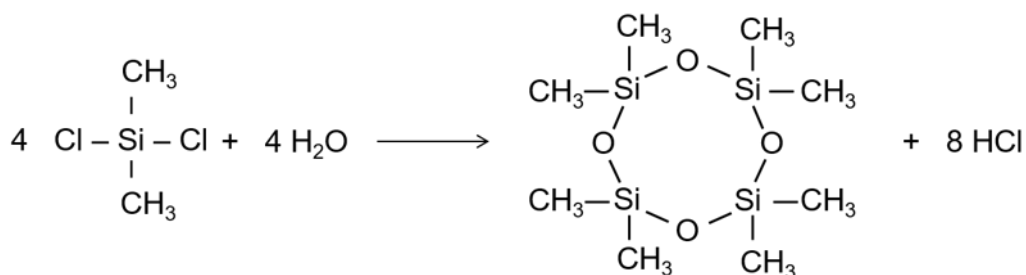
1.2.2 Silicone Polymerization Techniques

The commercial production of silicones begins with the Direct Process, which was developed independently in the early 1940s by Eugene Rochow in the United States and Richard Müller in Germany. The reaction (Scheme 1.1) is carried out in a fluidized bed of ground silicon metal with a copper catalyst, which is exposed to chloromethane gas at 300°C under pressure. The major product of the reaction is dichlorodimethylsilane, the principal precursor to making silicones.

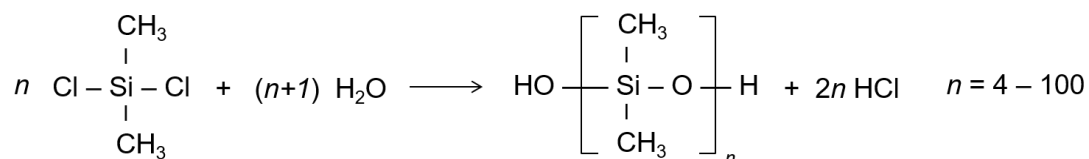


Scheme 1.1 The Direct Process to synthesis silicone precursor dichlorodimethylsilane

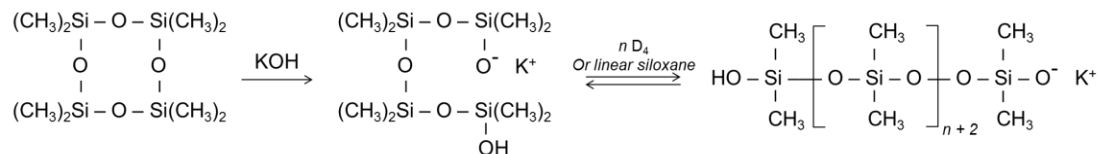
Linear and cyclic polyorganosiloxanes are formed by hydrolysis or methanolysis of organodichlorosilanes, typically dimethyldichlorosilane.² Control of the process favors formation of cyclic siloxanes, such as octamethylcyclotetrasiloxane (D₄ or ^{Me}D₄) in Scheme 1.2, or linear oligomeric dimethylsiloxanes typically terminated with hydroxyl groups, Scheme 1.3. Polysiloxanes can then be formed either by equilibrating ring opening polymerization of cyclic organosiloxanes (Scheme 1.4) or by anionic catalyst (cationic catalysis is also possible). Polysiloxanes can also be formed by the polycondensation of linear oligomeric dimethylsiloxanes (Scheme 1.5; acid catalyzed).^{1,3} It is also possible to make siloxane based copolymers by copolymerizing D₄ with another cyclosiloxane with a different functionality such as phenyl, vinyl, alkyl, or trifluoropropyl.⁴



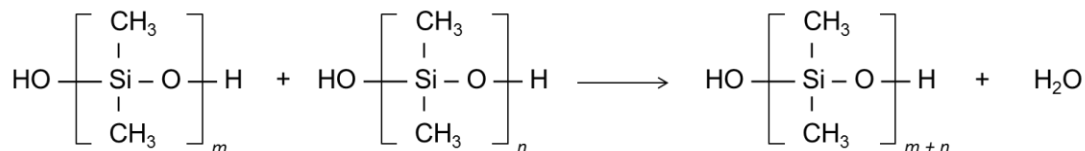
Scheme 1.2 Formation of octamethylcyclotetrasiloxane (D₄) via hydrolysis of dimethyldichlorosilane



Scheme 1.3 Formation of hydroxyl-terminated oligomeric dimethylsiloxanes via hydrolysis of dimethyldichlorosilane



Scheme 1.4 Ring opening polymerization of D₄ to PDMS



Scheme 1.5 Polycondensation of hydroxyl-terminated oligomeric dimethylsiloxanes to PDMS

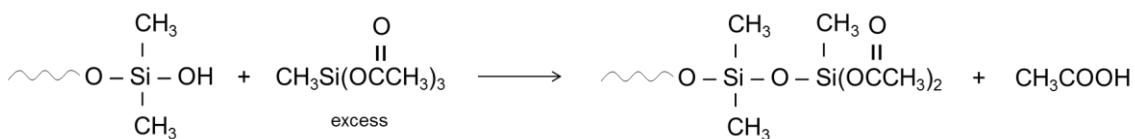
1.2.3 Types and Properties of Silicones

Silicone fluids are uncross-linked and branch free linear polysiloxanes that have a MDTQ formula of MD_xM where $x = 2 - 4000$. The functional groups on the D unit can be methyl (PDMS), phenyl, a mix of methyl and phenyl, a mix of methyl and hydrogen, a mix of methyl and alkyl, or trifluoropropyl. These high thermal stability fluids perform well at low temperatures and have good hydrophobic, release, antifriction, lubricating, dielectric, and damping properties.¹ Due to the excellent combination of properties silicone fluids have applications as heat transfer media, refrigerants, waterproof coatings, lubricants, and cosmetics (odorless, tasteless, physiologically inert).

Linear polysiloxanes with cross-linkable functional groups in the backbone or on the chain ends can be cured to form silicone elastomers in several different ways. These cross-linkable unsaturated C=C bonds can undergo radical polymerization with heat in the presence of a peroxide initiator and produce acid byproducts.⁵ Unsaturated C=C bonds from incorporated vinyl groups can also undergo hydrosilylative curing (in the presence of metal catalysts) with Si-H bonds in either the backbone or with short sidechain cross-linkers (i.e. methylhydrogensiloxanes), which does not form byproducts like radical curing with peroxides.¹ Increased cross-link density increases the modulus and hardness of the elastomer, but typically silica is also incorporated as a reinforcing filler, which increases

the tensile strength.^{6,7} Low cross-link densities can also be targeted to achieve very soft materials or gels.

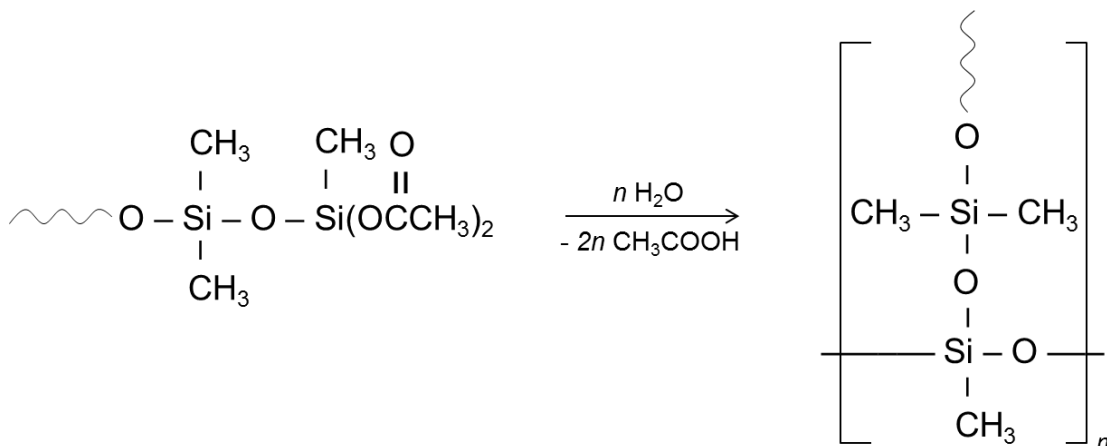
Silicone elastomers can also be cross-linked by ambient moisture at room temperature in so called one component and two component RTV (room temperature vulcanizing) silicones. These systems typically use a tin catalyst to achieve complete cure. One component RTV silicones are formulated from hydroxyl terminated polysiloxanes with an excess amount of methyltriacetoxysilane, which first reacts with the hydroxyl group to create reactive end groups (Scheme 1.6).⁸ The excess silane serves two purposes. First, the excess reduces the probability of two chain ends reacting with the same silane molecule. Second, the chain ends are blocked by two acetoxy groups which suppress cross-linking allowing the liquid to be sealed in containers for later use.



Scheme 1.6 Hydroxyl terminated polysiloxane reacting with methyltriacetoxysilane cross-linker to form end blocked intermediate for one component RTV silicone elastomer

On opening the container, the excess methyltriacetoxysilane and reactive chain ends are hydrolyzed by ambient moisture forming SiOH, which then reacts with remaining acetoxy groups to create the cross-linked elastomer and acetic acid byproduct (Scheme 1.7).⁸ Other hydrolyzable silanes can be used as cross-linkers, but all form byproducts such as alcohols, amines, or oximes. The corrosive nature of acetic acid, the condensation byproduct, can limit the use of RTV silicones.

Two component RTV silicones require the mixing of a hydroxyl functionalized polysiloxane and silane cross-linker at the time of use. They also use tin catalysts and produce byproducts, but do forego the intermediate end blocking reaction.



Scheme 1.7 Cross-linking of RTV silicone elastomer upon exposure to humidity

The final properties of silicone elastomers vary depending on cross-link density, filler type/amount, copolymerization, backbone structure, etc., which lead to very diverse applications. High thermal stability, hot air resistance, oxidation resistance, and flame retardancy make silicone elastomers ideal for tubing, gaskets, fixtures, sealants, and coatings in automotive and aerospace applications.⁹⁻¹¹

Due to their physiological inertness, silicone elastomers are used in food contact applications as well as medical applications such as prosthetics, implants, catheters, and heart valve seals.¹²⁻¹³ Silicone elastomers have strong adhesion to metal and glass substrates and provide a low surface energy, low friction, non-stick, hydrophobic surface suitable for applications in casting, mold making, mold release, water repellent coatings, anti-graffiti coatings, cookware, and the paper industry.¹⁴⁻¹⁶

Unlike silicone fluids and elastomers, which are linear polysiloxanes comprised of only D and M units, silicone resins also contain T and Q units. These tri- and tetra- functional units are used to create highly branched and cage-like networks with a high cross-link density. A combination of units is typically used to balance properties, for example, pure T-resins can be brittle, but adding D or M units increases elasticity and adhesion.¹ Similar hydrolysis and alcoholysis processes to those mentioned above are used to produce silicone resins. Silicone resins are also cured by the mechanisms mentioned above, with the most common method being metal catalyzed condensation.¹ A 2-D idealized silicone resin containing all four monomer units is shown in Figure 1.1

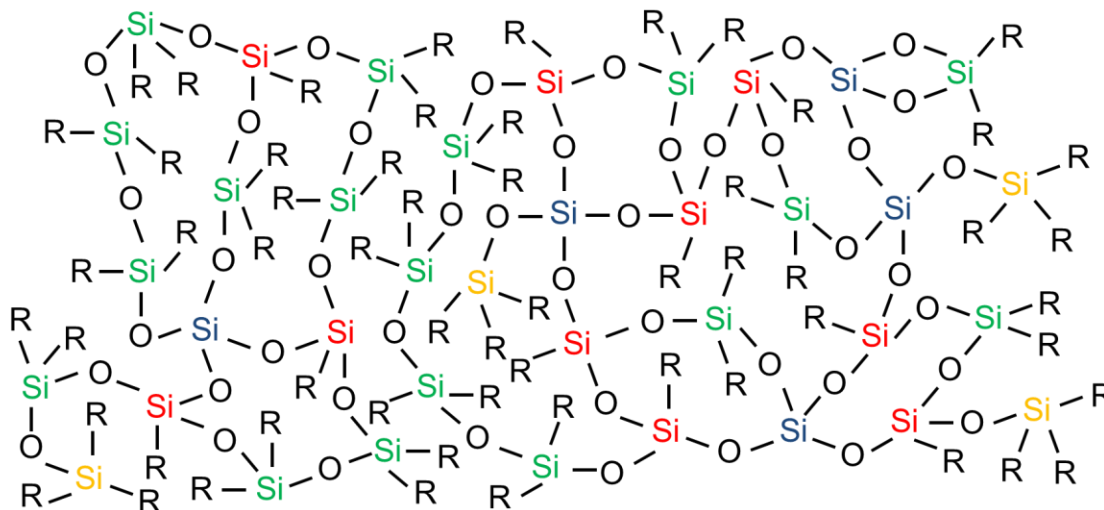


Figure 1.1 An idealized silicone resin structure, where R = methyl, phenyl, etc.; Orange Si = M unit, Green Si = D unit, Red Si = T unit, Blue Si = Q unit

Silicone resins combine high temperature, oxidation, and UV stability as well as resistance to acids, oils, and water making them ideal for many coating applications including release, hydrophobic, oleophobic, abrasion resistance, chemical resistance, anti-corrosion, protective, decorative, insulating, anti-fouling, sealants, and paints.^{1,14-16}

1.3 Introduction to Silsesquioxanes

The word silsesquioxane can be broken up into four terms that provide the general formula $(\text{RSiO}_{1.5})_n$: sil- (silicon), -sesqui- (one and a half), -ox- (oxygen), and -ane (hydrocarbon R group). Thus, the name itself indicates that silsesquioxanes (SQs) are comprised of T units ($\text{RSiO}_{1.5}$) where the ratio of R group to silicon to oxygen is 1:1:1.5. The R groups can be hydrogen or many different alkyl, alkenyl, aryl, arylene, or siloxy groups. This combination of organic R groups and inorganic Si-O-Si framework make SQs organic-inorganic hybrid materials with properties intermediate of ceramics and polymers. The inorganic component provides inertness and thermal and oxidative stability while the organic components can provide reactivity, polymer miscibility, and a wide range of functionalities.

These hybrid materials have unique and tailorable multi-functional properties that offer utility for a plethora of applications including components in polymer nanocomposites, catalyst, models for silica surfaces and heterogeneous catalysts, low-k dielectrics, antimicrobial agents, emitting layers in organic light-emitting diodes, and coatings.¹⁷⁻³⁹ In particular, SQs have been used to enhance the mechanical and thermal properties of many common polymers^{40,41} including PDMS as nanofillers and cross-linkers.^{7,42-45} Vinyl⁴²⁻⁴⁴ or epoxy⁴⁵ functionalized T₈ SQs were used as cross-linkers for vinyl or epoxy terminated linear PDMS chains to create cross-linked silicone rubbers.

SQs can have random, ladder, partial cage, or cage structures (Figure 1.2).⁴⁶⁻⁶⁴ Random SQs are polymeric and have no long-range order. Ladder structured SQs have been made on an oligomeric scale, but polymeric forms have not.⁴⁷ Partial cage structures are not fully condensed meaning they contain silanol groups at one or more cage corners. Cage structures, as well as random and ladder structures, are completely condensed without any -OH groups.

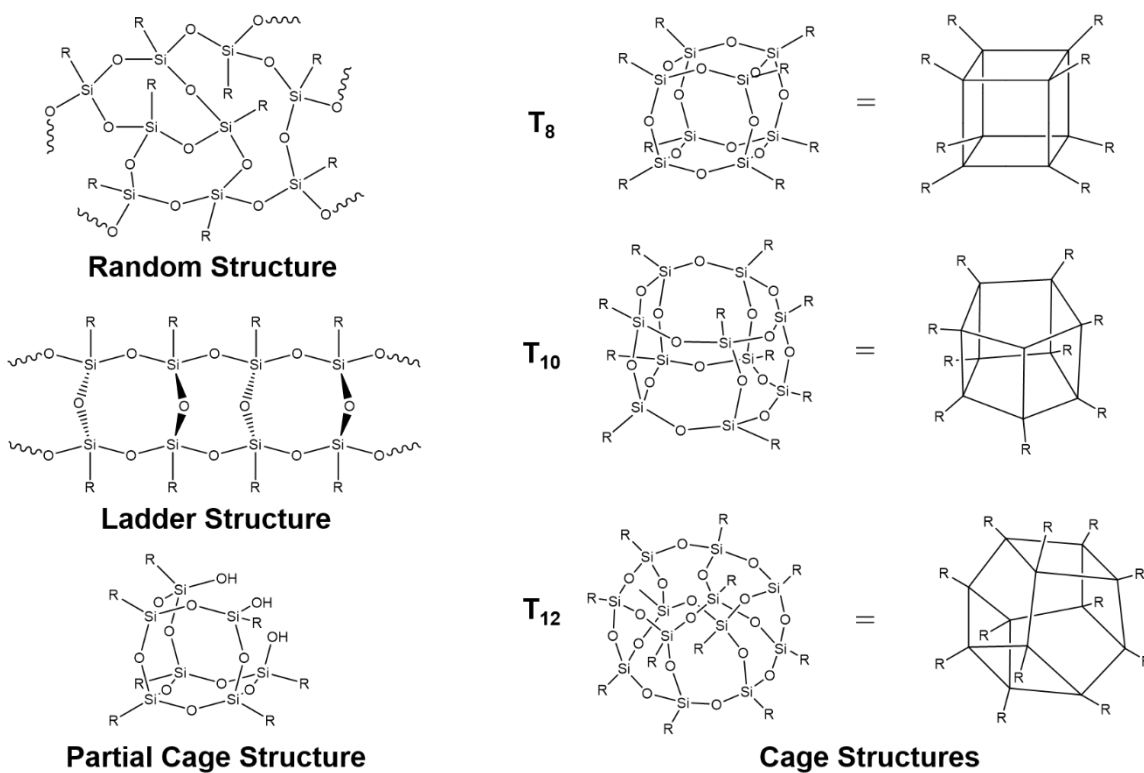
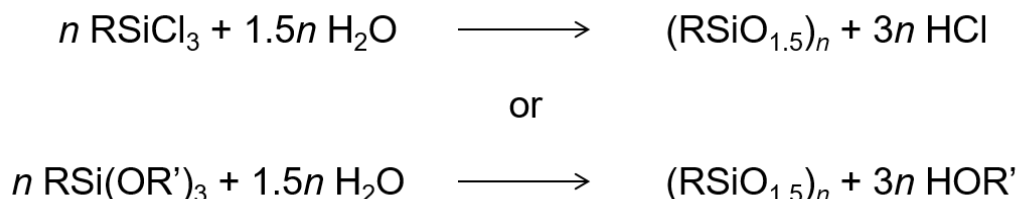


Figure 1.2 Silsesquioxane (SQ) structures^{47,65,66}

Typical SQ syntheses are by acid or base catalyzed hydrolysis and condensation of trichloro- or trialkoxy-silanes as shown in Scheme 1.8. This general route is a complex multi-step process where the structure of the final product is interdependent on the various reaction conditions and is slow with low yields.⁵⁸⁻⁶¹

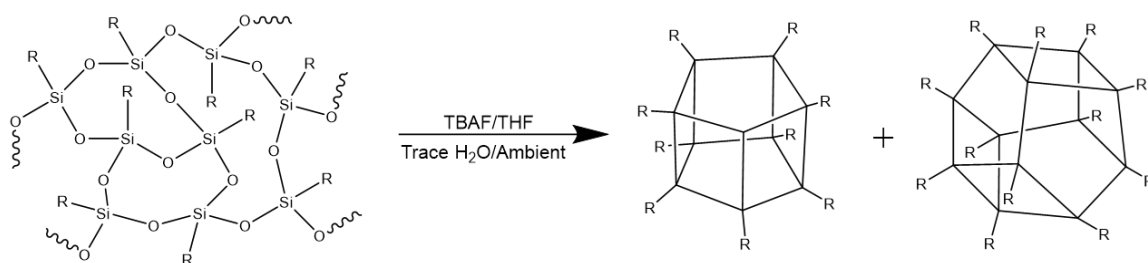


Scheme 1.8 Traditional hydrolytic condensation reaction to produce SQs

1.4 Introduction to Fluoride Ion Catalyzed Rearrangement Reactions

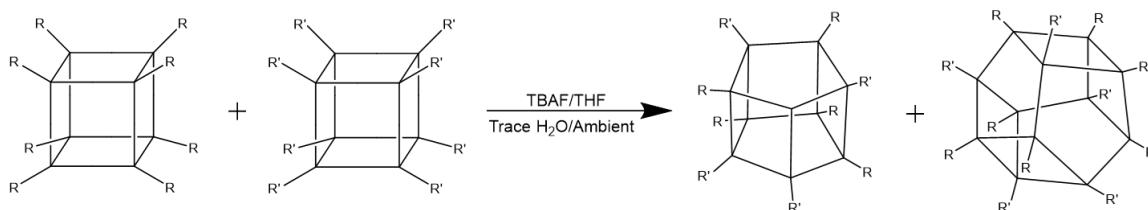
The inspiration for the silicone polymerization (Chapter 3), recycling (Chapter 4), and *in situ* modification (Chapter 5) methods developed for this dissertation come from the fluoride ion (F⁻) catalyzed rearrangement reaction developed by the Laine Group as a facile synthetic route to silsesquioxanes.⁶⁵⁻⁷⁰ Unlike traditional hydrolytic condensation reactions this route has much higher yields, > 98% in many cases, for T₁₀ and T₁₂ SQs.

The first example of F⁻ catalyzed rearrangement from our group used 1-2 mol% of tetrabutylammonium fluoride (TBAF) to convert polymeric SQs into discrete T₁₀ and T₁₂ SQ cages (Scheme 1.9).^{65,67} The cages were recovered by capturing the F⁻ with CaCl₂ to form insoluble CaF₂, filtering out the solid, and collecting the product by either solvent removal or precipitation. SQs with mixed vinyl/methyl and vinyl/phenyl were synthesized by rearranging polyvinylsilsesquioxane [vinylSiO_{1.5}]_n and polymethylsilsesquioxane [MeSiO_{1.5}]_n or polyphenylsilsesquioxane [PhSiO_{1.5}]_n in solution with the F⁻. The ratio of functional groups was statistically controlled by the ratio of starting materials.



Scheme 1.9 F^- catalyzed rearrangement of polymeric SQ into T_{10} and T_{12} SQ cages

Our group also showed that two mono-functional T_8 SQs rearrange in the presence of F^- to form T_{10} and T_{12} cages with statistically controlled mixed functionality (Scheme 1.10).⁶⁸ In this work, octaaminophenylsilsesquioxane [aminophenylSiO_{1.5}]₈ and octaphenylsilsesquioxane [phenylSiO_{1.5}]₈ were rearranged to create bifunctional SQs that were then reacted with a di-epoxy to create beads on a chain polymers.



Scheme 1.10 F^- catalyzed rearrangement of T_8 SQ into T_{10} and T_{12} SQ cages

The mechanism of the F^- catalyzed rearrangement reaction was mostly unknown until recently when Furgal *et al.* conducted an exhaustive experimental and computational analysis of likely reaction pathways.⁷⁰ This work focused on forming phenyl T_{10} SQ, decaphenylsilsesquioxane [PhSiO_{1.5}]₁₀, from different starting materials including [PhSiO_{1.5}]₈ and oligomeric or polymeric [PhSiO_{1.5}]_n. Yields up to 50% were achieved for the difficult to isolate [PhSiO_{1.5}]₁₀. The F^- catalyzed rearrangement mechanism was found to be highly complicated with many intermediate steps and the equilibration of many different soluble intermediate species, some of which are shown in Figure 1.3. The most likely pathway at RT based on activation energies was suggested to be a hybrid mechanism involving both F^- and water.

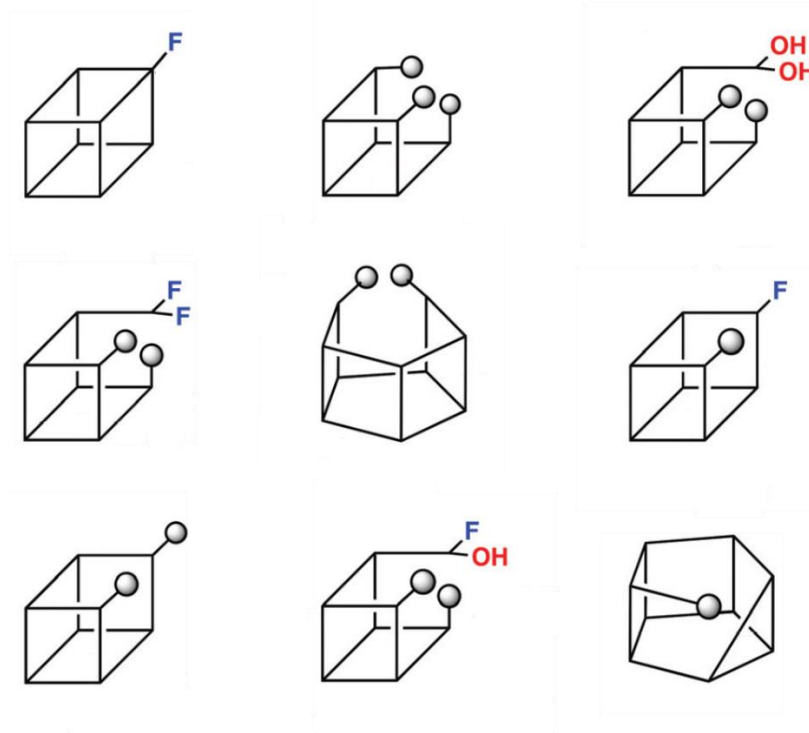


Figure 1.3 Soluble intermediate species during F^- catalyzed rearrangement of T_8 SQ, spheres represent capped corners⁷⁰

1.5 Overview of Polymer Recycling

A brief overview of the current status of plastic recycling provides perspective for the motivation and importance of work described later in Chapters 4 and 5. Large scale production of polymers only began in the 1950s, but today they are ubiquitous in modern society. Not only can polymers be found in an endless list of products essential to everyday life, but they can also be found in most aquatic and terrestrial ecosystems.

A recent study estimated that approximately 8.3 billion metric tons of plastic was produced globally between 1950 and 2015.⁷¹ The rate of plastic production continues to increase rapidly and nearly half of the total plastic production occurred in the last 13 years of the study's timeframe. After the start of commercial plastic production essentially all polymer products were discarded until 1980 when incineration and recycling techniques began to come online (Figure 1.4). Since then, the rates of incineration and recycling have increased to 24% and 18%, respectively, in 2014.

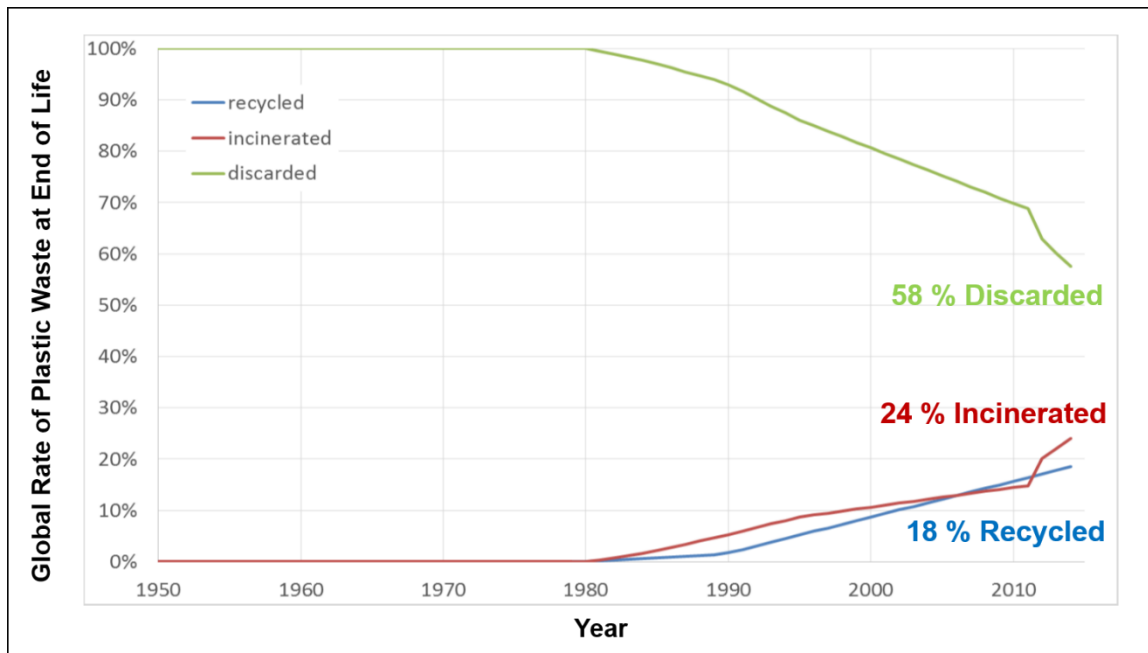


Figure 1.4 Global rates for recycling, incineration, and discard of all plastic waste⁷¹

In addition to, or perhaps in light of, understanding the history of plastic waste production and final destination, it is imperative that we look at what will happen in the future. The same study by Geyer *et al.* used historical trends to make the future projections shown in Figure 1.5. The cumulative plastic waste generated by 2050 was estimated to reach 26 billion metric tons (plus an additional 8 billion metric tons in fibers and additives not shown in the graph) with 12 billion metric tons discarded.⁷¹ In this context it is important to note that the term “discarded” means both landfilled and discarded into the environment where the polymers can be consumed by or kill animals and leach compounds into soil or water thereby creating numerous pathways for harmful substances to ultimately end up in human bodies as well.

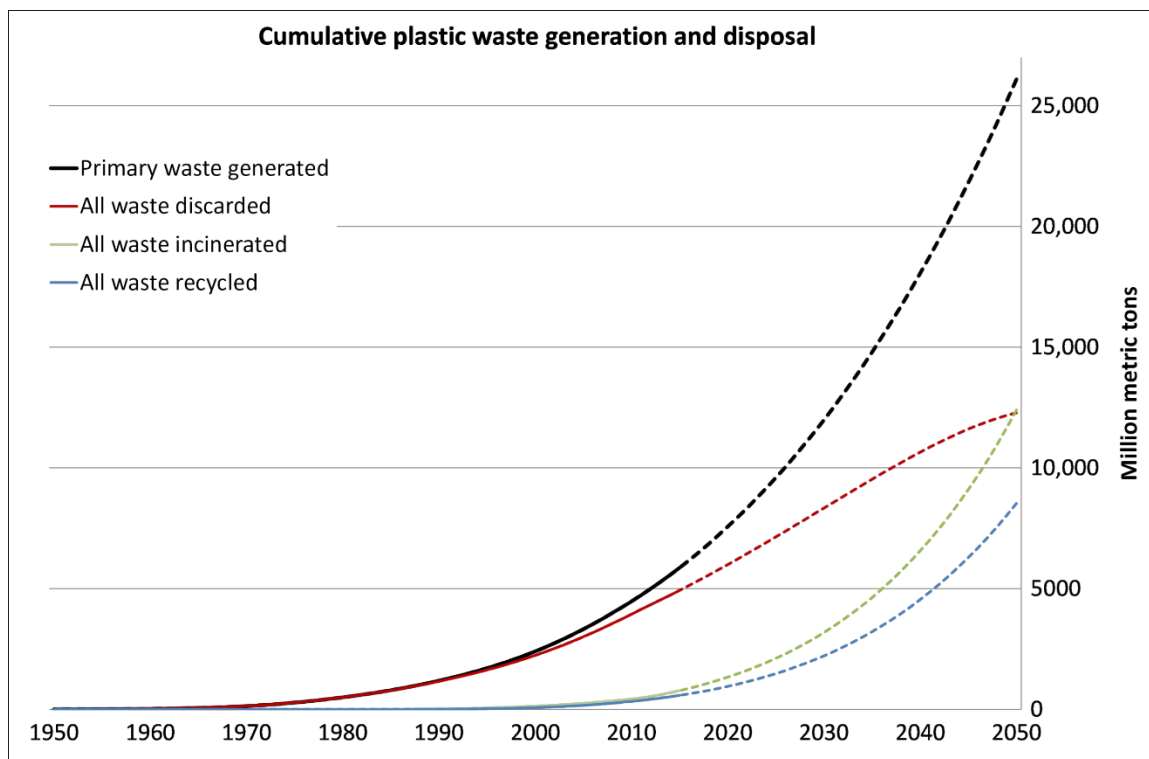


Figure 1.5 Cumulative global plastic waste generation and disposal, historical data and future projections represented by solid and dashed lines respectively⁷¹

The only plastic waste streams recycled on an industrial scale are thermoplastic polymers because they have a melting point at which they begin to flow. Heating a thermoplastic polymer adds thermal energy that allows for thermal motion of the polymer chains transforming it from a solid to a viscous liquid. Thus, a virgin thermoplastic product can be melted, reshaped, and cooled to hold a new shape for a new product. The most commonly recycled thermoplastics are: polyethylene terephthalate (PET), high density polyethylene (HDPE), low density polyethylene (LDPE), polypropylene (PP), polystyrene (PS), and polyvinylchloride (PVC).

Thermosetting polymers or thermosets account for 18% of all polymers produced annually⁷² and are difficult to recycle because they do not have a melting point. Thermosets have cross-links between the polymer chains that prevent the chain movement necessary for the material flow with heat (Figure 1.6). Therefore, thermosets are used in applications that require high operating temperatures instead of thermoplastics. At sufficiently high temperatures thermosets will degrade. Silicone resins, which are highly cross-linked, have high thermal stability for polymeric materials due to the cross-links as well the inorganic

siloxane, rather than organic carbon, backbone or network. The high thermal and oxidative stability makes recycling silicone rubbers and resins especially difficult as discussed later in Chapter 4.

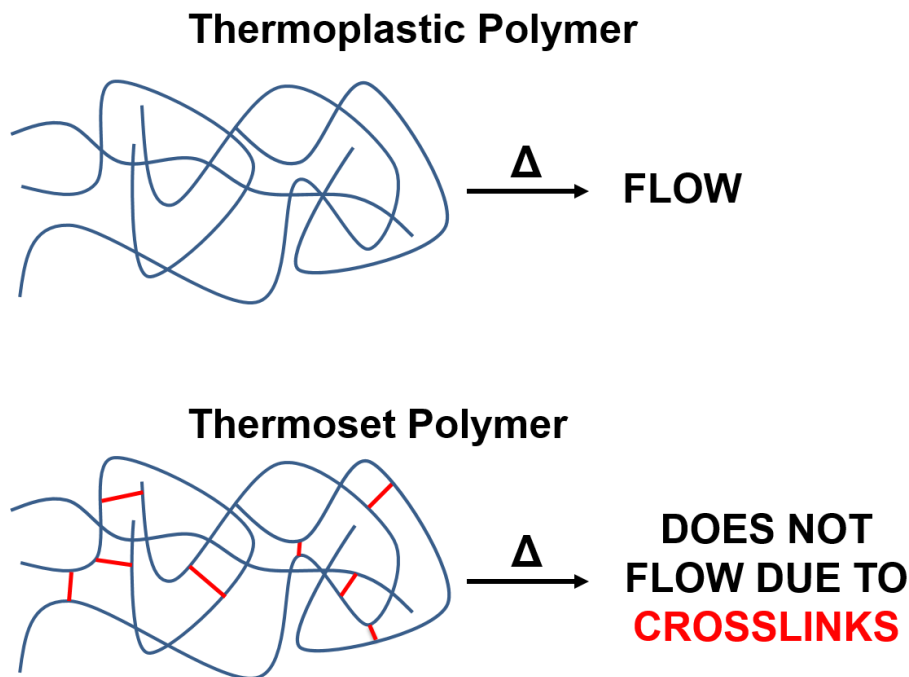


Figure 1.6 Schematic of thermoplastic and thermoset polymer behavior upon heating

One of the biggest obstacle to higher recycling rates of plastic waste is generally agreed to be the collection (and sorting) of plastic waste.^{73,74} However, as logistical, technological, and economic factors drive plastic waste collection forward, the scientific community needs to provide low cost, low energy, and easy to scale ways to recycle all plastic waste including difficult to recycle polymers like thermosets and specifically silicones.

Our research described in this dissertation presents a new technique for recycling silicones (Chapter 4) inspired by the F^- catalyzed rearrangement reaction used to synthesize SQs. This method is low energy, easy to scale, and allows for near 100% retention of key properties. Our new approach also presents an opportunity for the *in situ* modification of the recycled silicone (Chapter 5), thus providing the ability to enhance or modify key properties to potentially expand the applications of the recycled silicone.

1.6 References

1. Moretto, H. H.; Schulze, M.; Wagner, G. In *Ullmann's Encyclopedia of Industrial Chemistry*; Electronic Release, Wiley-VCH, Weinheim, 2012, Vol. 32, Chapter Silicones, pp 675-712.
2. Lu, P.; Paulasaari, J. K.; Weber, W. P. Reaction of Dimethyldichlorosilane, Phenylmethyldichlorosilane, or Diphenyldichlorosilane with Dimethyl Sulfoxide. Evidence for Silanone and Cyclodisiloxane Intermediates. *Organometallics* **1996**, *15*, 4649-4652.
3. Kojima, K.; Gore, C. R.; Marvel, C. S. Preparation of Polysiloxanes Having Terminal Carboxyl or Hydroxyl Groups. *J. Polym. Sci., Part A-1: Polym. Chem.* **1966**, *4*, 2325-2327.
4. Pouget, E.; Tonnar, J.; Lucas, P.; Lacroix-Desmazes, P.; Ganachaud, F.; Boutevin, B. Well-Architected Poly(dimethylsiloxane)-Containing Copolymers Obtained by Radical Chemistry. *Chem. Rev.* **2010**, *110*, 1233-1277.
5. Bischoff, R.; Cray, S. E. Polysiloxanes in Macromolecular Architecture. *Prog. Polym. Sci.* **1999**, *24*, 185-219.
6. Viallat, A.; Cohen-Addad, J. P.; Pouchelon, A. Mechanically Induced Sorption of Siloxane on Silica: Experimental and Theoretical Investigations of Chain Binding, Collective Behaviour and Multiple-Aggregate Processes. *Polymer* **1986**, *27*, 843-848.
7. Paul, D. R.; Mark, J. E. Fillers for Polysiloxane ("Silicone") Elastomers. *Prog. Polym. Sci.* **2010**, *35*, 893-901.
8. Colas, A.; Curtis, J. In *Biomaterials Science: An Introduction to Materials in Medicine*; Ratner, B. D., Hoffman, A. S., Schoen, F. J., Lemons, J. E., Eds.; Elsevier Academic Press: California, 2004; Chapter 2.3 Silicone Biomaterials: History and Chemistry, pp 80-86.
9. Murphy, C. M.; Saunders, C. E.; Smith, D. C. Thermal and Oxidation Stability of Polymethylphenylsiloxanes. *Ind. Eng. Chem.* **1950**, *42*, 2462-2468
10. Hanu, L. G.; Simon, G. P.; Cheng, Y. -B. Thermal Stability and Flammability of Silicone Polymer Composites. *Polym. Degrad. Stab.* **2006**, *91*, 1373-1379
11. Hamdani, S.; Longuet, C.; Perrin, D.; Lopez-Cuesta, J. M.; Ganachaud, F. Flame Retardancy of Silicone-Based Materials. *Polym. Degrad. Stab.* **2009**, *94*, 465-495.
12. Abbasi, F.; Mirzadeh, H.; Katbab, A. A. Modification of Polysiloxane Polymers for Biomedical Applications: A Review. *Polym. Int.* **2001**, *50*, 1279-1287.

13. Lucas, P.; Robin, J. J. In *Advances in Polymer Science: Functional Materials and Biomaterials*; Springer-Verlag: Berlin Heidelberg, 2007; Vol. 209, Chapter Silicone-Based Polymer Blends: An Overview of the Materials and Processes, pp 111-147.
14. Ma, M.; Hill, R.; Superhydrophobic Surfaces. *Curr. Opin. Colloid Interface Sci.* **2006**, *11*, 193-202.
15. Yilgor, E.; Yilgor, I. Silicone Containing Copolymers: Synthesis, Properties and Applications. *Prog. Polym. Sci.* **2014**, *39*, 1165-1195.
16. Gong, D.; Long, J.; Jiang, D.; Fan, P.; Zhang, H.; Li, L.; Zhong, M. Robust and Stable Transparent Superhydrophobic Polydimethylsiloxane Films by Duplicating via a Femtosecond Laser-Ablated Template. *ACS Appl. Mater. Interfaces* **2016**, *8*, 17511-17518.
17. Zhang, C.; Babonneau, F.; Bonhomme, C.; Laine, R.M.; Soles, C.L.; Hristov, H.A.; Yee, A.F. Highly Porous Polyhedral Silsesquioxane Polymers. Synthesis and Characterization. *J. Am. Chem. Soc.* **1998**, *120*, 8380-8391.
18. Sellinger, A.; Laine, R.M. Silsesquioxanes as Synthetic Platforms. 3. Photocurable, Liquid Epoxides as Inorganic/Organic Hybrid Precursors. *Chem. Mater.* **1996**, *8*, 1592-1593.
19. Choi, J.; Kim, S.G.; Laine, R.M. Organic/Inorganic Hybrid Epoxy Nanocomposites from Aminophenylsilsesquioxanes. *Macromol.* **2004**, *37*, 99-109.
20. Choi, J.; Yee, A.F.; Laine, R.M. Organic/Inorganic Hybrid Composites form Cubic Silsesquioxanes. Epoxy Resins of Octa(dimethylsiloxethylcyclohexyl-epoxide) silsesquioxane. *Macromol.* **2003**, *36*, 5666-5682.
21. Takamura, N.; Viculis, L.; Zhang, C.; Laine, R.M. Completely Discontinuous Organic/Inorganic Hybrid Nanocomposites by Self-Curing of Nanobuilding Blocks Constructed from Reactions of [HMe₂SiOSiO_{1.5}]₈ with Vinylcyclohexene. *Polym. Int.* **2007**, *56*, 1378-1391.
22. Asuncion, M.Z.; Laine, R.M. Silsesquioxane Barrier Materials. *Macromol.* **2007**, *40*, 555-562.
23. Feher, F.J.; Blanski, R.L. Olefin Polymerization by Vanadium-Containing Silsesquioxanes: Synthesis of a Dialkyl-oxo-vanadium (V) Complex that Initiates Ethylene Polymerization. *J. Am. Chem. Soc.* **1992**, *114*, 5886-5887.
24. Feher, F.J.; Budzichowski, T.A. Silsesquioxanes as Ligands in Inorganic and Organometallic Chemistry. *Polyhedron* **1995**, *14*, 3239-3253.

25. Ropartz, L.; Morris, R.E.; Schwarz, G.P.; Foster, D.F.; Cole-Hamilton, D.J. Dendrimer- Bound Tertiary Phosphines for Alkene Hydroformylation. *Inorg. Chem. Commun.* **2000**, *3*, 714-717.
26. Riollet, V.; Quadrelli, E.A.; Copéret, C.; Basset, J.-M.; Andersen, R.A.; Köhler, K.; Böttcher, R.-M.; Herdtweck, E. Grafting of [Mn(CH₂tBu)₂(tmeda)] on Silica and Comparison with Its Reaction with a Silsesquioxane. *Chem.-Eur. J.* **2005**, *11*, 7358-7365.
27. Feher, F.J.; Newman, D.A.; Walzer, J.F. Silsesquioxanes as Models for Silica Surfaces. *J. Am. Chem. Soc.* **1989**, *111*, 1741-1748.
28. Feher, F.J.; Budzichowski, T.A.; Blanski, R.L.; Weller, K.J.; Ziller, J.W. Facile Syntheses of New Incompletely Condensed Polyhedral Oligosilsesquioxanes: [(*c*-C₅H₉)₇Si₇O₉(OH)₃], [(*c*-C₇H₁₃)₇Si₇O₉(OH)₃], and [(*c*-C₇H₁₃)₆Si₆O₇(OH)₄]. *Organomet.* **1991**, *10*, 2526-2528.
29. Contreras-Torres, F.F.; Basiuk, V.A. "Imidazo[1,2-*a*]pyrazine-3,6-diones Derived from α -Amino Acids: A Theoretical Mechanistic Study of Their Formation via Pyrolysis and Silica-Catalyzed Process." *J. Phys. Chem. A* **2006**, *110*, 7431-7440.
30. Maschmeyer, T.; Klunduk, M.C.; Martin, C.M.; Shephard, D.S.; Thomas, J.M.; Johnson, B.F.G. "Modeling the Active Sites of Heterogeneous Titanium-Centred Epoxidation Catalysts with Soluble Silsesquioxane Analogues." *Chem. Comm.* **1997**, 1847-1848.
31. Duchateau, R.; Abbenhuis, H.C.L.; van Santen, R.A.; Meetsma, A.; Thiele, S.K.- H.; van Tol, M.F.H. Half-Sandwich Titanium Complexes Stabilized by a Novel Silsesquioxane Ligand: Soluble Model Systems for Silica-Grafted Olefin Polymerization Catalysts. *Organomet.* **1998**, *17*, 5222-5224.
32. Solans-Monfort, X.; Filhol, J. -S.; Copéret, C.; Eisenstein, O. Structure, Spectroscopic and Electronic Properties of a Well Defined Silica Supported Olefin Metathesis Catalyst, [(₂SiO)Re(₂CR)(=CHR)(CH₂R)], through DFT Periodic Calculations: Silica is Just a Large Siloxy Ligand. *New J. Chem.* **2006**, *30*, 842-850.
33. Leu, C. M.; Reddy, M.; Wei, K. -H.; Shu, C.-F. Synthesis and Dielectric Properties of Polyimide-Chain-End Tethered Polyhedral Oligomeric Silsesquioxane Nanocomposites. *Chem. Mater.* **2003**, *15*, 2261-2265.
34. Leu, C.-M.; Chang, Y. -T.; Wei, K. -H. Synthesis and Dielectric Properties of Polyimide-Tethered Polyhedral Oligomeric Silsesquioxane (POSS) Nanocomposites via POSS-Diamine. *Macromol.* **2003**, *36*, 9122-9127.
35. Liu, Y. -L.; Lee, H. -C. Preparation and Properties of Polyhedral Oligosilsesquioxane Tethered Aromatic Polyamide Nanocomposites through Michael Addition between

- Maleimide-Containing Polyamides and an Amino-Functionalized Polyhedral Oligosilsesquioxane. *J. Polym. Sci., Part A: Polym. Chem.*, **2006**, *44*, 4632-4643.
36. Chojnowski, J.; Fortuniak, W.; Rosciszewski, P.; Werel, W.; Lukasiak, J.; Kamysz, W.; Halasa, R. Polysilsesquioxanes and Oligosilsesquioxanes Substituted by Alkylammonium Salts as Antibacterial Biocides. *J. Inorg. Organomet. Polym. Mater.* **2006**, *16*, 219-230.
37. Majumdar, P.; Lee, E.; Gubbins, N.; Stafslie, S.J.; Daniels, J.; Thorson, C.J.; Chisolm, B.J. Synthesis and Antimicrobial Activity of Quaternary Ammonium- Functionalized POSS (Q-POSS) and Polysiloxane Coatings Containing Q-POSS. *Polymer* **2009**, *50*, 1124-1133.
38. Gromilov, S.A.; Basova, T.V.; Emel'yanov, D.Y.; Kuzmin, A.V.; Prokhorova, S.A. Layer Arrangement in the Structure of Octakis-(trimethylsiloxy)octasilsesquioxane and Dodecakis-(trimethylsiloxy)octasilsesquioxane. *J. Struct. Chem. (Engl. Trans.)* **2004**, *45*, 471-475.
39. Gromilov, S.A.; Emel'yanov, D.Y.; Kuzmin, A.V.; Prokhorova, S.A. Structural Organization of Layers in Octakis-(trimethylsiloxy)octasilsesquioxane. *J. Struct. Chem. (Engl. Trans.)* **2003**, *44*, 704-706
40. Tanaka, K.; Adachi, S.; Chujo, Y. Structure-Property Relationship of Octa-Substituted POSS in Thermal and Mechanical Reinforcements of Conventional Polymers. *J. Polym. Sci. A Polym. Chem.* **2009**, *47*, 5690-5697.
41. Wang, F.; Lu, X.; He, C. Some Recent Developments of Polyhedral Oligomeric Silsesquioxane (POSS)-Based Polymeric Materials. *J. Mater. Chem.* **2011**, *21*, 2775-2782.
42. Baumann, T.; Jones, T.; Wilson, T.; Saab, A.; Maxwell, R. Synthesis and Characterization of Novel PDMS Nanocomposites Using POSS Derivatives as Cross-Linking Filler. *J. Polym. Sci. A Polym. Chem.* **2009**, *47*, 2589-2596.
43. Chen, D.; Liu, Y.; Zhang, H.; Zhou, Y.; Huang, C.; Xiong, C. Influence of Polyhedral Oligomeric Silsesquioxanes (POSS) on Thermal and Mechanical Properties of Polydimethylsiloxane (PDMS) Composites Filled with Fumed Silica. *J. Inorg. Organomet. Polym.* **2013**, *23*, 1375-1382.
44. Bai, H.; Huang, C.; Jun, L.; Li, H. Modification of Liquid Silicone Rubber by Octavinyl-Polyhedral Oligosilsesquioxanes. *J. Appl. Polym. Sci.* **2016**, *133*, 43906.
45. Florea, N.; Lungu, A.; Badica, P.; Craciun, L.; Enculescu, M.; Ghita, D.; Ionescu, C.; Zgiran, R.; Iovu, H. Novel Nanocomposites Based on Epoxy Resin/Epoxy-Functionalized Polydimethylsiloxane Reinforced with POSS. *Composites Part B* **2015**, *75*, 226-234.

46. Voronkov, M.; Lavrentyev, V. Polyhedral Oligosilsesquioxanes and Their Homo Derivatives. *Top. Curr. Chem.* **1982**, *102*, 199–236.
47. Baney, R.; Itoh, M.; Sakakibara, A.; Suzuki, T. Silsesquioxanes. *Chem. Rev.* **1995**, *95*, 1409–1430.
48. Loy, D.; Shea, K. Bridged Polysilsesquioxanes - Highly Porous Hybrid Organic-Inorganic Materials. *Chem. Rev.* **1995**, *95*, 1431–1442.
49. Calzaferri, G. In *Tailor-Made Silicon-Oxygen Compounds, From Molecules to Materials*; Corriu, R., Jutzi, P., Eds.; Friedr. Vieweg & Sohn GmbH, Braunschweig/Weisbaden, Germany, 1996; Chapter *Silsesquioxanes*, pp 149-169.
50. Lichtenhan, J. In *Polymeric Materials Encyclopedia*; Salmone, J. C., Ed.; CRC Press, NY, 1996, vol. 10, Chapter *Silsesquioxane-Based Polymers*, pp. 7768–7777.
51. Pescarmona, P.; Maschmeyer, T. Oligomeric Silsesquioxanes: Synthesis, Characterization, and Selected Applications. *Aust. J. Chem.* **2001**, *54*, 583–596.
52. Li, G.; Wang, L.; Ni, H.; Pittman Jr., C. Polyhedral Oligomeric Silsesquioxane (POSS) Polymers and Copolymers: A Review. *J. Inorg. Organomet. Polym.* **2001**, *11*, 123–154.
53. Duchateau, R. Incompletely Condensed Silsesquioxanes: Versatile Tools in Developing Silica-Supported Olefin Polymerization Catalysts. *Chem. Rev.* **2002**, *102*, 3525–3542.
54. Abe, Y.; Gunji, T. Oligo- and Polysiloxanes. *Prog. Polym. Sci.* **2004**, *29*, 149–182.
55. Phillips, S.; Haddad, T.; Tomczak, S. Developments in Nanoscience: Polyhedral Oligomeric Silsesquioxane (POSS)-Polymers. *Curr. Opin. Solid State Mater. Sci.* **2004**, *8*, 21–29.
56. Kannan, R.; Salacinski, H.; Butler, P.; Seifalian, A. *Acc. Chem. Res.* **2005**, *38*, 879–884.
57. Laine, R. M. Nanobuilding Blocks Based on the $[\text{OSiO}_{1.5}]_x$ ($x = 6, 8, 10$) Octasilsesquioxanes. *J. Mater. Chem.* **2005**, *15*, 3725–3744.
58. Provas, A.; Matison, J. Silsesquioxanes: Synthesis and Applications. *Trends Polym. Sci.*, **1997**, *5*, 327–333.
59. Lickiss, P.; Rataboul, F. *Adv. Organomet. Chem.* Fully Condensed Polyhedral Oligosilsesquioxanes (POSS): From Synthesis to Application. **2008**, *57*, 1–116.

60. Chan, K.; Sonar, P.; Sellinger, A. Cubic Silsesquioxanes for Use in Solution Processable Organic Light Emitting Diodes (OLED). *J. Mater. Chem.* **2009**, *19*, 9103–9120.
61. Laine, R. M.; Roll, M. Polyhedral Phenylsilsesquioxanes. *Macromolecules* **2011**, *44*, 1073–1109.
62. Wu, J.; Mather, P. POSS Polymers: Physical Properties and Biomaterials Applications. *Polym. Rev.* **2009**, *49*, 25–63.
63. Cordes, D.; Lickiss, P.; Rataboul, F. Recent Developments in the Chemistry of Cubic Polyhedral Oligosilsesquioxanes. *Chem. Rev.* **2010**, *110*, 2081–2173.
64. Kuo, S. W.; Chang, F.C. POSS Related Polymer Nanocomposites. *Prog. Polym. Sci.* **2011**, *36*, 1649-1696.
65. Ronchi, M.; Sulaiman, S.; Boston, N.; Laine, R. M. Fluoride Catalyzed Rearrangements of Polysilsesquioxanes, Mixed Me, Vinyl T₈, Me, Vinyl T₁₀ and T₁₂ Cages. *Appl. Organometal. Chem.* **2010**, *24*, 551-557.
66. Furgal, J.; Jung, J. H.; Goodson III, T.; Laine, R. M. Analyzing Structure-Photophysical Property Relationships for Isolated T₈, T₁₀, and T₁₂ Stilbenevinylsilsesquioxanes. *J. Am. Chem. Soc.* **2013**, *135*, 12259-12269.
67. Asuncion, M. Z.; Laine, R. M. Fluoride Rearrangement Reactions of Polyphenyl- and Polyvinylsilsesquioxanes as a Facile Route to Mixed Functional Phenyl, Vinyl T₁₀ and T₁₂ Silsesquioxanes. *J. Am. Chem. Soc.* **2010**, *132*, 3723-3736.
68. Jung, J. H.; Laine, R. M. Beads on a Chain (BOC) Polymers Formed from the Reaction of [NH₂PhSiO_{1.5}]_x[PhSiO_{1.5}]_{10-x} and [NH₂PhSiO_{1.5}]_x[PhSiO_{1.5}]_{12-x} Mixtures (x=2-4) with the Diglycidyl Ether of Bisphenol A. *Macromolecules* **2011**, *44*, 7263-7272.
69. Jung, J. H.; Furgal, J.; Goodson III, T.; Mizumo, T.; Schwartz, M.; Chou, K.; Vonnet, J. F.; Laine, R. M. 3-D Molecular Mixtures of Catalytically Functionalized [vinylSiO_{1.5}]₁₀/[vinylSiO_{1.5}]₁₂. Photophysical Characterization of Second Generation Derivatives. *Chem. Mater.* **2012**, *24*, 1883-1895.
70. Furgal, J.; Goodson III, T.; Laine, R. M. D_{5h} [PhSiO_{1.5}]₁₀ Synthesis via F⁻ Catalyzed Rearrangement of [PhSiO_{1.5}]_n. An Experimental/Computational Analysis of Likely Reaction Pathways. *Dalton Trans.* **2016**, *45*, 1025-1039
71. Geyer, R.; Jambeck, J. R.; Law, K. L. Production, Use, and Fate of All Plastics Ever Made. *Sci. Advances* **2017**, *3*, 1-5.

72. Ma, S.; Webster, D. C. Degradable Thermosets Based on Labile Bonds or Linkages: A Review. *Prog. Polym. Sci.* **2018**, *76*, 65-110.
73. Hopewell, J.; Dvorak, R.; Kosior, E. Plastics Recycling: Challenges and Opportunities. *Phil. Trans. R. Soc. B* **2009**, *364*, 2115-2126.
74. Cimpan, C.; Maul, A.; Jansen, M.; Pretz, T.; Wenzel, H. Central Sorting and Recovery of MSW Recyclable Materials: A Review of Technological State-of-the-Art, Cases, Practice and Implications for Materials Recycling. *J. Environ Manage.* **2015**, *156*, 181-199.

Chapter 2

Experimental Techniques

2.1 Materials

Phenyltriethoxysilane, octamethylcyclotetrasiloxane (D₄), (tridecafluoro-1,1,2,2-tetrahydrooctyl)triethoxysilane (PFS), methacryloxypropyltrimethoxysilane (MAS), vinyltrimethoxysilane, and fumed silica (12-20 nm) were purchased from Gelest, Inc. Acetone and tetrahydrofuran (THF) were purchased from VWR. Tetrabutylammonium fluoride (TBAF, 1.0 M in THF) and azobisisobutyronitrile (AIBN) were purchased from Sigma-Aldrich. SILRES REN 50 and ELASTOSIL E10 silicones were provided free from Wacker Chemie. All chemicals were used as received without further purification. Dodecaphenylsilsesquioxane (DDPS) was synthesized using previously reported methods.¹⁻¹¹ All reactions were conducted at room temperature in the presence of air.

2.2 Analytical Techniques

Thermal Gravimetric Analyses (TGA)

Thermal stability evaluated via a Q600 SDT simultaneous differential scanning calorimetry / TGA instrument (TA Instruments Inc., New Castle, DE). Thin monoliths were cast from solution. Samples (5-10 mg) were cut from the monoliths, loaded into alumina pans and ramped at 10°C/min to 1000°C in either a N₂ or air flow of 100 ml/min.

Differential Scanning Calorimetry (DSC)

Calorimetry studies were performed using a Q20 DSC instrument (TA Instruments Inc., New Castle, DE) with a N₂ flow rate of 50 ml/min. Samples (5-10 mg) were placed in a

crimped Tzero pan. Samples were heat at 20 °C/min and cooled at 10 °C/min to various desired temperatures.

Dynamic Mechanical Analyses (DMA)

All DMA experiments were performed using a Q800 DMA instrument (TA Instruments Inc., New Castle, DE) equipped with a single cantilever stage and in the presence of air. DMA sample bars were cut from cast monoliths to approximately 7 x 35 x 2 mm. Cured samples were polished on a wet polishing wheel with increasing grit 400 - 1600. Samples were ramped at 3 °C/min to various desired temperatures.

Thermomechanical Analyses (TMA)

All TMA experiments were performed using a Q400 TMA instrument (TA Instruments Inc., New Castle, DE) equipped with an expansion probe and under a N₂ flow rate of 50 ml/min. Cured samples were cut to approximately 2 x 5 x 5 mm. Heating and cooling ramp rates were 5 °C/min.

Scanning Electron Microscopy (SEM)

SEM was performed with a Hitachi S-3400N scanning electron microscope in variable pressure mode (15-50 Pa) with the backscatter electron detector set in composition mode and with an accelerating voltage of 5-10 kV.

Energy Dispersive X-ray Spectroscopy (EDS)

EDS was performed with a Bruker Nano X-Flash detector (410-M) equipped on the SEM with an accelerating voltage of 10-15 kV.

Gas Chromatography - Mass Spectrometry (GC-MS)

GC-MS analyses were done on a Thermo Scientific TRACE 1310 system equipped with a Thermo Scientific TG-5MS column (60 m length, 0.25 mm I.D., 0.25 µm film thickness, 5% diphenyl-/95% dimethylpolysiloxane stationary phase) and an ISQ LT single quadrupole mass spectrometer (electron impact ionization). Thermal desorption was

performed using a CDS Analytical Pyroprobe 5000 with a Tenax TA trap by heating ≈ 15 mg samples at $10^\circ\text{C}/\text{min}$ to 50°C above cure temperature and holding for 15 min.

Water Contact Angle Measurement

Droplets ($10\ \mu\text{L}$) of distilled water pipetted onto a coated surface were photographed edge-on and measured with the aid of PowerPoint. WCA measurements were repeated on three different areas of each coating and reported as an average with the standard deviation.

Wear Resistance

A 25×75 mm strip of the coating was abraded by rubbing a 100 g weighted ($2\ \text{kPa}$) piece of 2000 grit silicon carbide sandpaper back and forth at a rate of approximately $50\ \text{mm}/\text{s}$ (Figure 2.1). A combined back and forth motion was considered one wear cycle and WCAs were measured after 50, 100, 150, and 200 cycles. Wear tests were repeated on three different areas of each coating and an average WCA was reported with the standard deviation. This type of weighted sandpaper abrasion test has been used to test wear resistance on polymeric coatings and Milionis et al. recently reported in a review that a linear abrasion test method had the most potential as a universal standard for testing the durability of superhydrophobic coatings.¹²⁻¹⁴

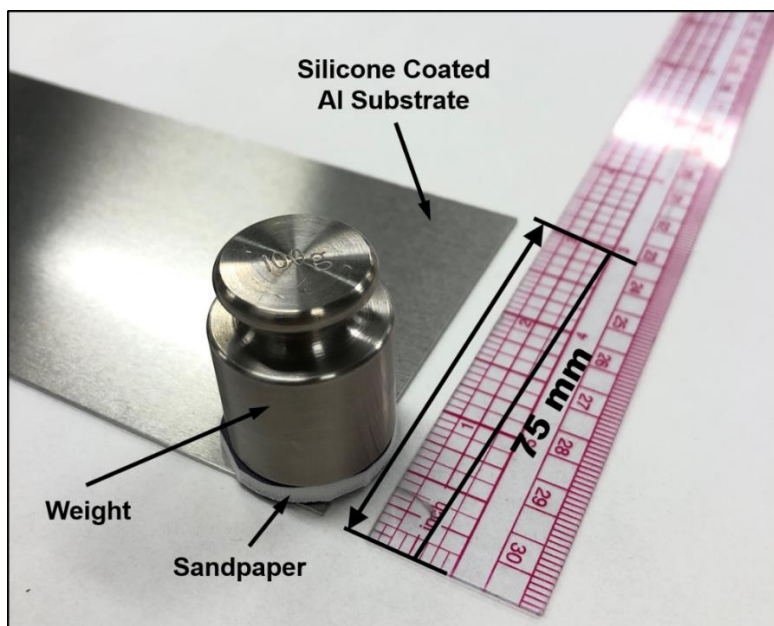


Figure 2.1 Linear wear test set up with 2000 grit sandpaper and 100g weight (2kPa)

Coating Adhesion

Standard tape adhesion tests were performed on coated substrates using an Elcometer 107 cross-hatch cutter to score a cross-hatch pattern into and through the coating thus exposing the substrate in the cuts. ASTM adhesive tape was then pressed onto the cross-hatch and peeled according to ASTM D3359 and evaluated on a 0B-5B scale from poor to excellent adhesion.

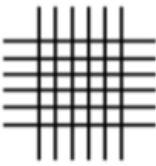
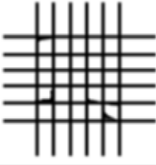
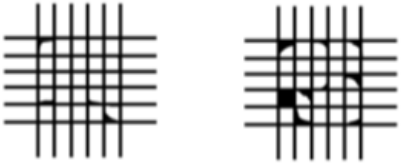
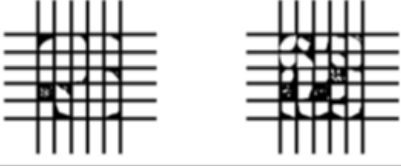
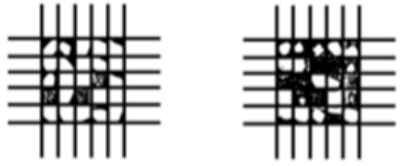
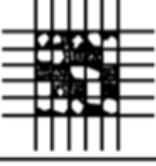
CLASSIFICATION OF ADHESION TEST RESULTS		
CLASSIFICATION	PERCENT AREA REMOVED	SURFACE OF CROSS-CUT AREA FROM WHICH FLAKING HAS OCCURRED FOR SIX PARALLEL CUTS AND ADHESION RANGE BY PERCENT
5B	0% None	
4B	Less than 5%	
3B	5 – 15%	
2B	15 – 35%	
1B	35 – 65%	
0B	Greater than 65%	

Figure 2.2 Coating tape adhesion test scale according to ASTM D3359¹⁵

Fourier-Transform Infrared Spectroscopy (FTIR)

FTIR spectra in the range 4000 - 400 cm^{-1} were recorded with a Bruker Alpha Platinum Attenuated Total Reflection Infrared (ATR-IR) spectrometer. Samples were either thin films or cast monoliths with smooth surfaces for adequate contact.

2.3 Synthetic Methods

2.3.1 Synthesis of Dodecaphenylsilsesquioxane (DDPS)

Dodecaphenylsilsesquioxane (DDPS) was synthesized using previously described methods.¹⁻¹¹ To a dry single neck 1000 ml round bottom flask equipped with magnetic stirring was added 100 g phenyltriethoxysilane, 400 ml THF, 44 ml distilled water, and 20 ml TBAF (1.0M in THF). After 48 h a white precipitate started to form. The reaction was allowed to stir at RT in air for 4 weeks. The precipitate was filtered and washed with THF. The white powder was dried at 75°C for 18 h. The yield was 52.80 g (98%).

2.3.2 Synthesis of Silicone Resins

Fluoride Ion Catalyzed Rearrangement of DDPS and D₄ (1 Ph : 1 Me)

DDPS (2.50 g, 1.613 mmol), D₄ (0.718 g, 2.420 mmol), and TBAF 0.01 M in THF (28.96 g) were added to a dry single neck 250 ml round bottom flask equipped with magnetic stirring and stirred at RT for 7 d. Coating concentration was 10 wt % and the ratio of functional groups was 1 Ph : 1 Me.

Fluoride Ion Catalyzed Rearrangement of DDPS and D₄ (1 Ph : 4 Me)

DDPS (2.5 g, 1.613 mmol), D₄ (2.87 g, 9.676 mmol), and TBAF 0.01 M in THF (48.33 g) were added to a dry single neck 250 ml round bottom flask equipped with magnetic stirring and stirred at RT for 7 d. Coating concentration was 10 wt % and the ratio of functional groups was 1 Ph : 4 Me.

Fluoride Ion Catalyzed Rearrangement of DDPS and D₄ (2 Ph : 1 Me)

DDPS (10.0 g, 6.452 mmol), D₄ (1.435 g, 4.841 mmol), and TBAF 0.04 M in THF (102.92 g) were added to a dry single neck 250 ml round bottom flask equipped with magnetic stirring and stirred at RT for 7 d. Coating concentration was 10 wt % and the ratio of functional groups was 2 Ph : 1 Me.

Fluoride Ion Catalyzed Rearrangement of DDPS, D₄, and PFS (1 Ph : 1 Me : 1 PFS)

DDPS (2.50 g, 1.613 mmol), D₄ (0.718 g, 2.420 mmol), PFS (9.879 g, 19.356 mmol), and TBAF 0.01 M in THF (117.87 g) were added to a dry single neck 250 ml round bottom flask equipped with magnetic stirring and stirred at RT for 7 d. Coating concentration was 10 wt % and the ratio of functional groups was 1 Ph : 1 Me : 1 PFS.

Fluoride Ion Catalyzed Rearrangement of DDPS, D₄, PFS, and MAS (1 Ph : 1 Me : 1 PFS : 1 MAS)

DDPS (2.50 g, 1.613 mmol), D₄ (0.718 g, 2.420 mmol), PFS (9.879 g, 19.356 mmol), MAS (4.807 g, 19.356 mmol), AIBN (159 mg, 0.968 mmol), and TBAF 0.01 M in THF (162.57 g) were added to a dry single neck 250 ml round bottom flask equipped with magnetic stirring and stirred at RT for 7 d. Coating concentration was 10 wt % and the ratio of functional groups was 1 Ph : 1 Me : 1 PFS : 1 MAS.

Fluoride Ion Catalyzed Rearrangement of DDPS, D₄, PFS, and MAS + 3 wt % silica nanoparticles

DDPS (2.50 g, 1.613 mmol), D₄ (0.718 g, 2.420 mmol), PFS (9.879 g, 19.356 mmol), MAS (4.807 g, 19.356 mmol), AIBN (159 mg, 0.968 mmol), SiO₂ (0.542 g, 9.021 mmol), and TBAF 0.01 M in THF (167.45 g) were added to a dry single neck 250 ml round bottom flask equipped with magnetic stirring and stirred at RT for 7 d. Coating concentration was 10 wt % and the ratio of functional groups was 1 Ph : 1 Me : 1 PFS : 1 MAS. Coating solution was sonicated in a sealed vial using a Branson ultrasonic bath (40kHz) for 30 min prior to application.

2.3.3 Recycling of Silicone Resins

Silicone resin monoliths were cast from 10 wt % solutions in open aluminum or Teflon dishes (i.d. = 75 mm). The solvent was allowed to evaporate in a fume hood overnight followed by heating to 50°C for 4 h, 100°C for 4 h, and the final temperature (up to 250°C) for 18 h. Cured resin pieces (2.0 g) were added to a dry single neck 250 ml round bottom flask equipped with magnetic stirring. TBAF/THF (18.0 g) solution at molar concentrations of either 0.1 M, 0.01 M, or 0.002 M was added to the flask and stirred until all solids dissolved. Recycled resins were spray coated or cast into monoliths and cured in the same manner as virgin resin as described below.

2.3.4 *In situ* Modification During Recycling of Silicone Resins

Monoliths of virgin silicone resin cured at 250°C were first recycled as described in section 2.3.3. Once all of the resin dissolved then DDPS, D₄, or PFS was added to the stirring solution to modify the ratio of functional groups as described below.

Fluoride Ion Catalyzed Recycling of 1 Ph : 1 Me Silicone Resin and Modification to 2 Ph : 1 Me Silicone Resin

To a dry single neck 250 ml round bottom flask equipped with magnetic stirring was added 1 Ph : 1 Me silicone resin (2.0 g, cured at 250°C) and TBAF 0.04 M in THF (18.0 g). The solid resin pieces were stirred for 7 days at ambient and were completely dissolved. DDPS (1.554 g, 1.002 mmol) was added along with additional TBAF 0.04 M in THF (13.99 g) to maintain a 10 wt % concentration of resin. All solids were dissolved after an additional 7 days stirring at RT in the presence of air.

Fluoride Ion Catalyzed Recycling of 1 Ph : 1 Me Silicone Resin and Modification to 1 Ph : 4 Me Silicone Resin

To a dry single neck 250 ml round bottom flask equipped with magnetic stirring was added 1 Ph : 1 Me silicone resin (2.0 g, cured at 250°C) and TBAF 0.01 M in THF (18.0

g). The solid resin pieces were stirred for 7 days at ambient and were completely dissolved. D₄ (1.338 g, 4.511 mmol) was added along with additional TBAF 0.01 M in THF (12.04 g) to maintain a 10 wt % concentration of resin. All solids were dissolved after an additional 7 days stirring at RT in the presence of air.

Fluoride Ion Catalyzed Recycling of 1 Ph : 1 Me Silicone Resin and Modification to 1 Ph : 4 Me : 1 PFS Silicone Resin

To a dry single neck 250 ml round bottom flask equipped with magnetic stirring was added 1 Ph : 1 Me silicone resin (2.0 g, cured at 250°C) and TBAF 0.01 M in THF (18.0 g). The solid resin pieces were stirred for 7 days at ambient and were completely dissolved. D₄ (1.338 g, 4.511 mmol) and PFS (4.604 g, 9.021 mmol) was added along with additional TBAF 0.01 M in THF (53.48 g) to maintain a 10 wt % concentration of resin. All solids were dissolved after an additional 7 days stirring at RT in the presence of air.

Fluoride Ion Catalyzed Recycling of SILRES Silicone Resin and Modification with 10 wt % DDPS

To a dry single neck 250 ml round bottom flask equipped with magnetic stirring was added SILRES silicone resin (2.0 g, cured at 250°C) and TBAF 0.01 M in THF (18.0 g). The solid resin pieces were stirred for 7 days at ambient and were completely dissolved. DDPS (0.20 g, 0.129 mmol) was added along with additional TBAF 0.01 M in THF (1.8 g) to maintain a 10 wt % concentration of resin. All solids were dissolved after an additional 7 days stirring at RT in the presence of air.

2.4 Coating Application

Coating solutions, 10 wt % resin in THF, were used throughout this work along with standard spraying conditions to maintain consistent coating thicknesses. Aluminum alloy 2024 coupons (0.81 x 76.2 x 152.4 mm) were cleaned with an aqueous alumina slurry to remove the oxidation layer, rinsed with distilled water, rinsed with acetone, and dried with an air flow. Clean and dry coupons were spray coated using a DeVilbiss gravity HVLP

spray gun with 10-15 psi of air flow. Coated samples were allowed to dry at ambient for 5 minutes before curing up to 250°C for 18 h. Coated samples were allowed to rest at ambient for at least 24 h before testing.

2.5 Monolith Casting

Thin (< 1 mm) monoliths of resin for TGA, DSC, FTIR, GC-MS, and EDS were cast from 10 wt % solutions in open aluminum or Teflon dishes (i.d. = 48 mm). The solvent was allowed to evaporate in a fume hood overnight followed by heating to 50°C for 4 h, 100°C for 4 h, and the final temperature (150°C, 200°C, or 250°C) for 18 h. Thicker (2-3 mm) monoliths for DMA and TMA studies were cast in larger (i.d. = 73 mm) Teflon dishes and required longer drying times at lower temperatures with slower ramps up to 100°C before heating to final a cure temperature of 250°C. Sample surfaces were polished smooth using a wet polishing wheel by increasing the grit from 400 to 1600.

2.6 References

1. Bassindale, A.R.; Pourny, M.; Taylor, P.G.; Hursthouse, M.B.; Light, M.E. Fluoride-Ion Encapsulation within a Silsesquioxane Cage. *Angew. Chem. Int. Ed.* **2003**, *42*, 3488-3490.
2. Bassindale, A.R.; Chen, H.; Liu, Z.; MacKinnon, I.A.; Parker, D.J.; Taylor, P.G.; Yang, Y.; Light, M.E. A Higher Yielding Route to Octasilsesquioxane Cages using Tetrabutylammonium Fluoride, Part 2: Further Synthetic Advances, Mechanistic Investigations and X-ray Crystal Structure Studies into the Factors that Determine Cage Geometry in the Solid State. *J. Organomet. Chem.* **2004**, *689*, 3287-3300.
3. Bassindale, A.R.; Parker, D.J.; Pourny, M.; Taylor, P.G.; Horton, P.N.; Hursthouse, M.B. Fluoride Ion Entrapment in Octasilsesquioxane Cages as Models for Ion Entrapment in Zeolites. Further Examples, X-ray Crystal Structure Studies, and Investigations into How and Why They May Be Formed. *Organomet.* **2004**, *23*, 4400-4405.
4. Anderson, S.E.; Bodzin, D.J.; Haddad, T.S.; Boatz, J.A.; Mabry, J.M.; Mitchell, C.; Bowers, M.T. Structural Investigation of Encapsulated Fluoride in Polyhedral Oligomeric Silsesquioxane Cages Using Ion Mobility Mass Spectrometry and Molecular Mechanics. *Chem. Mater.* **2008**, *20*, 4299-4309.
5. Asuncion, M.Z.; Laine, R.M. Fluoride Rearrangement Reactions of Polyphenyl- and Polyvinylsilsesquioxanes as a Facile Route to Mixed Functional Phenyl, Vinyl T₁₀ and T₁₂ Silsesquioxanes. *J. Am. Chem. Soc.* **2010**, *132*, 3723-3736.
6. Ronchi, M.; Sulaiman, S.; Boston, N.R.; Laine, R.M. Fluoride Catalyzed Rearrangements of Polysilsesquioxanes, Mixed Me, Vinyl T₈, Me, Vinyl T₁₀ and T₁₂ Cages. *Appl. Organometal. Chem.* **2010**, *24*, 551-557.
7. Jung, J.-H.; Laine, R.M. Beads on a Chain (BOC) Polymers Formed from the Reaction of [NH₂PhSiO_{1.5}]_x[PhSiO_{1.5}]_{10-x} and [NH₂PhSiO_{1.5}]_x[PhSiO_{1.5}]_{12-x} Mixtures (x=2-4) with the Diglycidyl Ether of Bisphenol A. *Macromolecules* **2011**, *44*, 7263-7272.
8. Jung, J.-H.; Furgal, J.C.; Goodson III, T.; Mizumo, T.; Schwartz, M.C.; Chou, K.; Vonnet, J.F.; Laine, R.M. 3-D Molecular Mixtures of Catalytically Functionalized [vinylSiO_{1.5}]₁₀/[vinylSiO_{1.5}]₁₂. Photophysical Characterization of Second Generation Derivatives. *Chem. Mater.* **2012**, *24*, 1883-1895.
9. Jung, J.-H.; Furgal, J.C.; Clark, S.C.; Schwartz, M.C.; Chou, K.; Laine, R. M. Copolymerization of [*p*-IPhSiO_{1.5}]₈, I8OPS] with Divinyl (DVB)- and Diethynylbenzene (DEB) gives Beads on a Chain (BoC) Polymers with Functionalized Beads. The DEB Systems Exhibit through Chain, Extended 3-D Conjugation in the Excited State. *Macromolecules*, **2013**, *46*, 7580-7590.

10. Furgal, J.C.; Jung, J.-H.; Goodson III, T.; Laine, R.M. Analyzing Structure-Photophysical Property Relationships for Isolated T₈, T₁₀, and T₁₂ Stilbenevinylsilsesquioxanes. *J. Am. Chem. Soc.* **2013**, *135*, 12259-12269.
11. Furgal, J.C.; Goodson III, T.; Laine, R.M. D_{5h} [PhSiO_{1.5}]₁₀ Synthesis *via* F⁻ Catalyzed Rearrangement of [PhSiO_{1.5}]_n. An Experimental/Computational Analysis of Likely Reaction Pathways. *Dalton Trans.* **2016**, *45*, 1025-1039.
12. Xue, F.; Jia, D.; Li, Y.; Jing, X. Facile Preparation of a Mechanically Robust Superhydrophobic Acrylic Polyurethane Coating. *J. Mater. Chem. A* **2015**, *3*, 13856-13863.
13. Wang, H.; Sun, F.; Wang, C.; Zhu, Y.; Wang, H. A Simple Drop-Casting Approach to Fabricate the Super-hydrophobic PMMA-PSF-CNFs Composite Coating with Heat-, Wear- and Corrosion-Resistant Properties. *Colloid Polym. Sci.* **2016**, *294*, 303-309.
14. Milionis, A.; Loth, E.; Bayer, I. Recent Advances in the Mechanical Durability of Superhydrophobic Materials. *Adv. Colloid Interface Sci.* **2016**, *229*, 57-79.
15. ASTM Standard D3359. Standard Test Methods for Rating Adhesion by Tape Test. ASTM: West Conshohocken, PA **2017**, 1-9.

Chapter 3

Silicone Resin Coatings via Fluoride Ion Catalyzed Rearrangement

Published: Krug, D. J.; Laine, R. M. *ACS Appl. Mater. Interfaces* **2017**, *9*, 8378-8383.

There have been many successful efforts to enhance the water shedding properties of hydrophobic and superhydrophobic coatings, but durability is often a secondary concern. Here we describe durable and hydrophobic coatings prepared via fluoride catalyzed rearrangement reaction of dodecaphenylsilsesquioxane [PhSiO_{1.5}]₁₂ (DDPS) with octamethylcyclotetrasiloxane (D₄). Hydrophobic properties and wear resistance are maximized by incorporating both low surface energy moieties and cross-linkable moieties into the siloxane network. Water contact angles as high as 150° ± 4° were achieved even after 150 wear cycles with SiC sandpaper (2000 grit, 2 kPa). These silicone resin coatings also have high thermal stabilities after curing at 250°C (T_{d5%} ≥ 340°C in air) due to the siloxane network with a maximum T_{d5%} of > 460°C measured for the system with the highest silsesquioxane content. The coating systems presented here offer a unique combination of hydrophobicity and mechanical/thermal stability and could greatly expand the utility of water repellent coatings.

3.1 Introduction

Hydrophobic and superhydrophobic surfaces continue to attract much attention due to their numerous potential applications including non-wetting,^{1,2} self-cleaning,³⁻⁵ anti-fogging,^{6,7} and low-adhesion properties.^{8,9} Hydrophobic and superhydrophobic surfaces are typically characterized as having static water contact angles (WCAs) of $>90^\circ$ and $>150^\circ$, respectively, as shown in Figure 3.1. The WCA of a smooth surface has been shown to be limited to $\approx 120^\circ$ for low surface energy materials like fluoropolymers, e.g. poly(tetrafluoroethylene), due to the small atomic radius and high electronegativity of fluorine.^{10,11}

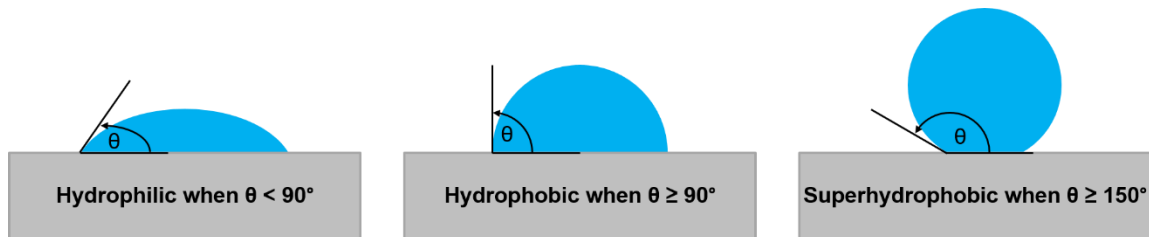


Figure 3.1 Schematic of water contact angles from hydrophilic to superhydrophobic

The surface of the lotus leaf has inspired researchers to explore nanoscale roughness to achieve higher WCAs in synthetic materials by mimicking the leaf's nanoscale wax covered microscale protrusions.¹² The lotus leaf WCA is about 160° (Figure 3.2), which provides self-cleaning properties as water rolling off the surface carries contaminants with it.^{3,13} This phenomenon, “the lotus-leaf effect,” arises from the surface morphology, which can be described by the Cassie-Baxter model (Figure 3.2) where air pockets are trapped between micro- and nano-structured features.^{14,15} The surface roughness maximizes the contact between water and air, which has a WCA of 180° .

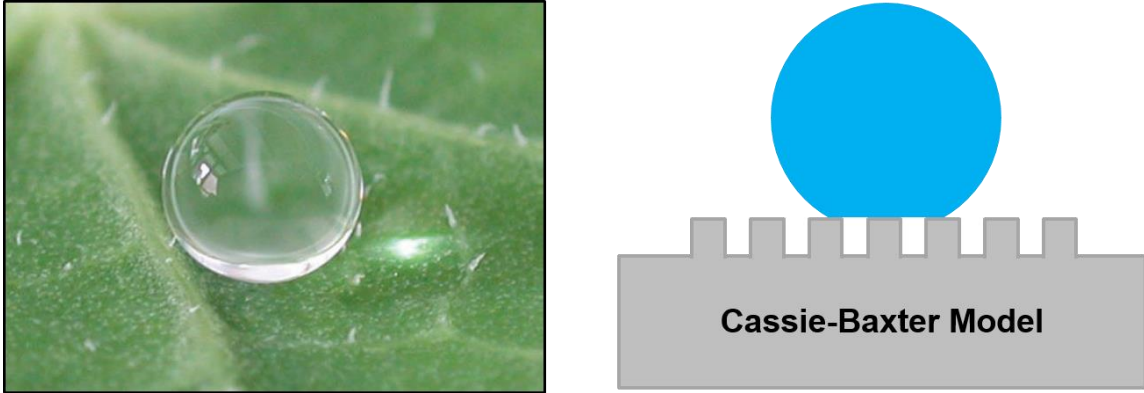


Figure 3.2 Water on a lotus leaf¹⁷ (left) and a schematic of the Cassie-Baxter model (right)

Many research groups have mimicked the lotus-leaf effect to successfully create surfaces with hierarchical scale roughness.^{16,17} Li et al. generated a WCA of 158.5° on an aligned, densely packed carbon nanotube (dia. \approx 60 nm) array, which increased to 166° after coating with fluoroalkylsiloxane.¹⁸ Shang et al. made superhydrophobic silica films (average particle size, APS \approx 100 nm) via sol-gel processing Si(OEt)₄ followed by a self-assembled monolayer of a fluoroalkylsilane, which resulted in a 165° WCA.¹⁹ Bravo et al. used layer-by-layer processing to stack layers of 20 and 50 nm (APS) silica nanoparticles on top of adhesive layers of a polysulfonate to make a superhydrophobic (160°) coating with high transparency on glass (Figure 3.3).²⁰ Qu et al. used nitric acid/hydrogen peroxide to etch metal alloys to create nano-scale roughness with WCAs of 150-160° after surface treating with fluoroalkylsilane.²¹

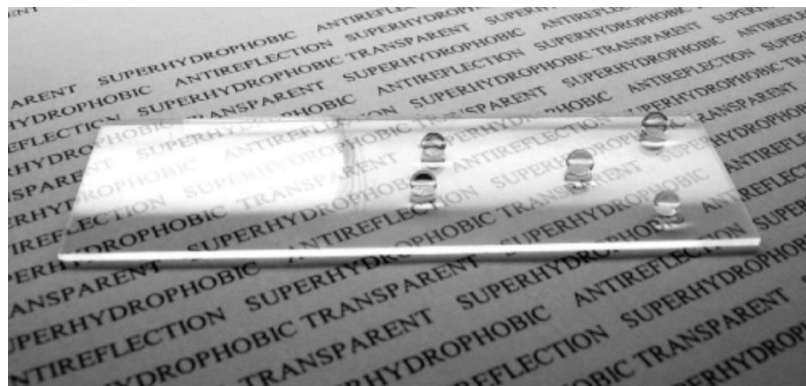


Figure 3.3 Superhydrophobic coating containing silica nanoparticles on glass²⁰

Perfluoroalkylsilane coatings offer very low surface energies, typically 14 mN/m (Table 3.1).^{20,22,23} Polydimethylsiloxane (PDMS) is also used extensively offering comparable low surface energy (20 mN/m),²⁴ good thermal and oxidative stability, low T_g , and biocompatibility.^{25,26} However, silicones are well known to exhibit poor mechanical properties and susceptibility to tearing as coating thicknesses increase.

Table 3.1 Surface energy of common polymers, aluminum, and glass

Material	Surface Energy (mN/m)
Polytetrafluoroethylene	14
Silicone	20
Polyethylene	31
Polyvinyl chloride	39
Nylon 66	43
Aluminum	≈ 500
Glass	≈ 1000

We too were able to make superhydrophobic coatings with the combination of silicone, perfluoroalkylsilane, and silica nanoparticles. Octamethylcyclotetrasiloxane (D₄) and (tridecafluoro-1,1,2,2-tetrahydrooctyl)triethoxysilane (PFS) along with a small amount of vinyltrimethoxysilane and 3 wt % silica nanoparticles (20 nm) were stirred in THF in the presence of fluoride ion. This fluoride rearrangement reaction as a pathway to silicone resin polymerization, described above in section 1.4 and in more detail below, was used to make a series of superhydrophobic coatings on aluminum substrates (Figure 3.4). An angled stream of water from a lab squeeze bottle onto the coated substrate bounces off at a deflected angle. Water droplets bounce off the surface and/or roll away. However, all efforts yielded highly friable coatings that could be easily worn away with a single rub of the finger.

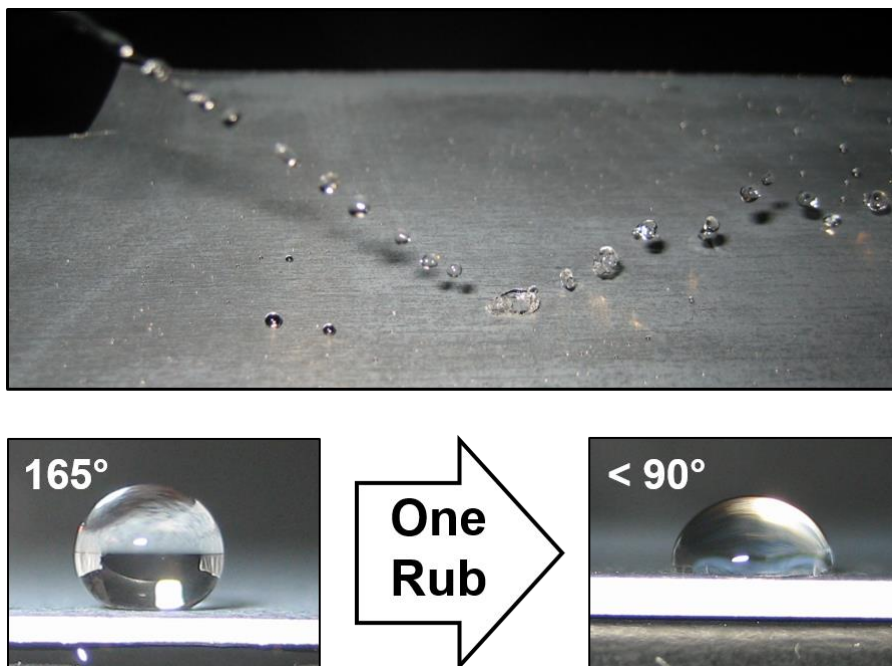


Figure 3.4 Water bounces off superhydrophobic silicone resin coating on Al substrate due to high WCA (top), but coating is easily worn away with a single finger rub (bottom)

Durability is often a secondary concern to the WCA when designing non-wetting biomimetic materials. Reviews on the topic identify the need to maximize durability and develop consistent methods for testing wear resistance in addition to high WCAs as a necessary requirement for widespread acceptance.^{1,2,23} Simple weighted sandpaper abrasion of coated surfaces has been used to test wear resistance and Milionis et al. recently reported in a review that a linear abrasion test like the method (section 2.2) used in this dissertation had the most potential as a universal standard for testing the durability of superhydrophobic coatings.²⁷⁻²⁹

One possible mechanism to improve the properties of silicones is with silsesquioxanes. SQs have been the subject of numerous review articles and are inorganic-organic hybrid nanocomposite materials with the empirical formula $\text{RSiO}_{1.5}$, where R can be a myriad of organic functional groups, and can have random, cage, or partial cage structures.³⁰⁻⁴⁸ The inorganic -Si-O-Si- cage or backbone provides thermal and oxidative stability while the attached organic moieties allow for polymer miscibility and functionalization. SQs have been shown to increase the mechanical and thermal properties of common polymers^{49,50}

including PDMS⁵¹⁻⁵⁴ as reinforcing nanofillers and cross-linkers for increased polymer network integrity.

Recently, our research group has devised a facile synthetic route to mono and mixed functionality SQs afforded by a fluoride ion (F⁻) catalyzed rearrangement of either polymeric SQ or T₈ SQs to create mono and mixed functionality T₁₀ and T₁₂ SQs as described in section 1.4.⁵⁵⁻⁶⁰ These functionality combination reactions occur at room temperature in THF with trace amounts of water and in high yields.⁶⁰ The capture of F⁻ is necessary to form discrete, isolable cage compounds. However, leaving F⁻ in solution and removing the solvent suspends the rearrangement of moieties and freezes them in place creating a scrambled silicone network. Final properties of these highly tailorable hybrid materials are controlled by the starting ratio of functional groups. The simplified suggested reaction pathway is shown in Figure 3.5.

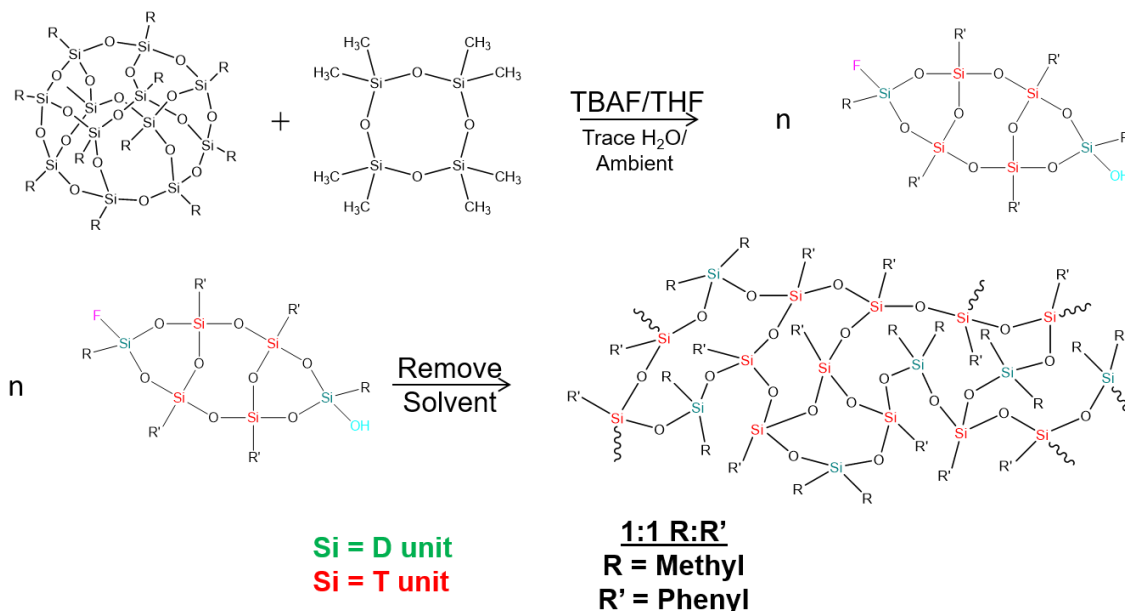


Figure 3.5 F⁻ catalyzed rearrangement reaction as a route to silicone resins

In this chapter, we describe the use of the patented⁶¹ fluoride rearrangement reaction described above for fabricating mixed functionality silicone resins for durable *and* hydrophobic coatings. The relationship between chemical composition, hydrophobicity, and durability is explored and discussed in the following sections in an effort to better understand and optimize these multifunctional materials.

The use of F^- as a catalyst rapidly equilibrates all $RSiO_{1.5}$ units in the coating system. These units are present in the form of silsesquioxane cage compounds.⁵⁵⁻⁶¹ The coating system *is not polymeric as applied, it only forms a polymer on drying (solvent evaporation) driven by the equilibration of all the $RSiO_{1.5}$ units.* A further aspect of this system is that if the coating does not meet target properties in a first trial, the coating solution can be modified simply by changing one or two components that are anticipated to lead to better properties and the system allowed to equilibrate before the next application. This type of *in situ* modification is explored in Chapter 5.

3.2 Experimental Procedures

The synthetic methods, processing techniques, and characterization procedures are described above in Chapter 2.

3.3 Results and Discussion

In the following sections, we first confirm the presence of the multiple functionalities successively added to the coating systems by FTIR. We then discuss the thermal stability of the coating systems following a typical curing temperature of 250°C. Thereafter we discuss coating properties, property optimization studies, and surface characterization followed by selected conclusions. It is important to note that dodecaphenylsilsesquioxane $[PhSiO_{1.5}]_{12}$ (DDPS) is insoluble in THF without the presence of fluoride ion catalyst. Rearrangement of the SQ, siloxanes, and silanes into soluble hybrid species only occurs with fluoride ion catalyst and results in a clear coating solution.

In addition to the model silicone compound comprised only of methyl (from D₄) and phenyl (from DDPS), systems with the addition of (tridecafluoro-1,1,2,2-tetrahydrooctyl)triethoxysilane (PFS) and methacryloxypropyltrimethoxysilane (MAS) were made to increase hydrophobicity and crosslink density, respectively (Figure 3.6). An additional coating system was made with 3 wt % silica nanoparticles to further increase

hydrophobicity and wear resistance. An initial coating solution concentration study was conducted to ensure adequate coverage of Al substrates during spray coating. Coating concentrations of 5 to 25 wt % were examined by SEM (Figures A.1 - A.4) and 10 wt % was found to be the minimum concentration necessary for uniform, complete coverage.

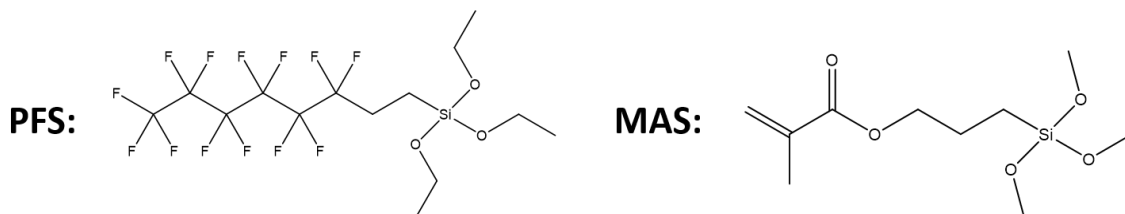


Figure 3.6 Structures of PFS and MAS added to coating systems for multi-functionality

3.3.1 FTIR Study

FTIR spectra of the coatings after 200 wear cycles (Figure 3.7) were identical to their respective spectra before wear testing. This indication of robustness helps explain the retention of high WCAs after wear resistance testing as described later. Benzene ring stretches at 1596 and 1432 cm^{-1} confirm the presence of phenyl groups in all four coatings. The symmetric C–H deformation vibrations of Si–CH₃ at 1261 cm^{-1} in the DDPS + D₄ coating confirms the presence of methyl groups from the D₄. This signal is partly obscured and appeared as a slight shoulder on the strong C–F stretch at 1236 cm^{-1} in the three coatings that have PFS; C–F was also observed at 1192 cm^{-1} . However, Si–CH₃ rocking at 804 cm^{-1} was detected in all coatings.

All spectra have Si–O–Si antisymmetric stretching peaks at 1131 and 1010-1030 cm^{-1} , which indicates the formation of a siloxane network. Absence of signals for Si–OH stretching at 920 cm^{-1} and O–H stretching at 3300 cm^{-1} indicates the elimination of silanols and that the siloxane network is well condensed. Both coatings polymerized with MAS show the C=O stretch at 1735 cm^{-1} from the ester group.

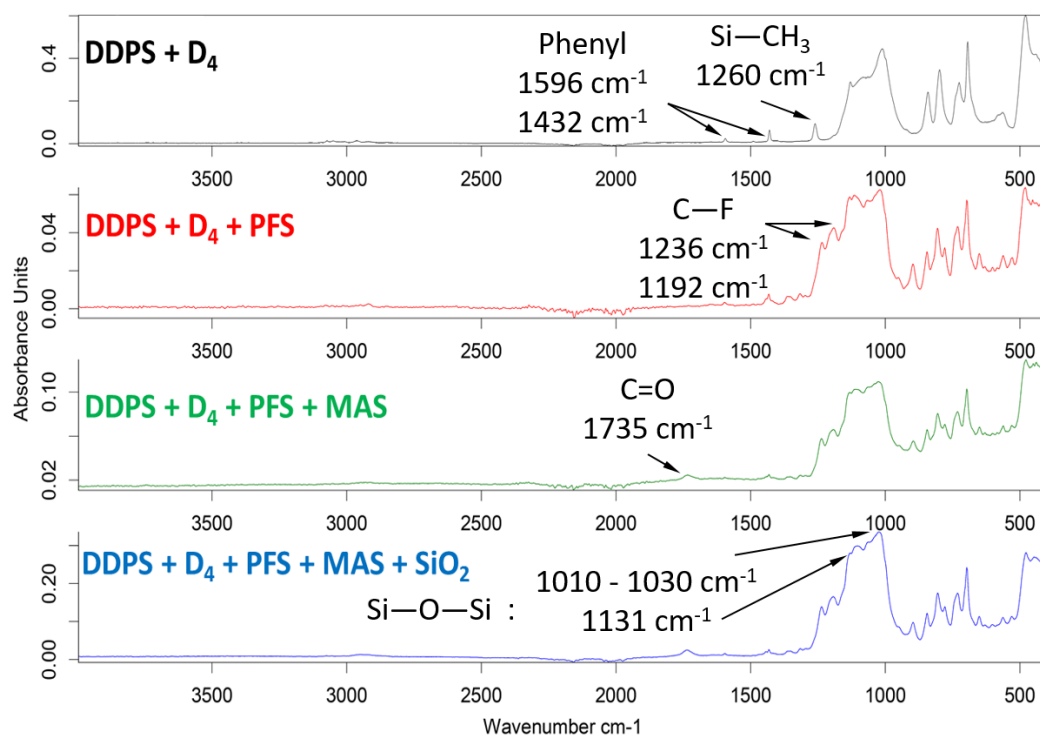


Figure 3.7 FTIRs of silicone resin coatings with successive incorporation of functionalities

3.3.2. Thermal Behavior

Thermal stabilities (Table 3.2) of the cured hybrid coatings were measured as the temperature at 5% mass loss ($T_{d5\%}$) via TGA in N_2 (Figure 3.8) and air (Figure 3.9). All cured coatings exhibited high thermal stability, $\geq 340^\circ\text{C}$ in air. The DDPS + D_4 coating had the highest thermal stability ($T_{d5\%}$) of 464°C in air. This is attributed to the high inorganic content from the silica core of the DDPS and siloxane ring of the D_4 . The amount of PFS added to the system was relatively large to achieve a 1:1:1 ratio of functional groups: phenyl, methyl, and perfluoroalkyl. This results in a coating with a higher organic content and lower thermal stability ($T_{d5\%} = 340^\circ\text{C}$ in air). Thermal stability increases to $T_{d5\%} = 343^\circ\text{C}$ in air with the addition of MAS. The ratio of functional groups is maintained at 1:1:1:1 (phenyl, methyl, perfluoroalkyl, methacrylate) and so there is less PFS than MAS by mass. MAS has fewer carbons per molecule compared to PFS and the methacrylate groups free radical polymerize to form crosslinks. Both of these factors increase thermal

stability. The subsequent addition of 3 wt % silica increases the $T_{d5\%}$ to 350°C in air due to the increased inorganic content.

Table 3.2 Thermal stability of hybrid coatings (T at 5% mass loss via TGA)

Coating System	Avg. $T_{d5\%}$ (N ₂)	Avg. $T_{d5\%}$ (Air)
DDPS + D ₄	473 ± 5 °C	464 ± 1 °C
DDPS + D ₄ + PFS	351 ± 1 °C	340 ± 2 °C
DDPS + D ₄ + PFS + MAS	368 ± 2 °C	343 ± 1 °C
DDPS + D ₄ + PFS + MAS + SiO ₂	384 ± 4 °C	350 ± 3 °C

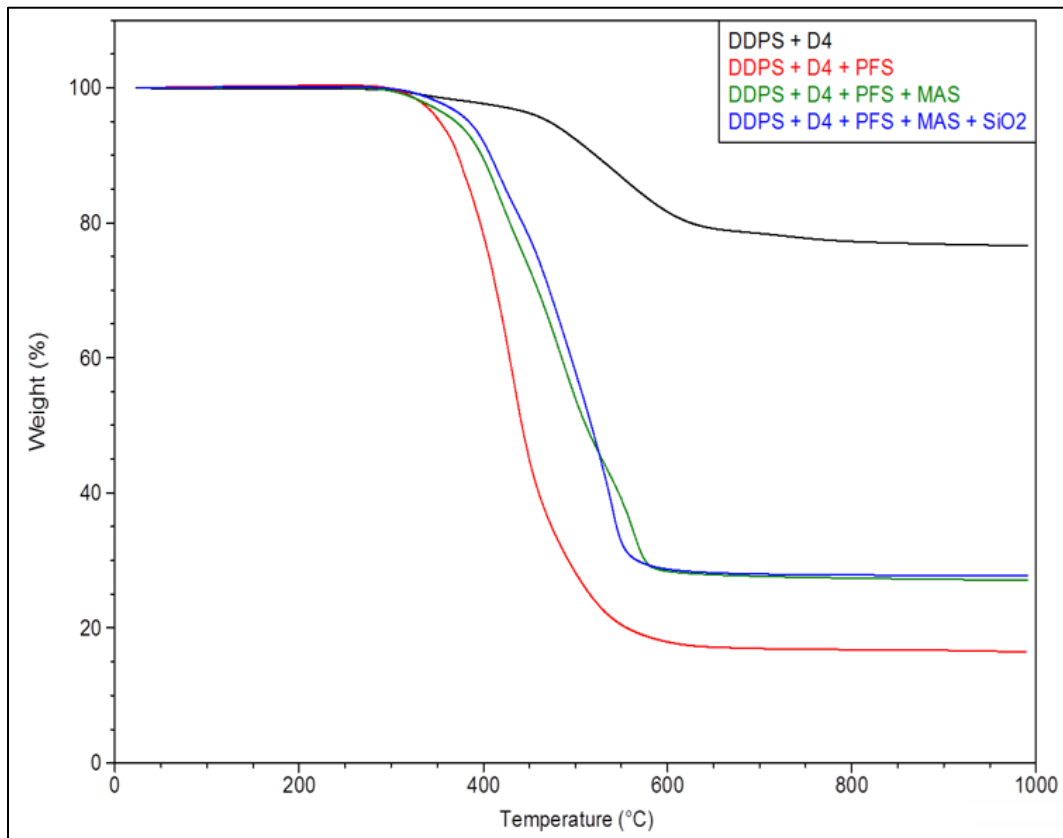


Figure 3.8 Typical TGAs of silicone resins in N₂

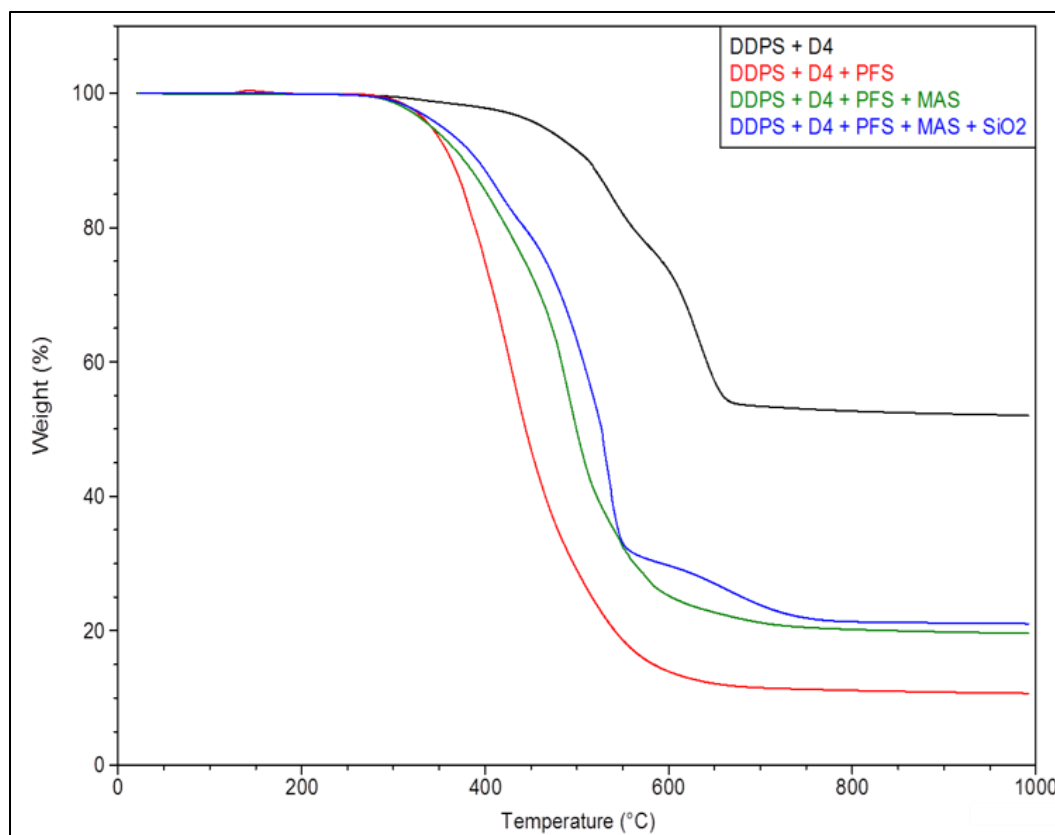


Figure 3.9 Typical TGAs of silicone resins in air

3.3.3 Wear Resistance

Initial WCAs of 90-100° indicate all silicone resin coatings are inherently hydrophobic (Figure 3.10, Table 3.3). The DDPS + D₄ coating maintains a relatively constant WCA of 95° during the wear resistance test indicating it is robust and not prone to surface roughening. Such a durable coating would be well suited for high temperature applications where smoothness is critical over a lifetime of wear.

The other three coatings exhibit increases in WCA with increases in wear cycles. This is attributed to surface roughening of the added polymeric functionalities. The perfluoroalkyl chains added to the coating (DDPS + D₄ + PFS) are softer than the phenyl groups from the DDPS or the Me groups from the D₄ and can therefore be roughened by the sandpaper wear cycles, but are not worn away to any significant degree because they are part of the polymer network via the siloxane linkages. The surface roughness of the

DDPS + D₄ + PFS reaches a steady plateau with a WCA of 115° maintained after 150 and 200 wear cycles.

Subsequently, methacrylate groups were added to further increase wear resistance at higher wear cycles by increasing crosslink density via free radical polymerization. These rigid crosslinks enhance the mechanical properties of the baseline silicone coatings developed here. The resulting coating (DDPS + D₄ + PFS + MAS) offers WCA increases ($\approx +20^\circ$) compared to the DDPS + D₄ + PFS coatings after 100 and 150 cycles because although the coating is roughened by wear, the improved network integrity enhanced by the increased crosslink density prevents complete degradation of the coating. The addition of 3 wt % silica nanoparticles (APS = 20 nm) to the coating system (DDPS + D₄ + PFS + MAS + SiO₂) shows a larger increase in WCA, which peaks at 150° after 150 wear cycles. Silica introduces a nano-scale roughness that likely creates a hierarchical structure not present in the other coatings. Silica also increases the wear resistance (i.e. 143° after 200 wear cycles) due to its inherent hardness and higher modulus. As wear continues throughout the test and new surfaces are created, more silica nanoparticles are exposed resulting in a maximum WCA of 150° after 150 wear cycles.

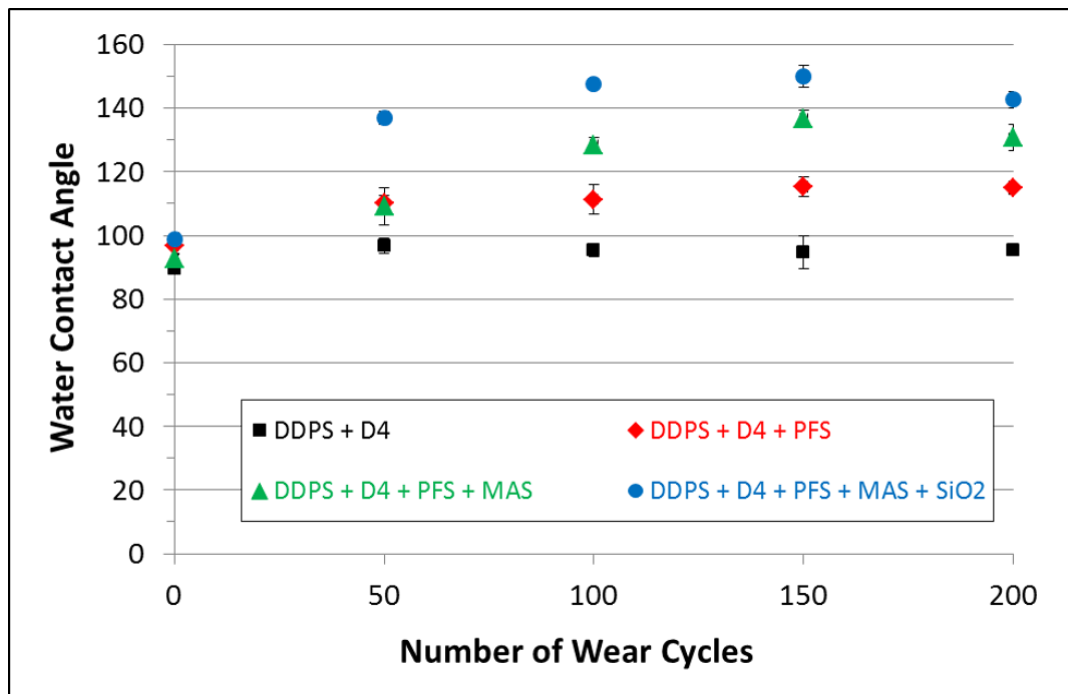


Figure 3.10 WCA of silicone resin coatings cured at 250°C versus wear cycles with 100 g weighted 2000 grit sandpaper

Table 3.3 WCA versus wear cycles on silicone resin coatings

Coating System	Wear Cycles				
	0	50	100	150	200
DDPS + D ₄	90 ± 0.5°	97 ± 2°	95 ± 2°	95 ± 5°	95 ± 1°
DDPS + D ₄ + PFS	97 ± 3°	110 ± 2°	111 ± 4°	115 ± 3°	115 ± 2°
DDPS + D ₄ + PFS + MAS	93 ± 2°	109 ± 6°	128 ± 2°	137 ± 3°	131 ± 4°
DDPS + D ₄ + PFS + MAS + SiO ₂	99 ± 2°	137 ± 2°	148 ± 0.5°	150 ± 4°	143 ± 3°

SEM-EDS analyses (Figure 3.11) show that all coating systems are uniform except DDPS + D₄ + PFS. The low surface tension and relatively high concentration of PFS (75 wt % of coating) causes the coating to de-wet from the Al alloy surface forming islands (Figure 3.11e). The addition of MAS provides a coating (DDPS + D₄ + PFS + MAS) that adequately wets the Al alloy surface during application and spreads uniformly. The PFS concentration with respect to the coating is reduced from 75 to 55 wt %, which raises the surface energy and allows better wetting during coating application (Figure 3.11i).

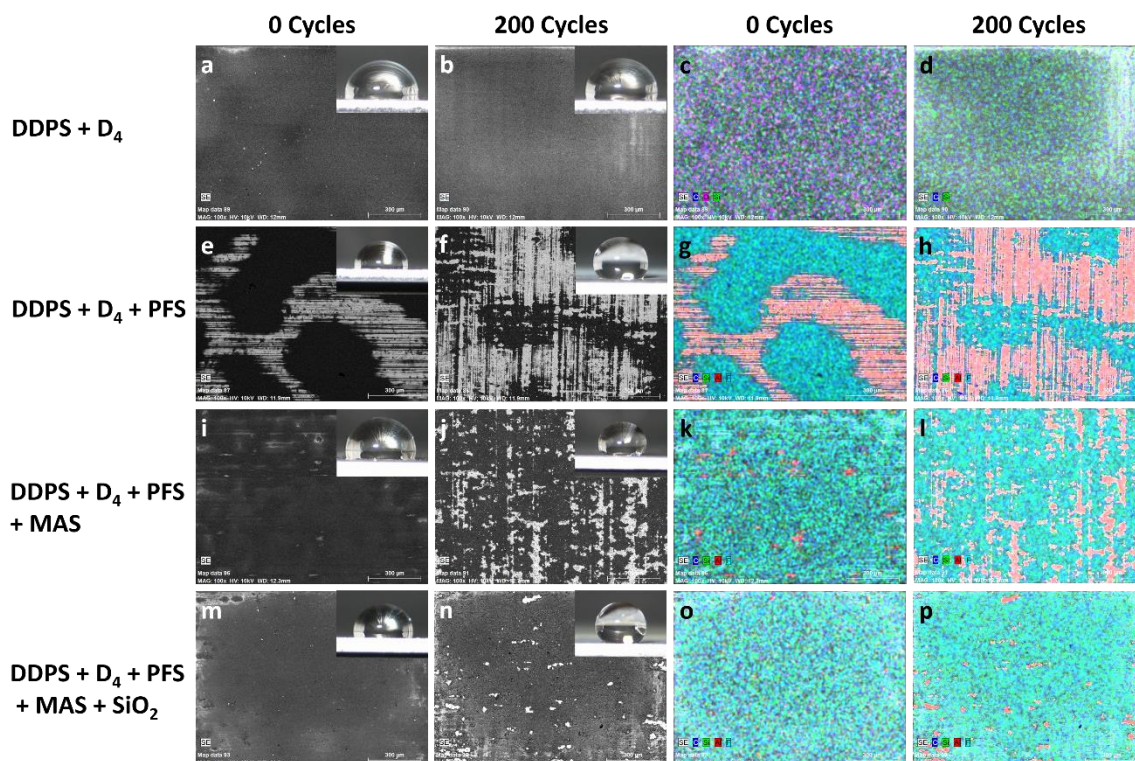


Figure 3.11 SEM-EDS images with WCA photo insets of coatings before and after 200 wear cycles. (a-d) DDPS + D₄, (e-h) DDPS + D₄ + PFS, (i-l) DDPS + D₄ + PFS + MAS,

(m-p) DDPS + D₄ + PFS + MAS + SiO₂. Magnification 100x, scale bar 300 μm. EDS map colors: Red = Al, Blue = C, Green = Si, Light Blue = F.

The integrity of the DDPS + D₄ coating (Figure **3.11a-d**) remains intact from 0 to 200 wear cycles, in agreement with the observed steady WCA (ca. 95°) versus wear. Even after 200 wear cycles the EDS spectra of the DDPS + D₄ coating showed no Al from the substrate. The DDPS + D₄ + PFS coating showed the most wear (Figure **3.11e-h**) as seen by the exposure of the Al alloy in the SEM images and EDS (Al = red on elemental map overlay) after 200 wear cycles. This coating loss is attributed to lower adhesion to the substrate due to poor wetting during application. Despite the obvious wear, enough DDPS + D₄ + PFS coating remains adhered to the surface to achieve a WCA of 115° after 200 wear cycles. As discussed above, wear resistance increases with inclusion of MAS to the coating system (DDPS + D₄ + PFS + MAS) due to higher crosslink density. The SEM-EDS analysis offers further evidence for this improved wear resistance from the preservation of coating integrity after 200 wear cycles (Figure **3.11i-l**) due to better wetting and adhesion. Figure **3.11m-o** shows that addition of silica nanoparticles further increased the coating integrity as expected due to their abrasion resistance properties and the results of the wear resistance test.

Overall, the EDS mapping suggests uniform distribution of functional groups because even low surface energy perfluoroalkyl chains are detected (as F, light blue) in all areas where the coating is present before and after wear (Figure **3.12**). The F⁻ rearrangement reaction scrambles the SQ, siloxane, and silanes randomly and does not favor local aggregation of moieties or phase separation despite surface energy differences. This suggests that not only are the low surface energy moieties uniformly distributed, but so are the methacrylate crosslinks that enhance wear resistance. Combination of wear and heat resistance along with a high WCA creates many opportunities for these materials where common weak superhydrophobic coatings fail. Possible applications include coated fabrics that resist laundering wear, easy to clean surfaces in hospitals and kitchens, and non-stick or anti-fouling coatings on metal and ceramic surfaces.

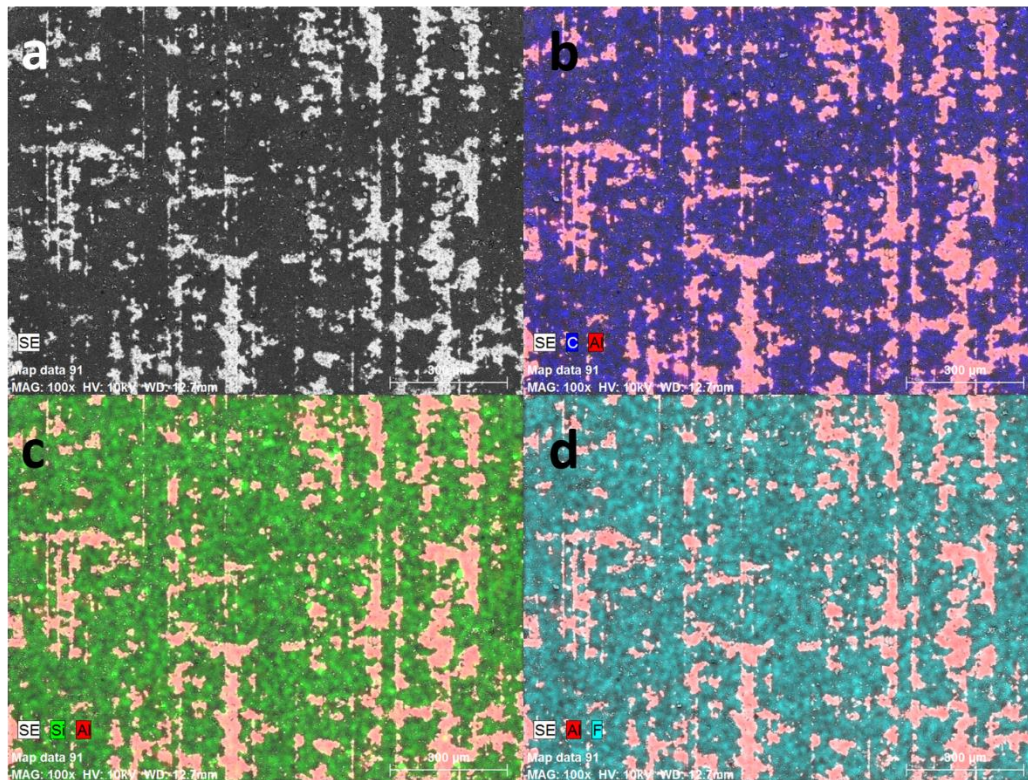


Figure 3.12 SEM-EDS images of a silicone resin coating (DDPS + D₄ + PFS + MAS) after 200 wear cycles suggests uniform distribution of functional groups: SEM, EDS maps where a) Al = red and b) C = blue, c) Si = green, d) F = light blue. Magnification 100x, scale bar 300 µm.

3.4 Conclusions

Hydrophobic or superhydrophobic properties of coatings are often maximized with the sacrifice of wear resistance and vice versa. Here we have developed a simple route to making multifunctional silicone resin coatings via a fluoride catalyze rearrangement reaction that affords the possibility to maximize both durability and water repellency. These silicone-methacrylate copolymers exhibit high WCAs, up to 150°, even after being worn with sandpaper. The robustness is in part attributed to the silicone network formed from when solvent is removed and the F⁻ scrambled network is frozen in place. This siloxane network gives these materials high thermal stabilities of $\geq 340^{\circ}\text{C}$ and even up to 460°C when the organic composition is minimized.

The possible applications for a low surface energy, wear resistant, and thermally stable coating are wide ranging from automotive and aerospace to medical and energy generation. Perhaps more exciting is that this work demonstrates a facile route to multifunctional silicones where the final properties are limited only by the imagination put into the functionalities of the silicone building blocks a formulator uses.

We reiterate again that the coating system is not polymeric as applied and only forms a polymer on drying (solvent evaporation) driven by the equilibration of all $\text{RSiO}_{1.5}$ units. Furthermore, the coating system can be modified “on the fly” because of this rapid equilibration process before application, which will be explored in Chapter 6. Very few other coating systems allow *in situ* modification.

3.5 References

1. Verho, T.; Bower, C.; Andrew, P.; Franssila, S.; Ikkala, O.; Ras, R. Mechanically Durable Superhydrophobic Surfaces. *Adv. Mater.* **2011**, *23*, 673-678.
2. Xue, C. H.; Ma, J. Z. Long-Lived Superhydrophobic Surfaces. *J. Mater. Chem. A* **2013**, *1*, 4146-4161.
3. Sun, T.; Feng, L.; Gao, X.; Jiang, L. Bioinspired Surfaces with Special Wettability. *Acc. Chem. Res.* **2005**, *38*, 644-652.
4. Parkin, I.; Palgrave, R. Self-Cleaning Coatings. *J. Mater. Chem.* **2005**, *15*, 1689-1695.
5. Ganesh, V.; Raut, H.; Nair, A.; Ramakrishna, S. A Review on Self-cleaning Coatings. *J. Mater. Chem.* **2011**, *21*, 16304-16322.
6. Lai, Y.; Tang, Y.; Gong, J.; Gong, D.; Chi, L.; Lin, C.; Chen, Z. Transparent Superhydrophobic/Superhydrophilic TiO₂-Based Coatings for Self-Cleaning and Anti-Fogging. *J. Mater. Chem.* **2012**, *22*, 7420-7426.
7. Faustini, M.; Nicole, L.; Boissiere, C.; Innocenzi, P.; Sanchez, C.; Grosso, D. Hydrophobic, Antireflective, Self-Cleaning, and Antifogging Sol-Gel Coatings: An Example of Multifunctional Nanostructures Materials for Photovoltaic Cells. *Chem. Mater.* **2010**, *22*, 4406-4413.
8. Jin, M.; Feng, X.; Xi, J.; Zhai, J.; Cho, K.; Feng, L.; Jiang, L. Super-Hydrophobic PDMS Surface with Ultra-Low Adhesive Force. *Macromol. Rapid Commun.* **2005**, *26*, 1805-1809.
9. Bhushan, B.; Jung, Y.; Koch, K. Micro-, Nano- and Hierarchical Structures for Superhydrophobicity, Self-Cleaning and Low Adhesion. *Philos. Trans. R. Soc., A* **2009**, *367*, 1631-1672.
10. Hare, E.; Shafrin, E.; Zisman, W. Properties of Films of Adsorbed Fluorinated Acids. *J. Phys. Chem.* **1954**, *58*, 236-239.
11. Nishino, T.; Meguro, M.; Nakamae, K.; Matsushita, M.; Ueda, Y. The Lowest Surface Free Energy Based on -CF₃ Alignment. *Langmuir* **1999**, *15*, 4321-4323.
12. Barthlott, W.; Neinhuis, C. Purity of the Sacred Lotus, or Escape from Contamination in Biological Surfaces. *Planta* **1997**, *202*, 1-8.
13. Koch, K.; Bhushan, B.; Barthlott, W. Multifunctional Surface Structures of Plants: An Inspiration for Biomimetics. *Prog. Mater. Sci.* **2009**, *54*, 137-178.

14. Cassie, A.; Baxter, S. Wettability of Porous Surfaces. *Trans. Faraday Soc.* **1944**, *40*, 546–551.
15. Nosonovsky, M. Multiscale Roughness and Stability of Superhydrophobic Biomimetic Interfaces. *Langmuir* **2007**, *23*, 3157-3161.
16. Yan, Y. Y.; Gao, N., Barthlott, W. Mimicking Natural Superhydrophobic Surfaces and Grasping the Wetting Process: A Review on Recent Progress in Preparing Superhydrophobic Surfaces. *Adv. Colloid Interface Sci.* **2011**, *169*, 80-105.
17. Blossey, R. Self-Cleaning Surfaces - Virtual Realities. *Nat. Mater.* **2003**, *2*, 301-306.
18. Li, H.; Wang, X.; Song, Y.; Liu, Y.; Li, Q.; Jiang, L.; Zhu, D. Super-“Amphiphobic” Aligned Carbon Nanotube Films. *Angew. Chem., Int. Ed.* **2001**, *40*, 1743-1746.
19. Shang, H. M.; Wang, Y.; Limmer, S. J.; Chou, T. P.; Takahashi, K.; Cao, G. Z. Optically Transparent Superhydrophobic Silica-Based Films. *Thin Solid Films* **2005**, *472*, 37-43.
20. Bravo, J.; Zhai, L.; Wu, Z.; Cohen, R. E.; Rubner, M. F. Transparent Superhydrophobic Films Based on Silica Nanoparticles. *Langmuir* **2007**, *23*, 7293-7298.
21. Qu, M.; Zhang, B.; Song, S.; Chen, L.; Zhang, J.; Cao, X. Fabrication of Superhydrophobic Surfaces on Engineering Materials by a Solution-Immersion Process. *Adv. Func. Mater.* **2007**, *17*, 593-596.
22. Brokar, S.; Jankova, K.; Siesler, H.; Hvilsted, S. New Highly Fluorinated Styrene-Based Materials with Low Surface Energy Prepared by ATRP. *Macromolecules* **2004**, *37*, 788-794.
23. Guo, Z.; Liu, W.; Su, B. L. Superhydrophobic Surfaces: From Natural to Biomimetic to Functional. *J. Colloid Interface Sci.* **2011**, *353*, 335-355.
24. Ma, M.; Hill, R.; Superhydrophobic Surfaces. *Curr. Opin. Colloid Interface Sci.* **2006**, *11*, 193-202.
25. Yilgor, E.; Yilgor, I. Silicone Containing Copolymers: Synthesis, Properties and Applications. *Prog. Polym. Sci.* **2014**, *39*, 1165-1195.
26. Gong, D.; Long, J.; Jiang, D.; Fan, P.; Zhang, H.; Li, L.; Zhong, M. Robust and Stable Transparent Superhydrophobic Polydimethylsiloxane Films by Duplicating via a Femtosecond Laser-Ablated Template. *ACS Appl. Mater. Interfaces* **2016**, *8*, 17511-17518.

27. Xue, F.; Jia, D.; Li, Y.; Jing, X. Facile Preparation of a Mechanically Robust Superhydrophobic Acrylic Polyurethane Coating. *J. Mater. Chem. A* **2015**, *3*, 13856-13863.
28. Wang, H.; Sun, F.; Wang, C.; Zhu, Y.; Wang, H. A Simple Drop-Casting Approach to Fabricate the Super-hydrophobic PMMA-PSF-CNFs Composite Coating with Heat-, Wear- and Corrosion-Resistant Properties. *Colloid Polym. Sci.* **2016**, *294*, 303-309.
29. Milionis, A.; Loth, E.; Bayer, I. Recent Advances in the Mechanical Durability of Superhydrophobic Materials. *Adv. Colloid Interface Sci.* **2016**, *229*, 57-79.
30. Voronkov, M.; Lavrentyev, V. Polyhedral Oligosilsesquioxanes and Their Homo Derivatives. *Top. Curr. Chem.* **1982**, *102*, 199-236.
31. Baney, R.; Itoh, M.; Sakakibara, A.; Suzuki, T. Silsesquioxanes. *Chem. Rev.* **1995**, *95*, 1409-1430.
32. Loy, D.; Shea, K. Bridged Polysilsesquioxanes - Highly Porous Hybrid Organic-Inorganic Materials. *Chem. Rev.* **1995**, *95*, 1431-1442.
33. Calzaferri, G. In *Tailor-Made Silicon-Oxygen Compounds, From Molecules to Materials*; Corriu, R., Jutzi, P., Eds.; Friedr. Vieweg & Sohn GmbH, Braunschweig/Weisbaden, Germany, 1996; Chapter *Silsesquioxanes*, pp 149-169.
34. Lichtenhan, J. In *Polymeric Materials Encyclopedia*; Salmone, J. C., Ed.; CRC Press, NY, 1996, vol. 10, Chapter *Silsesquioxane-Based Polymers*, pp. 7768-7777.
35. Provatas, A.; Matison, J. Silsesquioxanes: Synthesis and Applications. *Trends Polym. Sci.*, **1997**, *5*, 327-333.
36. Pescarmona, P.; Maschmeyer, T. Oligomeric Silsesquioxanes: Synthesis, Characterization, and Selected Applications. *Aust. J. Chem.* **2001**, *54*, 583-596.
37. Li, G.; Wang, L.; Ni, H.; Pittman Jr., C. Polyhedral Oligomeric Silsesquioxane (POSS) Polymers and Copolymers: A Review. *J. Inorg. Organomet. Polym.* **2001**, *11*, 123-154.
38. Duchateau, R. Incompletely Condensed Silsesquioxanes: Versatile Tools in Developing Silica-Supported Olefin Polymerization Catalysts. *Chem. Rev.* **2002**, *102*, 3525-3542.
39. Abe, Y.; Gunji, T. Oligo- and Polysiloxanes. *Prog. Polym. Sci.* **2004**, *29*, 149-182.
40. Phillips, S.; Haddad, T.; Tomczak, S. Developments in Nanoscience: Polyhedral Oligomeric Silsesquioxane (POSS)-Polymers. *Curr. Opin. Solid State Mater. Sci.* **2004**, *8*, 21-29.

41. Kannan, R.; Salacinski, H.; Butler, P.; Seifalian, A. *Acc. Chem. Res.* **2005**, *38*, 879–884.
42. Laine, R. Nanobuilding Blocks Based on the $[\text{OSiO}_{1.5}]_x$ ($x = 6, 8, 10$) Octasilsesquioxanes. *J. Mater. Chem.* **2005**, *15*, 3725–3744.
43. Lickiss, P.; Rataboul, F. *Adv. Organomet. Chem.* Fully Condensed Polyhedral Oligosilsesquioxanes (POSS): From Synthesis to Application. **2008**, *57*, 1–116.
44. Chan, K.; Sonar, P.; Sellinger, A. Cubic Silsesquioxanes for Use in Solution Processable Organic Light Emitting Diodes (OLED). *J. Mater. Chem.* **2009**, *19*, 9103–9120.
45. Wu, J.; Mather, P. POSS Polymers: Physical Properties and Biomaterials Applications. *Polym. Rev.* **2009**, *49*, 25–63.
46. Cordes, D.; Lickiss, P.; Rataboul, F. Recent Developments in the Chemistry of Cubic Polyhedral Oligosilsesquioxanes. *Chem. Rev.* **2010**, *110*, 2081–2173.
47. Laine, R.; Roll, M. Polyhedral Phenylsilsesquioxanes. *Macromolecules* **2011**, *44*, 1073–1109.
48. Kuo, S. W.; Chang, F.C. POSS Related Polymer Nanocomposites. *Prog. Polym. Sci.* **2011**, *36*, 1649–1696.
49. Tanaka, K.; Adachi, S.; Chujo, Y. Structure-Property Relationship of Octa-Substituted POSS in Thermal and Mechanical Reinforcements of Conventional Polymers. *J. Polym. Sci., Part A: Polym. Chem.* **2009**, *47*, 5690–5697.
50. Wang, F.; Lu, X.; He, C. Some Recent Developments of Polyhedral Oligomeric Silsesquioxane (POSS)-Based Polymeric Materials. *J. Mater. Chem.* **2011**, *21*, 2775–2782.
51. Baumann, T.; Jones, T.; Wilson, T.; Saab, A.; Maxwell, R. Synthesis and Characterization of Novel PDMS Nanocomposites Using POSS Derivatives as Cross-Linking Filler. *J. Polym. Sci., Part A: Polym. Chem.* **2009**, *47*, 2589–2596.
52. Chen, D.; Liu, Y.; Zhang, H.; Zhou, Y.; Huang, C.; Xiong, C. Influence of Polyhedral Oligomeric Silsesquioxanes (POSS) on Thermal and Mechanical Properties of Polydimethylsiloxane (PDMS) Composites Filled with Fumed Silica. *J. Inorg. Organomet. Polym.* **2013**, *23*, 1375–1382.
53. Florea, N.; Lungu, A.; Badica, P.; Craciun, L.; Enculescu, M.; Ghita, D.; Ionescu, C.; Zgirian, R.; Iovu, H. Novel Nanocomposites Based on Epoxy Resin/Epoxy-

- Functionalized Polydimethylsiloxane Reinforced with POSS. *Composites, Part B* **2015**, *75*, 226-234.
54. Bai, H.; Huang, C.; Jun, L.; Li, H. Modification of Liquid Silicone Rubber by Octavinyl-Polyhedral Oligosilsesquioxanes. *J. Appl. Polym. Sci.* **2016**, *133*, 43906.
55. Asuncion, M.; Laine, R. Fluoride Rearrangement Reactions of Polyphenyl- and Polyvinylsilsesquioxanes as a Facile Route to Mixed Functional Phenyl, Vinyl T₁₀ and T₁₂ Silsesquioxanes. *J. Am. Chem. Soc.* **2010**, *132*, 3723-3736.
56. Ronchi, M.; Sulaiman, S.; Boston, N.; Laine, R. Fluoride Catalyzed Rearrangements of Polysilsesquioxanes, Mixed Me, Vinyl T₈, Me, Vinyl T₁₀ and T₁₂ Cages. *Appl. Organometal. Chem.* **2010**, *24*, 551-557.
57. Jung, J. H.; Laine, R. Beads on a Chain (BOC) Polymers Formed from the Reaction of [NH₂PhSiO_{1.5}]_x[PhSiO_{1.5}]_{10-x} and [NH₂PhSiO_{1.5}]_x[PhSiO_{1.5}]_{12-x} Mixtures ($x=2-4$) with the Diglycidyl Ether of Bisphenol A. *Macromolecules* **2011**, *44*, 7263-7272.
58. Jung, J. H.; Furgal, J.; Goodson III, T.; Mizumo, T.; Schwartz, M.; Chou, K.; Vonet, J. F.; Laine, R. 3-D Molecular Mixtures of Catalytically Functionalized [vinylSiO_{1.5}]₁₀/[vinylSiO_{1.5}]₁₂. Photophysical Characterization of Second Generation Derivatives. *Chem. Mater.* **2012**, *24*, 1883-1895.
59. Furgal, J.; Jung, J. H.; Goodson III, T.; Laine, R. Analyzing Structure-Photophysical Property Relationships for Isolated T₈, T₁₀, and T₁₂ Stilbenevinylsilsesquioxanes. *J. Am. Chem. Soc.* **2013**, *135*, 12259-12269.
60. Furgal, J.; Goodson III, T.; Laine, R. D_{5h} [PhSiO_{1.5}]₁₀ Synthesis via F⁻ Catalyzed Rearrangement of [PhSiO_{1.5}]_n. An Experimental/Computational Analysis of Likely Reaction Pathways. *Dalton Trans.* **2016**, *45*, 1025-1039
61. Laine, R.; Asuncion, M.; Krug, D. Synthesis and Processing of New Silsesquioxane/Siloxane Systems. US20140120243

Chapter 4

Recycling Silicone Resins

Published: Krug, D. J.; Asuncion, M. Z.; Laine, R. M. *ACS Omega* **2019**, *4*, 3782-3789.

Silicone resins are traditional thermoset polymers with an inorganic backbone affording chemical inertness and high thermal stability, which also makes them inherently difficult to recycle by traditional methods. Here we demonstrate that catalytic amounts of fluoride ion (F^-) at room temperature solubilize highly cross-linked silicone resins initially cured up to 250°C. After solubilization equilibria are achieved, solvent is removed to reform the polymer network. Coatings on aluminum substrates and monoliths of virgin and recycled silicone resins were evaluated for hydrophobicity, wear resistance, substrate adhesion, and thermal stability. Silicones recycled under optimized conditions retained nearly 100% wear resistance, thermal stability, and adhesion properties. In some instances, the recycled coatings offer properties superior to the virgin materials.

4.1 Introduction

Polysiloxanes (polyorganosiloxanes) are commonly referred to as silicones. Commercial silicones are used as fluids, elastomers, or in resin forms with properties based on structural differences that rely on various compositions of mono-, di-, tri- and tetra-valent units with the respective symbols and general formulas: M = R₃SiO_{1/2} (siloxo), D = R₂SiO_{2/2} (siloxane), T = R₁SiO_{1/2} (silsesquioxane), and Q = SiO_{4/2} (silicate).

Their low glass transition temperatures, thermal stabilities, chemical inertness, and low coefficients of friction make silicones useful in many applications in the automotive, aerospace, cookware, and medical industries.¹ D units can be linked to form linear polysiloxane (silicones) as low to high molecular weight fluids. The R groups are typically methyl (most commercially useful silicone: polydimethylsiloxane, PDMS, Figure 4.1), phenyl, a mix of methyl and phenyl, a mix of methyl and hydrogen, a mix of methyl and alkyl, or trifluoropropyl.

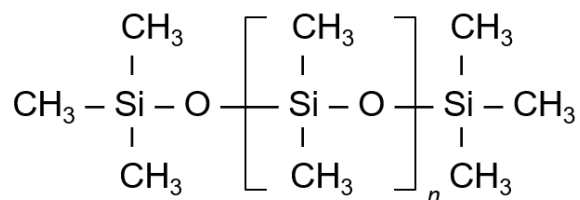


Figure 4.1 Structure of PDMS

Linear polysiloxanes with cross-linkable functional groups along the backbone or on the chain ends cure to form silicone elastomers. Increasing the cross-link density increases the moduli and hardness from soft gels to hard rubbers, which lead to very diverse applications. High thermal stability, hot air resistance, oxidative resistance, and flame retardancy make silicone elastomers ideal for tubing, gaskets, fixtures, sealants, and coatings in automotive and aerospace applications.²⁻⁴

Due to their physiological inertness, silicone elastomers are used in food contact applications as well as medical applications such as prosthetics, implants, catheters, and heart valve seals.^{5,6} Silicone elastomers exhibit strong adhesion to metal and glass substrates and provide a low surface energy, low friction, non-stick, hydrophobic surface

suitable for applications in casting, mold making, mold release, water repellent coatings, anti-graffiti coatings, cookware, and the paper industry.⁷⁻⁹

Unlike silicone fluids and elastomers, silicone resins also contain T and Q units. These tri- and tetra- functional units create highly branched and cage-like networks with high cross-link densities, especially compared to silicone elastomers. Combinations of units are typically used to balance properties. For example, pure T-resins can be brittle, but adding D or M units increases elasticity and adhesion.¹ Silicone resins combine high temperature, oxidation, and UV stabilities as well as resistance to acids, oils, and water making them ideal for many coating applications including release, hydrophobic, oleophobic, abrasion resistance, chemical resistance, anti-corrosion, protective, decorative, insulating, anti-fouling, sealants, and paints.^{1,7-9}

Many of silicone's favorable properties are attributed to their robust inorganic siloxane backbones and crosslinks. However, since thermosets do not melt like thermoplastics, it makes it much more difficult to recycle and reuse them. Thermoset polymer recycling is classified into three categories: mechanical, thermal, and chemical recycling (Figure 4.2).

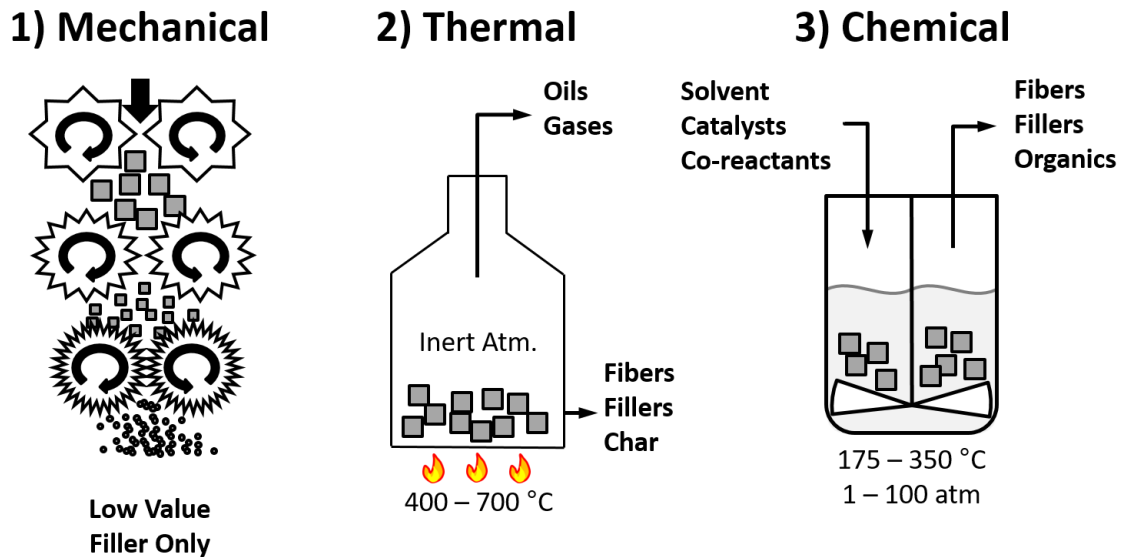


Figure 4.2 Three types of thermoset polymer or composite recycling

Mechanical recycling involves grinding the thermoset to a powder and using a low loading as filler in a chemically similar polymer, which often results in a reduction of mechanical properties.^{10,11} Thermosets can be thermally recycled (burned) to generate energy and recover fillers, but the process is energy intensive due to silicone's high thermal stability and creates unwanted greenhouse gases. In fact, when recycling multi-material systems, such as electronic waste (cell phones), silicone components are removed from the system prior to thermal recycling due to its high decomposition temperature and decomposition products (silica) that favor char formation from the organic containing components.¹²

Chemical recycling of silicones has focused on depolymerizing silicone fluids and cross-linked silicone rubbers into monomers that subsequently need to be repolymerized as a route to only partial replacement of virgin materials. Early research focused on aminolysis to cleave Si-O bonds to create silylamines and alcohol (Figure 4.3).^{13,14} Cast films of silicone rubber recycled in *n*-butylamine showed a 40% loss of tensile strength and 20% loss in percent elongation at break.

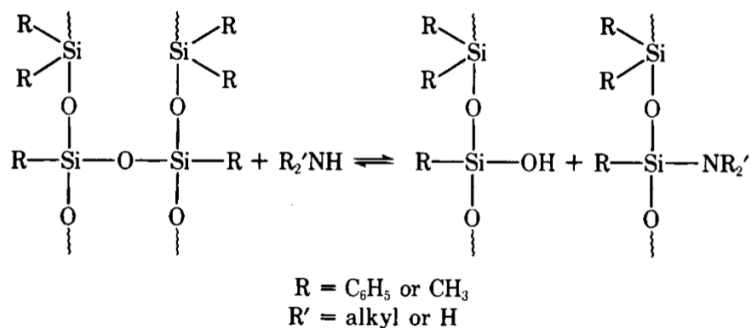


Figure 4.3 Aminolysis of silicone rubber yields 20-40% loss in mechanical properties¹³

Okamoto et al. explored alcoholysis of PDMS oils and cross-linked rubbers in a pressure reactor with the aid of metal halide catalysts and dimethyl carbonate.¹⁵ The metal halide polarizes the siloxane bond at the chain end as methanol attacks the Si-O to form methoxysilane and a shorter polysiloxane chain (Figure 4.4). Dimethyl carbonate reacts with the water co-product to form methanol and carbon dioxide. Depolymerization times are long because the reaction progresses only at the chain ends by cleaving one monomer

at a time. The use of pressure reactors in bulk recycling is also an economical and scalability challenge.

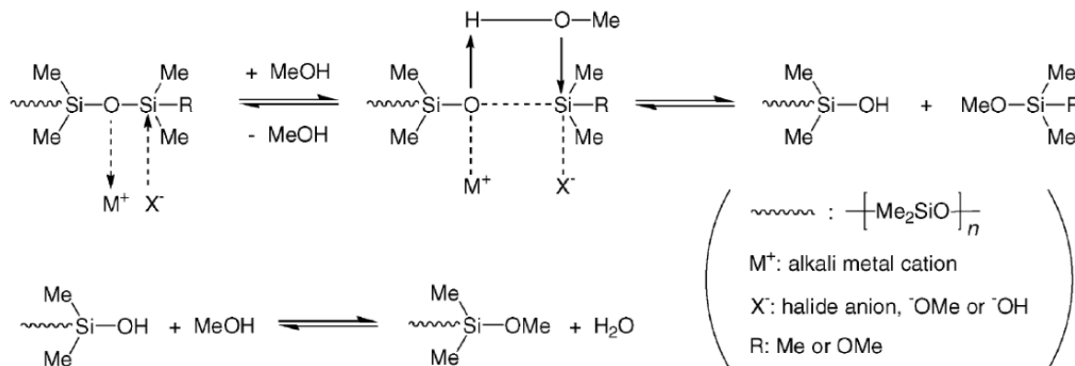


Figure 4.4 Alcoholysis of silicone oil/rubber requires a pressure reactor¹⁵

Enthaler and coworkers used iron and zinc catalysts to activate Si-O bonds in PDMS and cleave them with benzoyl fluoride, benzyl chloride, or acetic anhydride to make silicon containing monomers.¹⁶⁻¹⁹ These depolymerization reactions typically require high temperature, high pressure, long reaction times, and produce acid byproducts with low yields. The same researchers later used boron trifluoride etherate (BF₃OEt₂) to depolymerize PDMS at lower temperatures.^{20,21} Large quantities of BF₃OEt₂ (0.75 - 2 equivalents per polymer repeat unit) and complex isolation techniques were required to generate 75-87% yields of monomers that require further reaction to become useful products.

Researchers have also built-in recyclable crosslinks to polysiloxanes to promote de-crosslinking as opposed to depolymerization of siloxanes units. Guo et al. modified tetramethyltetra vinyl-cyclotetrasiloxane with furan by thiol-ene reaction forming thermally reversible crosslinks via Diels-Alder reactions with bismaleimide (Figure 4.5).²² De-crosslinking took place at 120°C via the retro Diels-Alder reaction forming a liquid that was reshaped and cooled to a solid. The low de-crosslinking temperature may be useful in some applications, but limits the thermal stability usually expected of silicones.

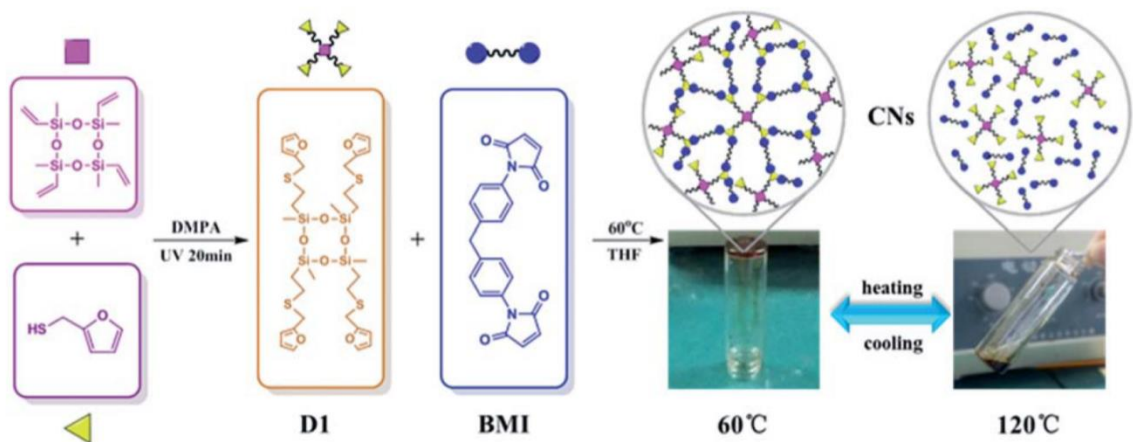


Figure 4.5 Thermally reversible cross-links incorporated into silicone²²

Disulfide bonds with dynamic covalent behavior incorporated into a silicone provides photo-reversible cross-links (e.g. sunlight, Figure 4.6).²³ Mechanical property retention of $\approx 80\%$ was achieved by first pulverizing the cross-linked silicone and then pressing and irradiating it for up to 48 h with a xenon lamp or natural sunlight. Both studies employed polymers structurally designed to be depolymerizable limiting usefulness to niche applications and does not address recycling common and widely used silicones.

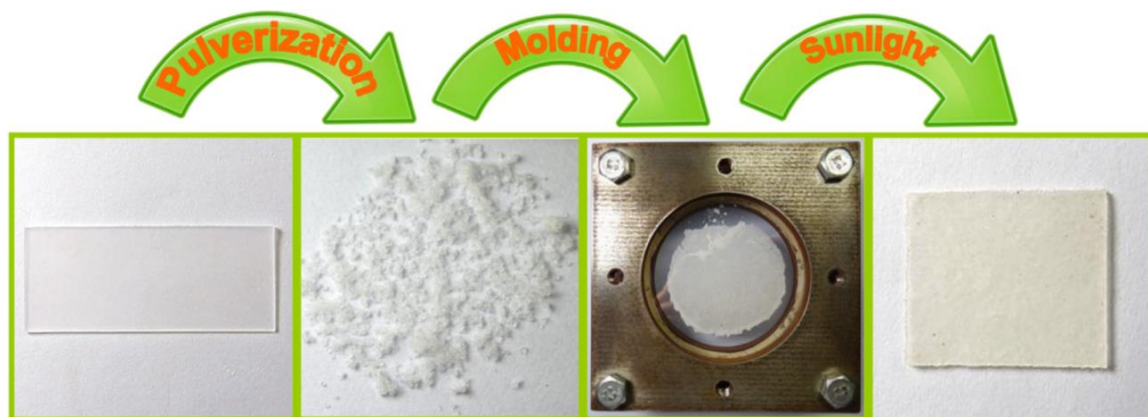


Figure 4.6 Silicone rubber with disulfide bond containing cross-links that are reversible with sunlight²³

Presently, chemical recycling efforts with silicones have mainly focused on depolymerizing silicone fluids, linear silicones, and some cross-linked silicone rubbers into monomers that subsequently need to be repolymerized as a partial replacement of virgin

materials.¹³⁻²³ Studies on recycling silicone *resins* directly are lacking. Silicone resins are more challenging to recycle than silicone rubber due to the presence of T and Q units, which significantly increases the crosslink density compared to rubber elastomers. Re-use of the collected monomers requires traditional, multi-step silicone polymerization and curing techniques, thus they require the same amount of energy, reagents, etc. as in the production of virgin silicones.

This type of down cycling usually re-uses recovered materials in lower demanding or lower value products. A chemical recycling approach for silicone fluids, rubbers, *and* resins that is low energy/cost with $\approx 100\%$ yields and $\approx 100\%$ retention of properties would be very attractive for the widespread silicone industry. More valuable yet would be to create a closed loop recycling process where the recycled silicone can be reused for the same application.

In this chapter, we report an entirely new method to recycle traditionally difficult to process thermosetting silicone resins, with mixed phenyl/methyl functionality recycled in one step by fluoride ion catalyzed rearrangement at ambient temperature and pressure and show near 100% retention of measured properties. Our research group has previously demonstrated fluoride (F^-) ion catalyzed rearrangement of polymeric silsesquioxanes (or T-resins), T_8 silsesquioxane (SQ) cages, or $RSi(OEt)_3$ into T_{10} and T_{12} cages on removal of F^- .²⁴⁻²⁹

These facile reactions occur at room temperature in THF with trace amounts of water and a F^- source such as tetrabutylammonium fluoride (nBu_4NF , TBAF) and form discrete SQ cages. Furgal et al. has proposed possible mechanistic pathways for these F^- mediated rearrangement reactions based on exhaustive experimental analyses and modeling studies.²⁹ Rearrangement of T (and D and Q) silicon units involve complex, multiple intermediate processes leading to equilibria among many intermediate species.²⁹ Reaction intermediates continue to reorganize and eventually lead to discrete cages with mixed functionalities upon fluoride removal.

As discussed above in Chapter 3, we showed that leaving F^- in solution with D and T silicone units and removing the solvent generates random polysiloxane networks forming hydrophobic and wear resistant coatings with mixed functionalities based on starting materials.³⁰ In this work we reintroduce F^- to cured thermoset silicone resins to solubilize

them in one step under ambient conditions, recast/recoat, and evaluate the retention of key properties. These studies are performed with the model mixed phenyl/methyl silicone resin made from DDPS and D4 from the previous chapter. The simplified proposed reaction scheme is shown in Figure 4.7. Thereafter, commercially available silicone rubber and resin are also recycled with our new method.

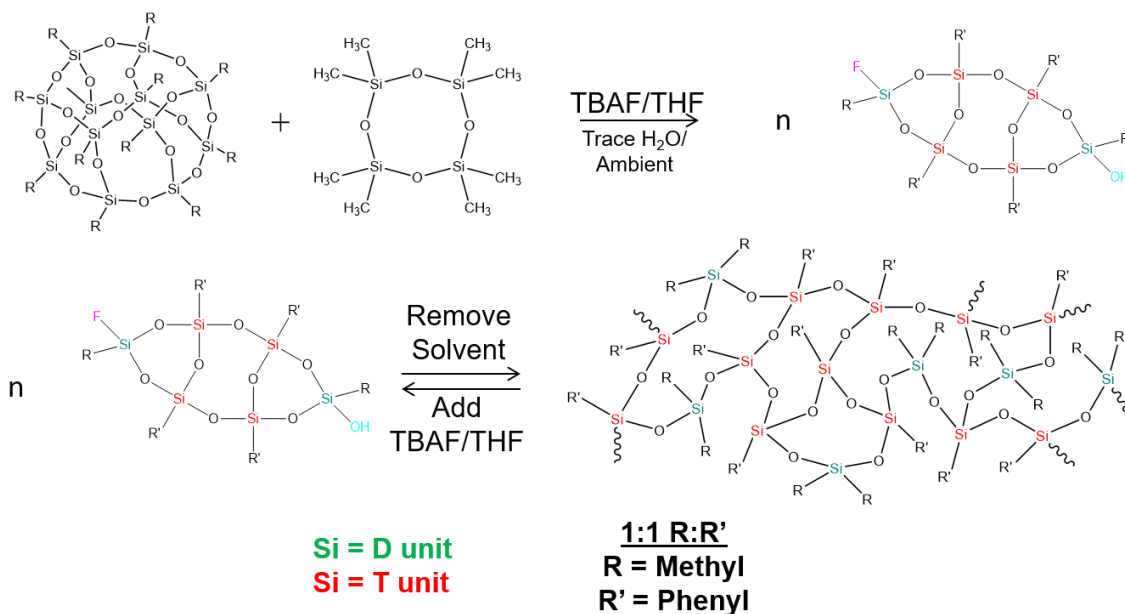


Figure 4.7 F⁻ catalyzed rearrangement as a new method for recycling silicones

4.2 Experimental Procedures

The synthetic methods, processing techniques, and characterization procedures are described above in Chapter 2.

4.3 Results and Discussion

In the following sections, we first investigate the influence of cure temperature on the key properties (hydrophobicity, wear resistance, adhesion, and thermal/oxidative stability) of the prime (virgin) silicone resin to establish a baseline. We then explore the influence of

fluoride ion concentration in the recycling reaction solution on final properties of recycled silicone resins. This work focuses on the model mixed phenyl/methyl silicone resin synthesized from DDPS and D₄ via F⁻ catalyzed rearrangement. Thereafter, we employ optimized recycling conditions to recycle commercially relevant silicone resin.

4.3.1 Prime Silicone Resin Properties vs Cure Temperature

The model silicone resin made from DDPS and D₄ has a 1 Me : 1 Ph ratio and 2 T units : 1 D unit. At this ratio of T:D units the cross-link density of the resin is very high as each T unit creates a crosslink, especially compared to silicone rubber elastomers, which have far fewer cross-linkable functionalities. Consistent solution concentrations (10 wt % silicone) in TBAF/THF ensured uniform thickness of spray coatings on Al 2024 coupons. Wear resistance was evaluated by a linear abrasion test method where the change in water contact angle (WCA) is measured after 50 wear cycle increments (back and forth = one cycle) with a 100 g weighted 2000 grit sandpaper. This simple wear resistance test (detailed in Chapter 2) has been used often and is considered a reliable technique for evaluating polymer thin films.³¹⁻³³

All prime coatings had consistent initial average WCAs between 90-92° with little deviation (Figure 4.8), but after 50-200 wear cycles coatings cured at 150°C and 200°C had higher and more variable WCAs. The WCA increase, attributed to surface roughening from the sandpaper, indicates the coatings were not as hard and abrasion resistant as coatings cured at 250°C, which exhibit steady and consistent WCA after 200 wear cycles. Higher cure temperatures decrease plasticizing volatiles and increase crosslink densities as will be evidenced later.

SEM-EDS images of prime silicone resin coatings before and after wear resistance and after tape adhesion testing are very similar (Figures 4.9 - 4.11). Little to no wear shows on the surface. However, the coating cured at the lowest temperature, 150°C, appears to have a non-uniform thickness based on the variation in color of the image. In BSE composition mode heavier elements are lighter on the grayscale, which indicates the dark areas are carbon rich from the coating and the light areas have less coating and more of the substrate

(Al) reads through. Adhesion test results vs temperature are all the highest rating (5B) with no coating removal.

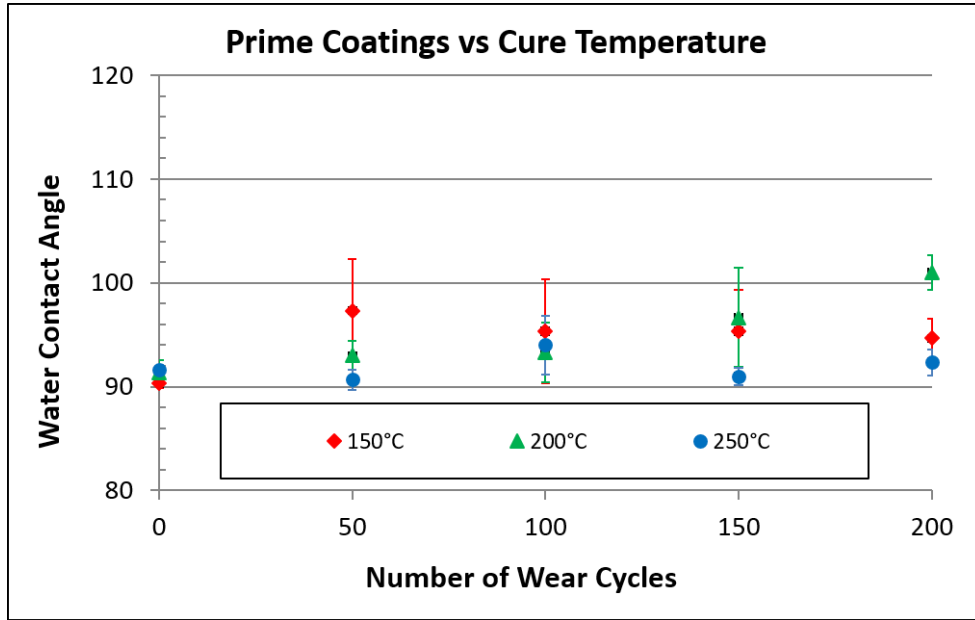


Figure 4.8 Effect of cure temperature on wear resistance of prime silicone resin coatings

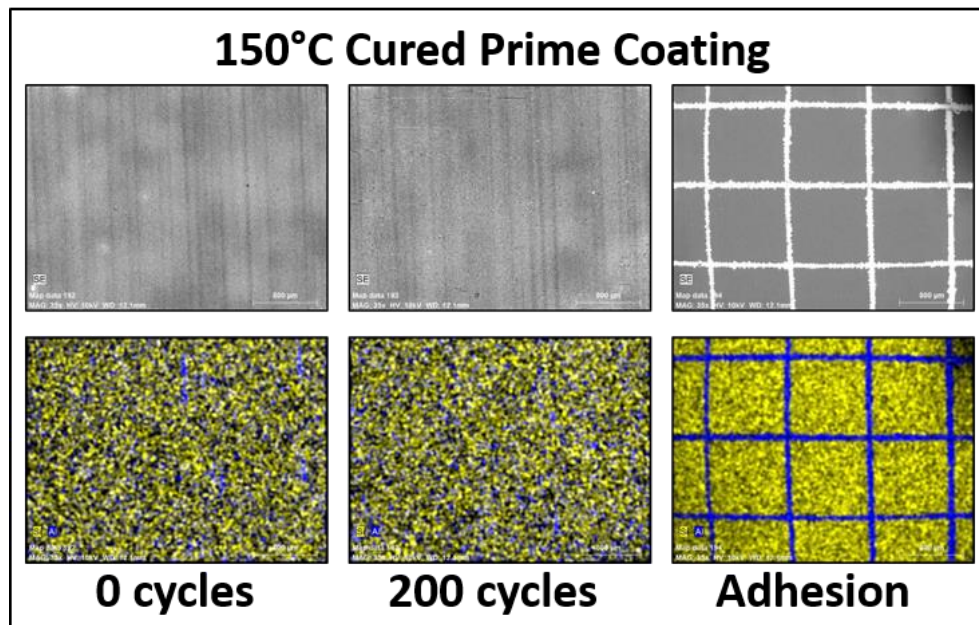


Figure 4.9 SEM-EDS images of prime silicone resin coatings cured at 150°C before and after 200 wear cycles and cross-hatch tape adhesion test. Wear micrograph magnification 100x, scale bar 300 μm . Cross-hatch magnification 35x, scale bar 800 μm , EDS map: yellow = Si, blue = Al.

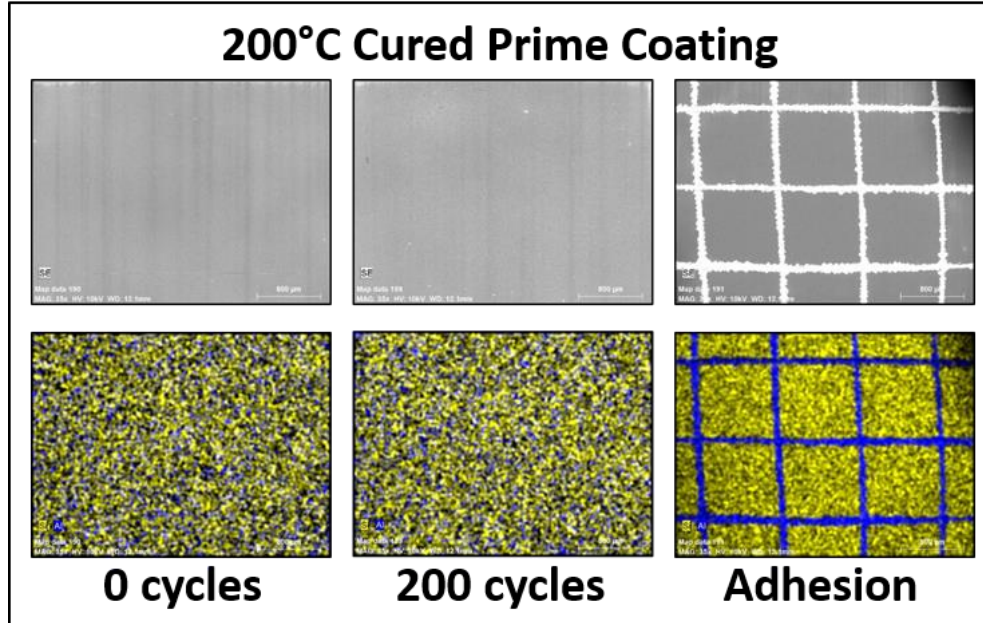


Figure 4.10 SEM-EDS images of prime silicone resin coatings cured at 200°C before and after 200 wear cycles and cross-hatch tape adhesion test. Wear micrograph magnification 100x, scale bar 300 μm. Cross-hatch magnification 35x, scale bar 800 μm, EDS map: yellow = Si, blue = Al.

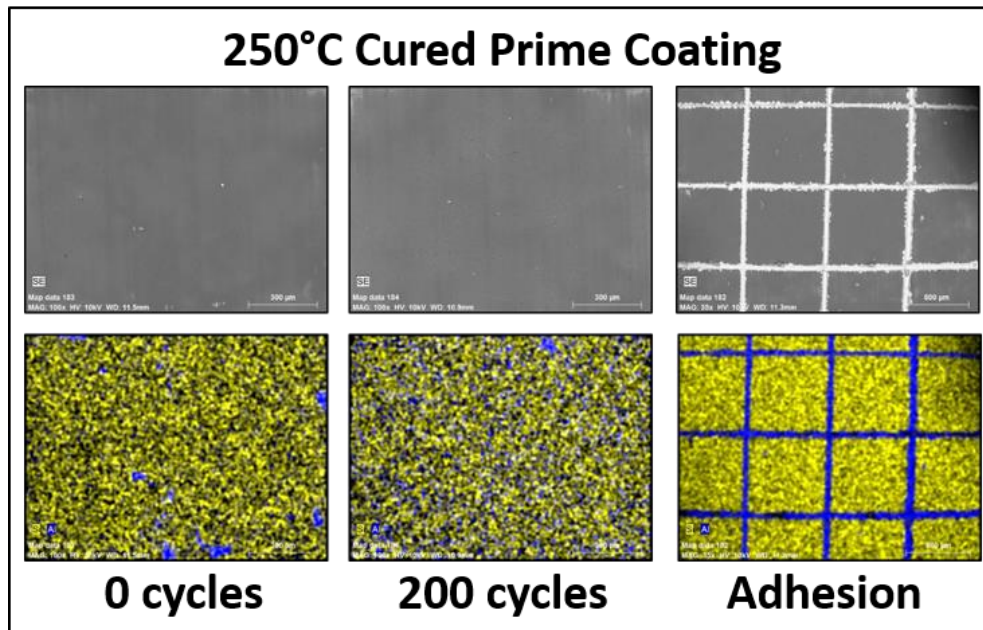


Figure 4.11 SEM-EDS images of prime silicone resin coatings cured at 250°C before and after 200 wear cycles and cross-hatch tape adhesion test. Wear micrograph magnification 100x, scale bar 300 μm. Cross-hatch magnification 35x, scale bar 800 μm, EDS map: yellow = Si, blue = Al.

The thermal stability of the prime silicone resin, identified as the average temperature at 5% mass loss ($T_{d5\%}$) via TGA in air, also increased with an increase in cure temperature (Figure 4.12). This confirms the highest cure temperature is optimal with a maximum $T_{d5\%}$ of 483 ± 7 °C. $T_{d5\%}$ of the resin cured at 200°C was slightly lower, 470 ± 6 °C, but both resins exhibit two main mass losses between 400-575°C and 575-700°C, attributed to the methyl/phenyl groups and char, respectively. Resin cured at the lowest temperature of 150°C had a 130°C lower $T_{d5\%}$ (353 ± 5 °C) due to a third mass loss below 400°C attributed to volatiles, which were elucidated by gas chromatography – mass spectrometry (GC-MS).

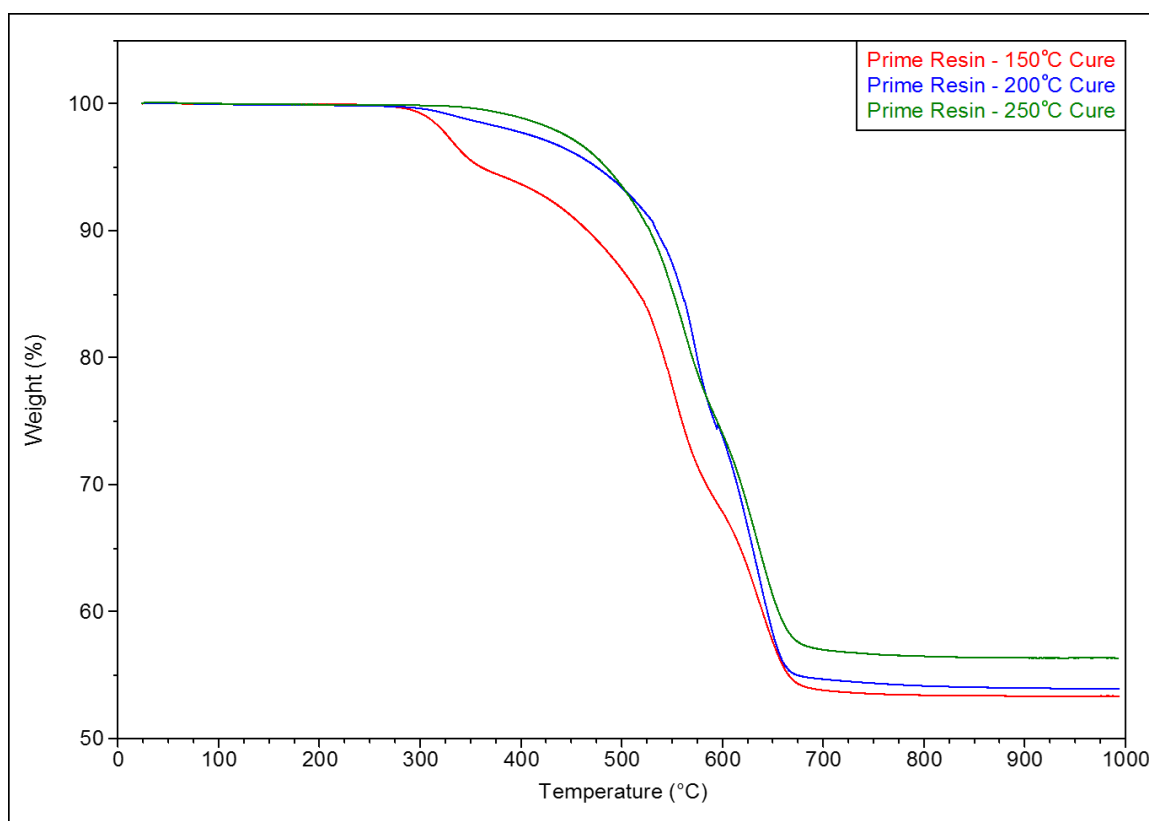


Figure 4.12 Typical TGAs in air of prime silicone resins cured at increasing temperatures

A sample of silicone resin cured at 150°C was heated to 200°C in a closed thermal desorption system to evolve only the volatiles that would come off from increasing the cure temperature from 150°C to 200°C (Figure 4.13a), which were then injected into the GC-MS. The most abundant compound detected was tributylamine (413 ppm, 46% of total volatiles), which has a boiling point of 214°C and is the main decomposition product of

TBAF. The second most abundant compound was butylated hydroxytoluene (BHT, 123 ppm, 14% of total volatiles), which has a boiling point of 265°C and was the inhibitor in the THF. These and other TBAF and BHT decomposition products (Figure D.1) accounted for 93% of the total volatiles detected. These byproducts can act as plasticizing impurities that lower network integrity, cross-link density, thermal stability, wear resistance, and adhesion. Cyclic siloxanes D₃, D₄, and D₅, which are common silicone degradation products, were detected in small quantities totaling 2.5% of volatiles.

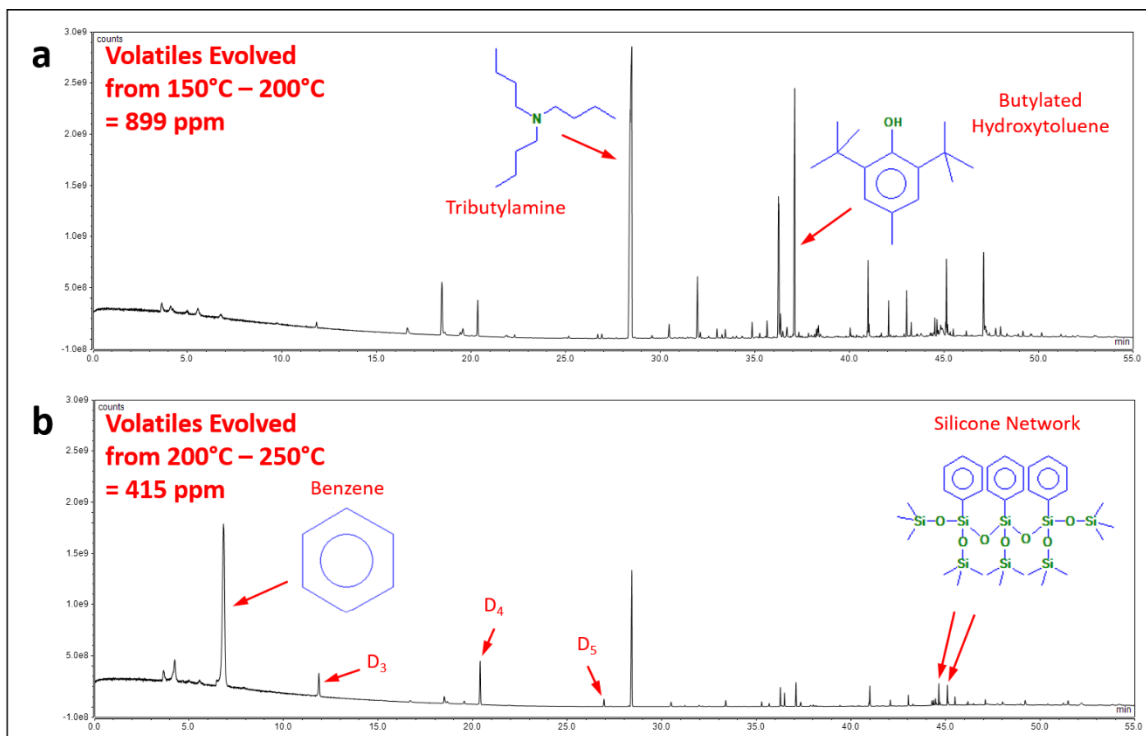
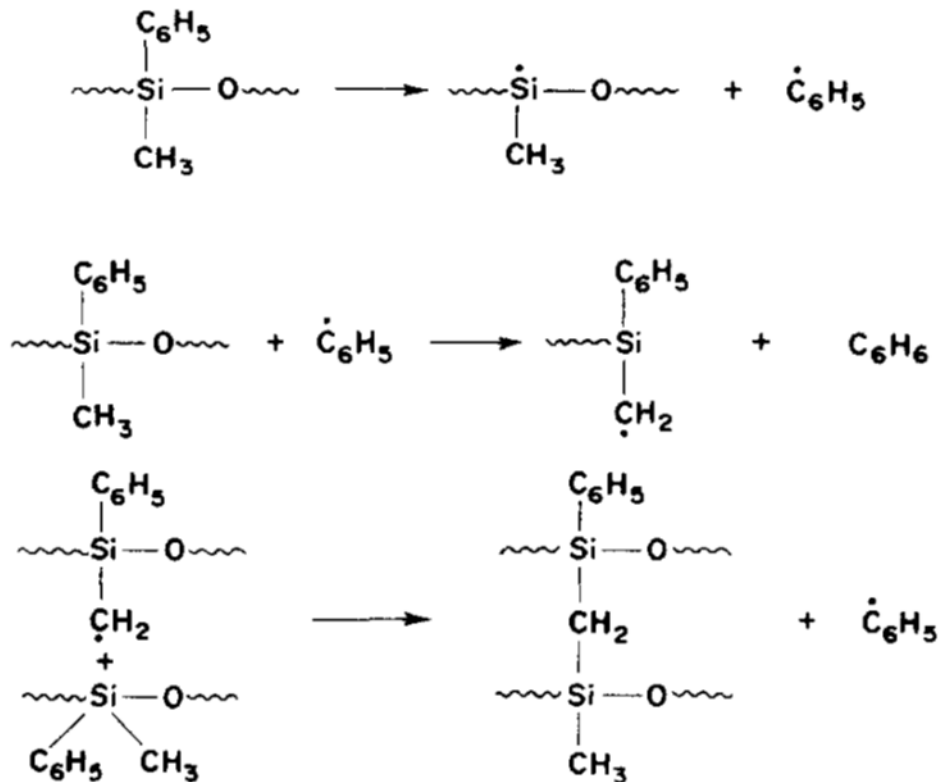


Figure 4.13 GC-MS of prime silicone resin a) cured at 150°C and tested at 150°C – 200°C, and b) cured at 200°C and tested at 200°C – 250°C to determine volatile content at different cure temperatures.

Silicone resin cured at 200°C was heated to 250°C under similar conditions to evolve only the volatiles that would come off from increasing cure from 200°C to 250°C (Figure 4.13b), which were then analyzed by GC-MS. Total amount of tributylamine, BHT, and TBAF/BHT decomposition products decreased to 116 ppm, 86% less than the resin cured at 150°C. Cyclic siloxane oligomer degradation products accounted for 10% of total volatiles. The primary compound detected was benzene (243 ppm), which accounted for 59% of all volatiles. Benzene was only detected from the resin on heating to 250°C.

A widely accepted free radical sequence (Scheme 4.1) first proposed by Sobolevski accounts for benzene evolution from mixed methyl/phenyl polysiloxanes.³⁴⁻³⁶ Si-C scission generates a phenyl radical (C₆H₅) that abstracts a hydrogen from a methyl group to form benzene (boiling point = 80°C). This also forms a methylene groups that attacks another Si atom creating a cross-link and displacing another phenyl radical. The process generates benzene while increasing cross-link density. Continuation of the process creates degradation products of small sections of the silicone network like bis[di(trimethylsiloxyl)phenylsiloxyl]trimethylsiloxylphenylsiloxane (Figure 4.13b). As the silicone resin is heated its cross-link density increases further increasing its thermal stability. The large T_{d5%} increase from raising the cure temperature up to 250°C shown above can be explained by the GC-MS findings of decreased total volatile species, increased cross-link density, and reduced organic content from benzene generation.



Scheme 4.1 Free radical sequence of phenyl/methyl silicones at elevated temperature³⁴⁻³⁶

This high degree of cross-link density for the model mixed phenyl/methyl silicone resin cured at 250°C can be calculated from the dynamic mechanical analysis (DMA) thermogram (Figure 4.14) using the rubber elasticity theory:

$$\frac{E_r}{3RT_r} = \gamma_e$$

where E_r is the storage modulus in the rubbery plateau, R is the universal gas constant, T is the temperature in the rubbery plateau taken at 30°C above the glass transition temperature (T_g), and γ_e is the cross-link density as cross-linked points per unit volume. The T_g , 237°C, taken from the peak of the $\tan \delta$ curve is quite high for a silicone, but this is expected for a highly cross-linked silicone resin. The high cross-link density, 1630 mol/m³, is a result of the high amount of T units, which is 2 T : 1 D. A second smaller peak in the $\tan \delta$ curve was observed at a lower temperature, which is likely a β transition attributed to side chain movement and small localized movements in the backbone.³⁷

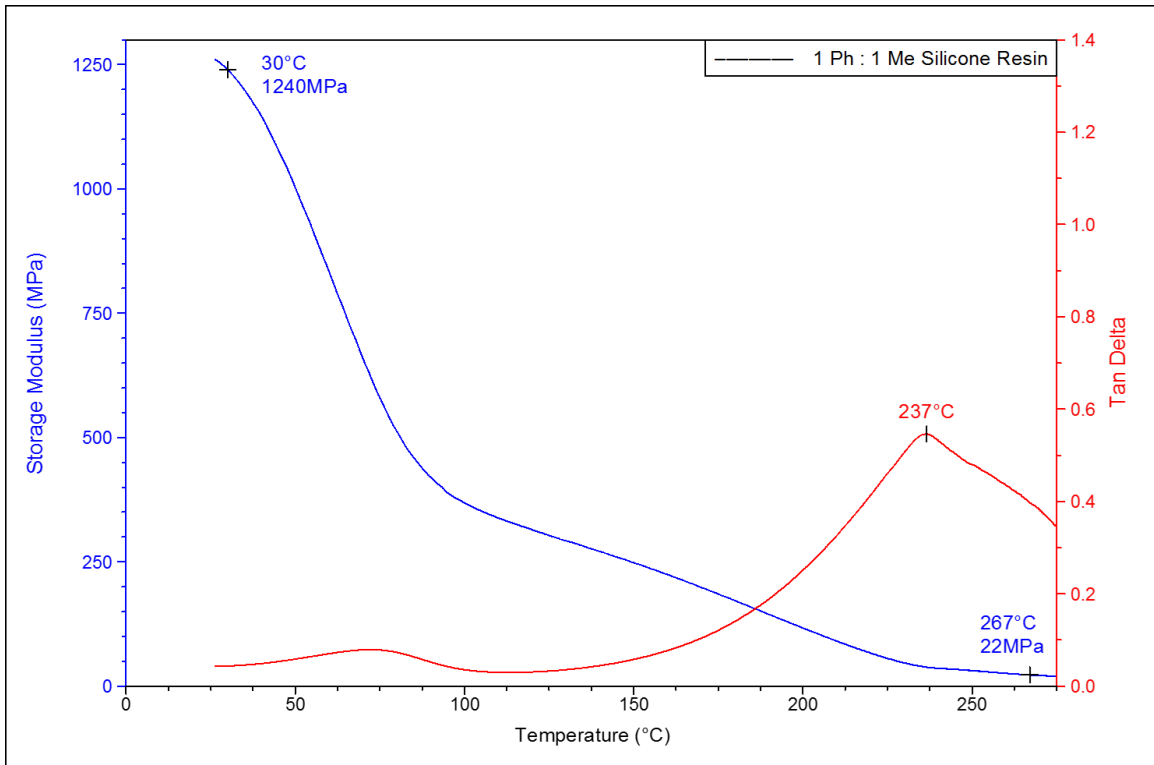


Figure 4.14 DMA of the model mixed phenyl/methyl silicone resin

The T_g of polymers are often measured by DSC and TMA as well. However, TMA is one to two orders of magnitude less sensitive to this transition than DMA and DSC is even less. Therefore it is not surprising that the T_g was not detected by DSC (Figure B.1). A T_g was detected in the first heat of the TMA thermogram (Figure 4.15) around 233°C, which is in agreement with the DMA results. However, there was not a T_g in the second heat after enthalpic relaxation occurred during the first heat and the transition had become so broad it was undetectable. The TMA also measures the dimensional change upon heating from which the coefficient of linear thermal expansion (CLTE) is calculated. It is interesting to note that the CLTE of the model silicone resin at high temperatures is $240 \mu\text{m}/(\text{m}\cdot^\circ\text{C})$, which is relatively low for a silicone as will be seen later.

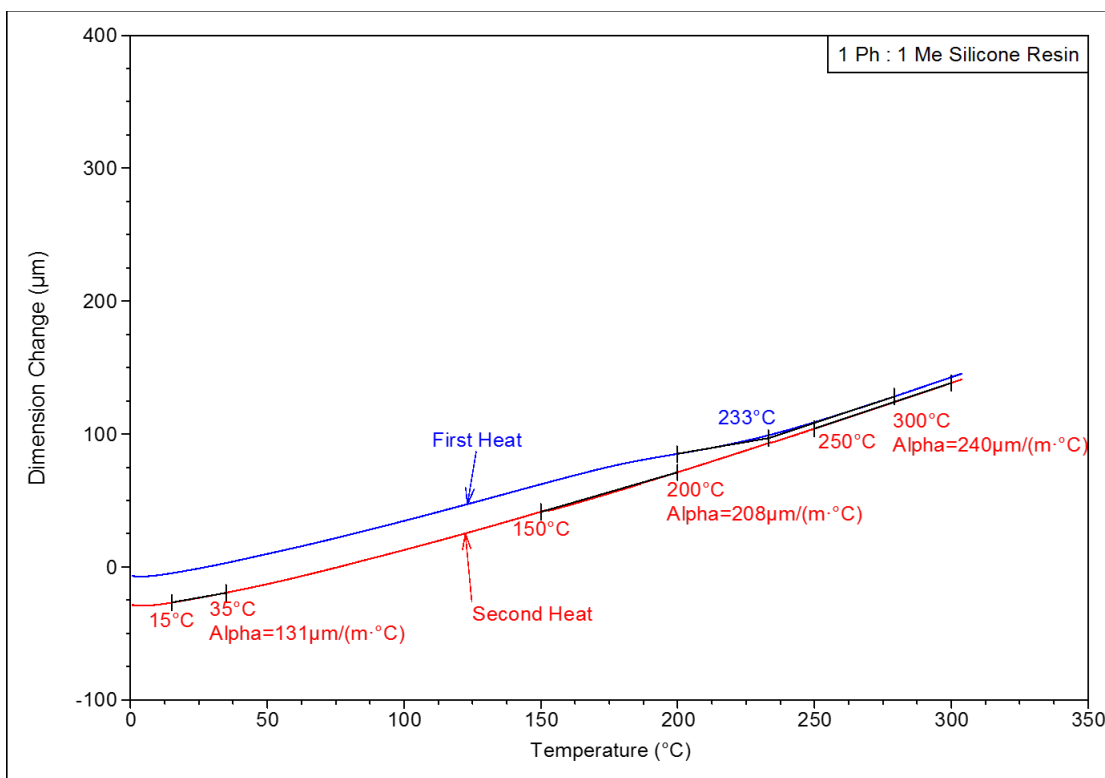


Figure 4.15 TMA of the model mixed phenyl/methyl silicone resin

4.3.2 Effect of Fluoride Ion Concentration on Recycled Silicone Resin Properties

Thin monoliths of resin were cast and cured at 250°C to produce enough material for recycling reactions. The cured resin was insoluble in THF without an F^- source. Three

concentrations were tested by controlling the molarity of the TBAF/THF: 0.002 M, 0.01 M, and 0.1 M. Dissolution time decreased with increasing F^- concentration (Table 4.1).

Dissolution of resin in 0.001 M TBAF/THF was attempted, but after stirring for 7 d the solution remained cloudy with solids. After increasing the $[F^-]$ to 0.002 M TBAF/THF the solution became clear within 24 h thus identifying the minimum threshold of F^- necessary to disassociate the silicone network into soluble species. The reaction was repeated with 0.002 M TBAF initially and the resin dissolved in approximately 6 d. The recycled resins were spray coated, cast, and tested in the same manner as described previously for prime resin samples.

Table 4.1 Cured (250°C) silicone resin dissolution time vs $[F^-]$

TBAF/THF Molarity	Dissolution Time (h)
0.002 M	144
0.01 M	18
0.1 M	6

Figure 4.16 shows the influence of $[F^-]$ in the recycling solution on the wear resistance of the recycled silicone resin coatings cured at 250°C. The initial WCA of the resin recycled in 0.01 M TBAF was similar to the prime coating. The coating of resin recycled with the highest $[F^-]$ solution, 0.1 M TBAF, was hydrophilic with an initial WCA $< 90^\circ$. The coating was non-uniform with patches of Al substrate exposed and exhibited a significant loss of coating after 200 wear cycles (Figure 4.17). The high $[F^-]$ could have resulted in the formation of many Si-F bonds in the polymer that readily converted to hydrophilic Si-OH in the presence of adventitious water and were continually replenished as wear created new surfaces. Formation of Si-F bonds would also prevent formation of Si-O_{3/2} or SQ linkages thus reducing the cross-link density and wear resistance. F was not detected by EDS in any of the thin films or in monoliths of resin recycled with 0.002 or 0.01 M TBAF, but F was present in the monolith cast from resin recycled with 0.1 M TBAF

solution (Figure 4.18). Thus, the fluorine remains in the recycled resin, but under optimal recycling conditions, 0.01M TBAF, the amount is too low to be detected by EDS.

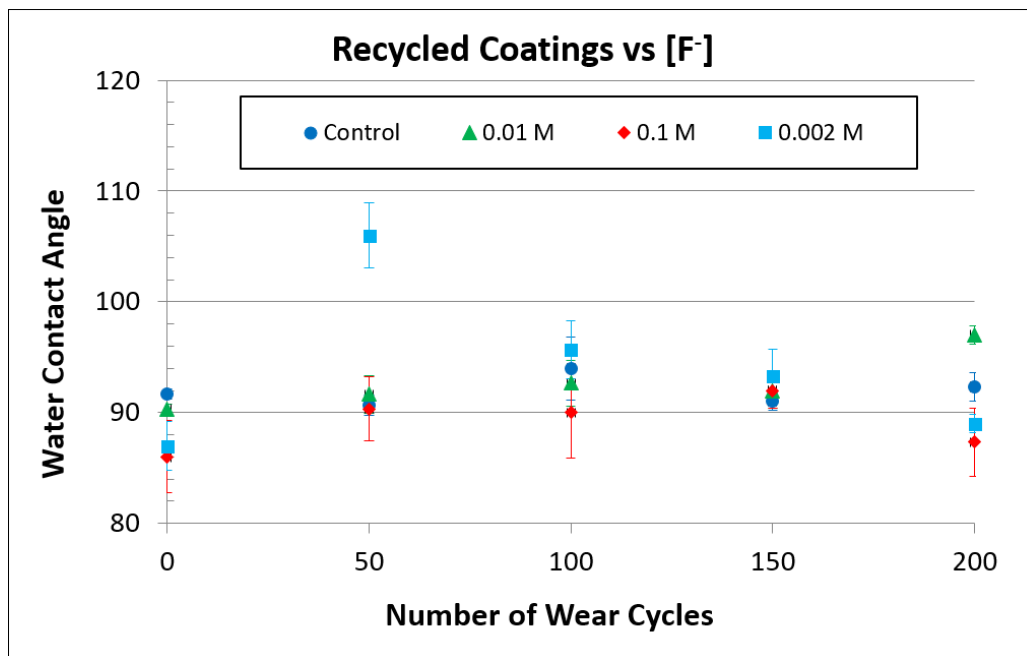


Figure 4.16 WCA vs number of wear cycles at various [F⁻]

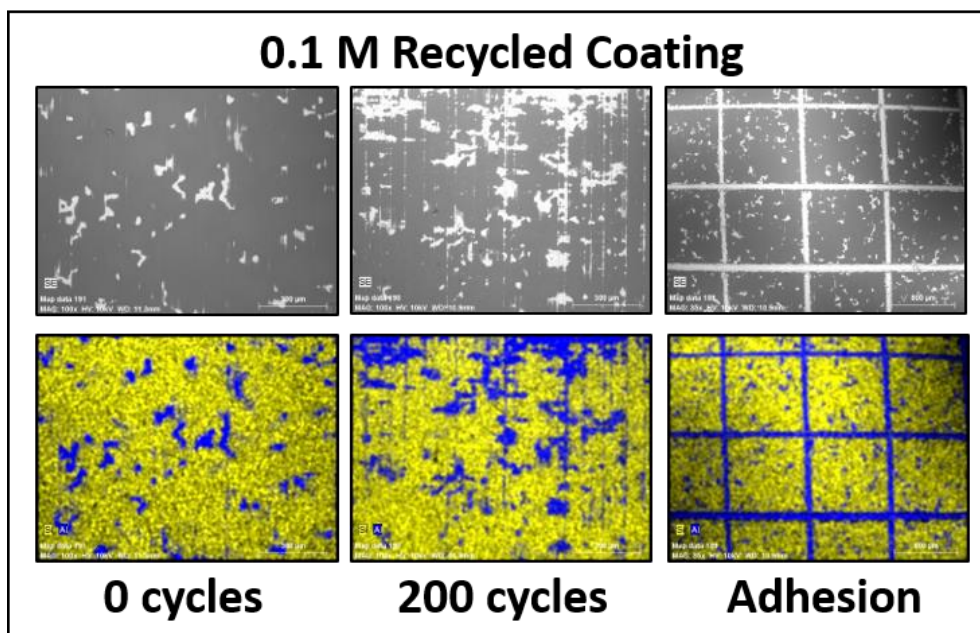


Figure 4.17 SEM-EDS images of recycled (0.1M TBAF/THF) silicone resin coatings cured at 250°C before and after 200 wear cycles and cross-hatch tape adhesion test. Wear

micrograph magnification 100x, scale bar 300 μm . Cross-hatch magnification 35x, scale bar 800 μm , EDS map: yellow = Si, blue = Al.

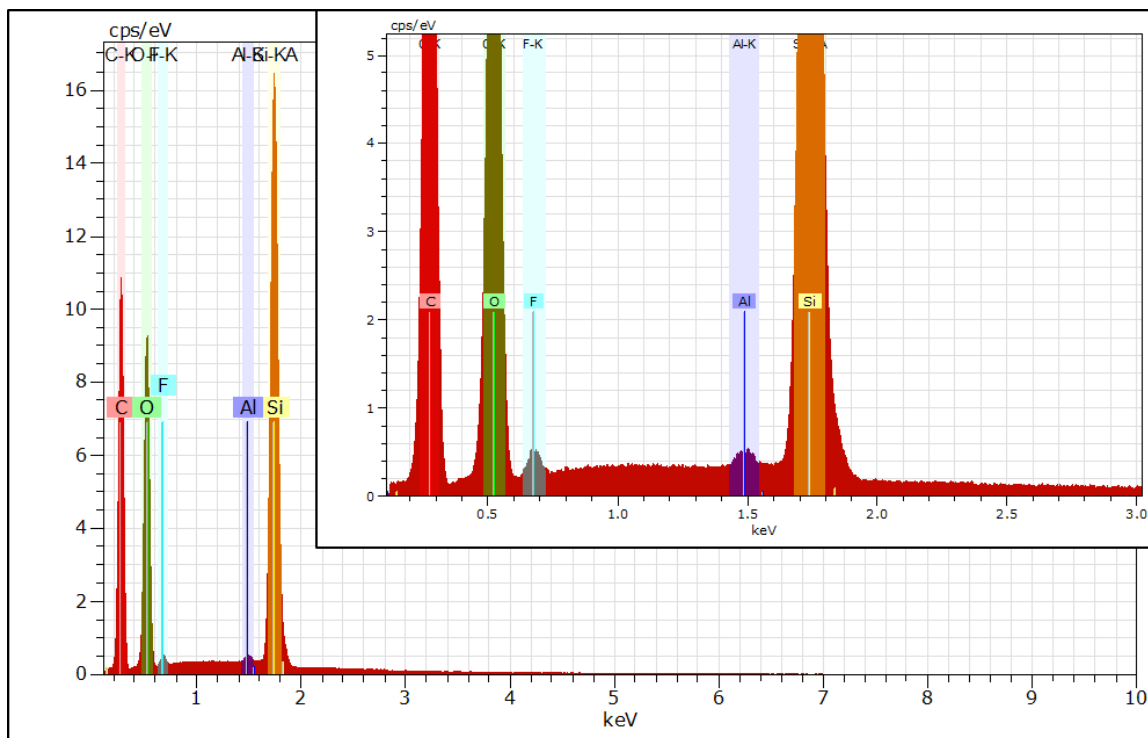


Figure 4.18 EDS shows F in silicone resin recycled with 0.1 M TBAF/THF

As stated above, the minimum $[\text{F}^-]$ required to dissolve the highly cross-linked silicone resin was 0.002 M TBAF/THF. The coating from this recycled resin was also non-uniform (Figure 4.19), hydrophilic both initially and after 200 wear cycles (Figure 4.16), and soft enough to roughen after 50 wear cycles as suggested by the WCA increase from $87^\circ \pm 2^\circ$ to $106^\circ \pm 3^\circ$. An F^- deficient system may lead to an insufficient number of active Si atoms necessary to reform the highly cross-linked network upon solvent removal resulting in poor wear resistance. The coating system also displayed the worst substrate adhesion of all experiments due to the inadequate reformation of the resin network.

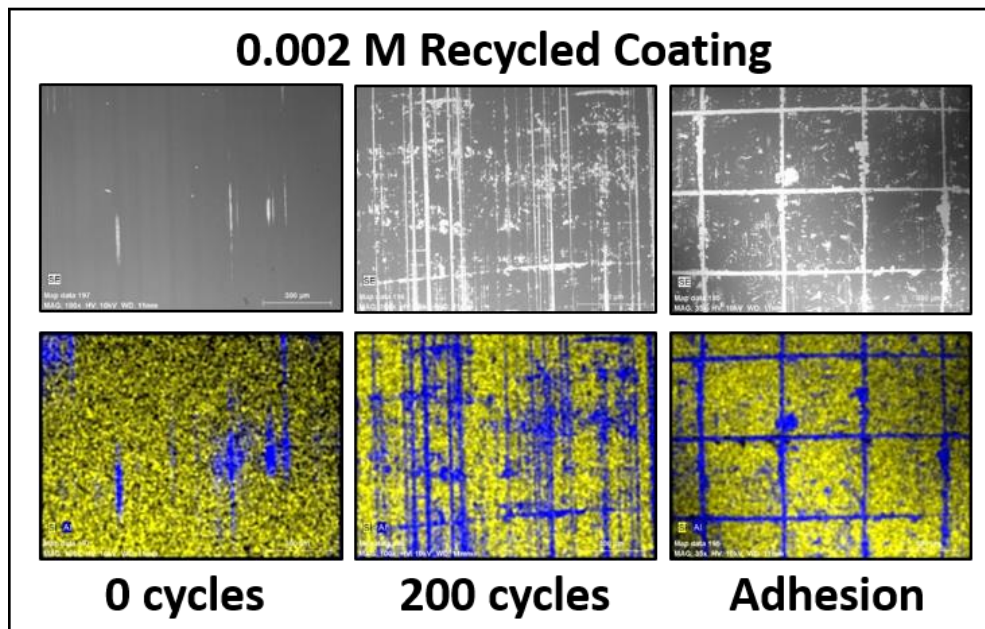


Figure 4.19 SEM-EDS images of recycled (0.002M TBAF/THF) silicone resin coatings cured at 250°C before and after 200 wear cycles and cross-hatch tape adhesion test. Wear micrograph magnification 100x, scale bar 300 μm . Cross-hatch magnification 35x, scale bar 800 μm , EDS map: yellow = Si, blue = Al.

The optimal [F] for recycling the model phenyl/methyl silicone resin was determined to be 0.01 M TBAF/THF. SEM-EDS images of these recycled resin coatings after 200 wear cycles show an intact and complete coating layer with no exposure of Al coupon substrate (Figure 4.20). The coating integrity and adhesion appears to be very similar to the prime coatings (Figure 4.11). Coating adhesion test results also indicated excellent adhesion to the Al substrate. When cured at 250°C, this model silicone resin forms a hard, adherent, wear resistant, and hydrophobic coating that can be easily recycled and reapplied with retention of key mechanical properties.

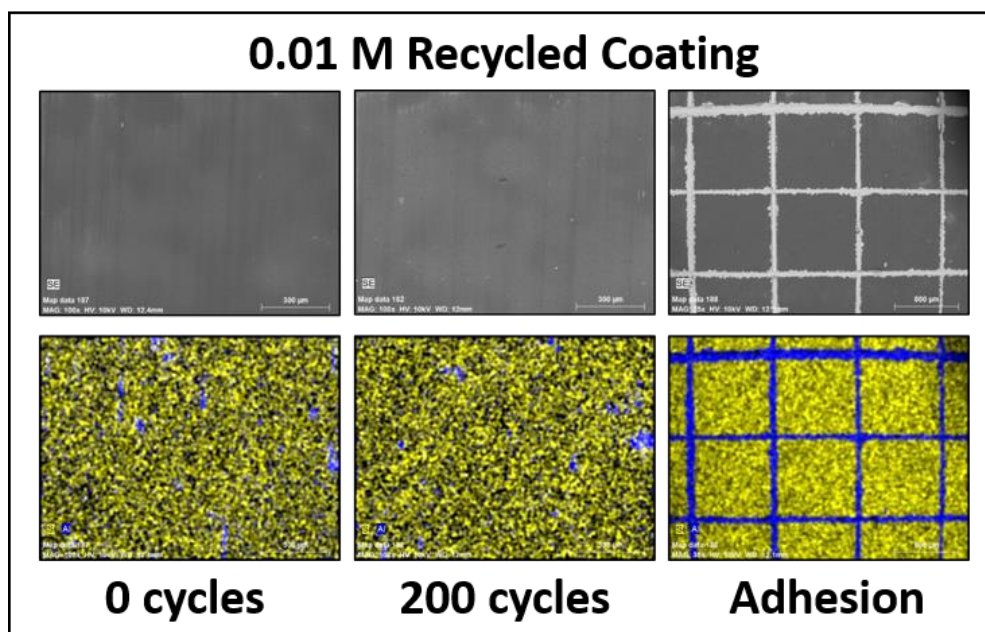


Figure 4.20 SEM-EDS images of recycled (0.01M TBAF/THF) silicone resin coatings cured at 250°C before and after 200 wear cycles and cross-hatch tape adhesion test. Wear micrograph magnification 100x, scale bar 300 μm . Cross-hatch magnification 35x, scale bar 800 μm , EDS map: yellow = Si, blue = Al.

Resins recycled with 0.01 M TBAF had nearly the same $T_{d5\%}$ as the prime resin indicating no significant loss of thermal stability (Figure 4.21, Table 4.2). GC-MS showed similar levels of volatiles in both the prime and 0.01 M TBAF recycled resin cured at 250°C (Figure 4.22). This evidence suggests that the dissolution and reformation of the silicone under these conditions sufficiently rebuilds a robust network. However, the $T_{d5\%}$ of silicone resin recycled with 0.1 M TBAF decreased 51°C to 432 ± 6 °C due to a mass loss event below 400°C. This is attributed to the order of magnitude increase in TBAF concentration, which resulted in a 5x increase in TBAF degradation products (Figure 4.23). In addition, a 2x increase benzene detected suggests the F^- promotes benzene evolution. The presence of F in the silicone network would create less steric hindrance, compared to a phenyl group, for the phenyl radical to abstract an H from a neighboring methyl group per the free radical mechanism described above (Scheme 4.1).

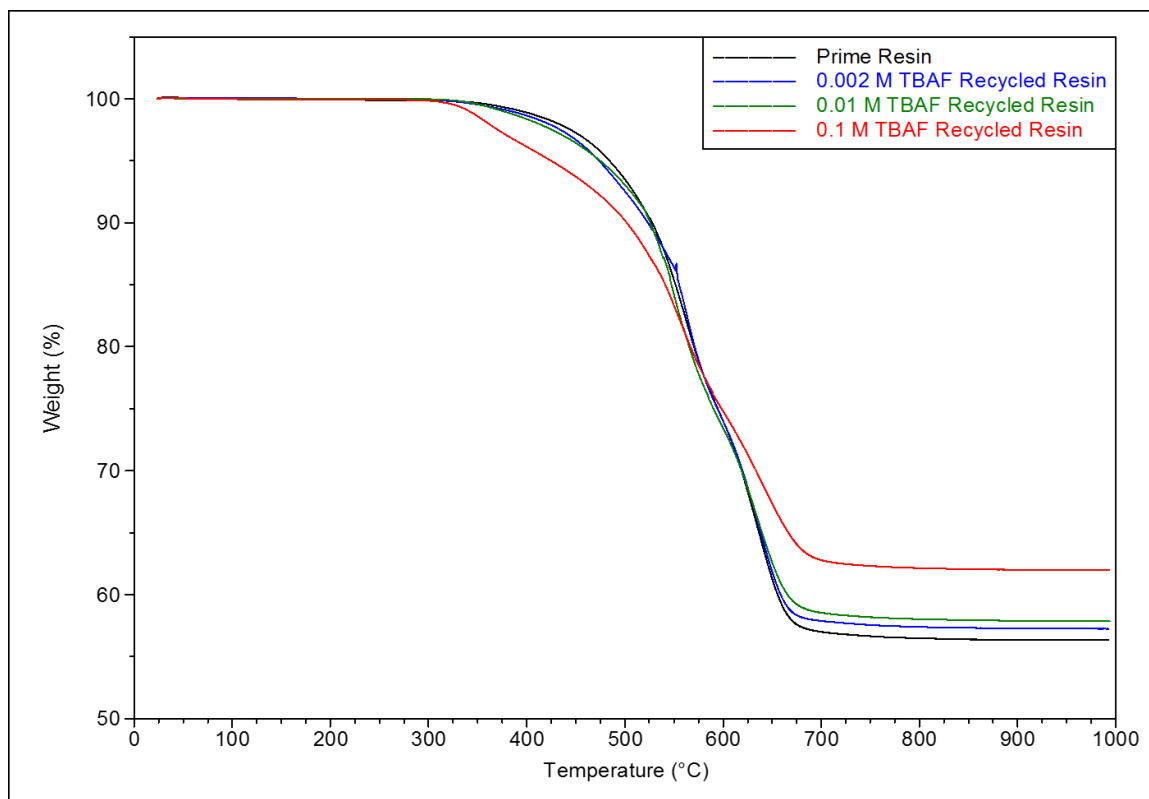


Figure 4.21 Typical TGAs in air of prime and recycled silicone resins with increasing [F⁻]

Table 4.2 Silicone resin thermal stability vs [F⁻]

TBAF/THF Molarity	Avg. T _{d5%}	Δ Avg. T _{d5%}
Prime	483 ± 7 °C	-
0.002 M	472 ± 2 °C	- 11 °C
0.01 M	478 ± 2 °C	- 5 °C
0.1 M	432 ± 6 °C	- 51 °C

A study of cure temperature versus recycled silicone resin properties at the optimal F⁻ concentration was also conducted and is provided in Appendix C. The trends were similar to the cure temperature study for the prime silicone resin essentially confirming 250°C is the optimal cure temperature.

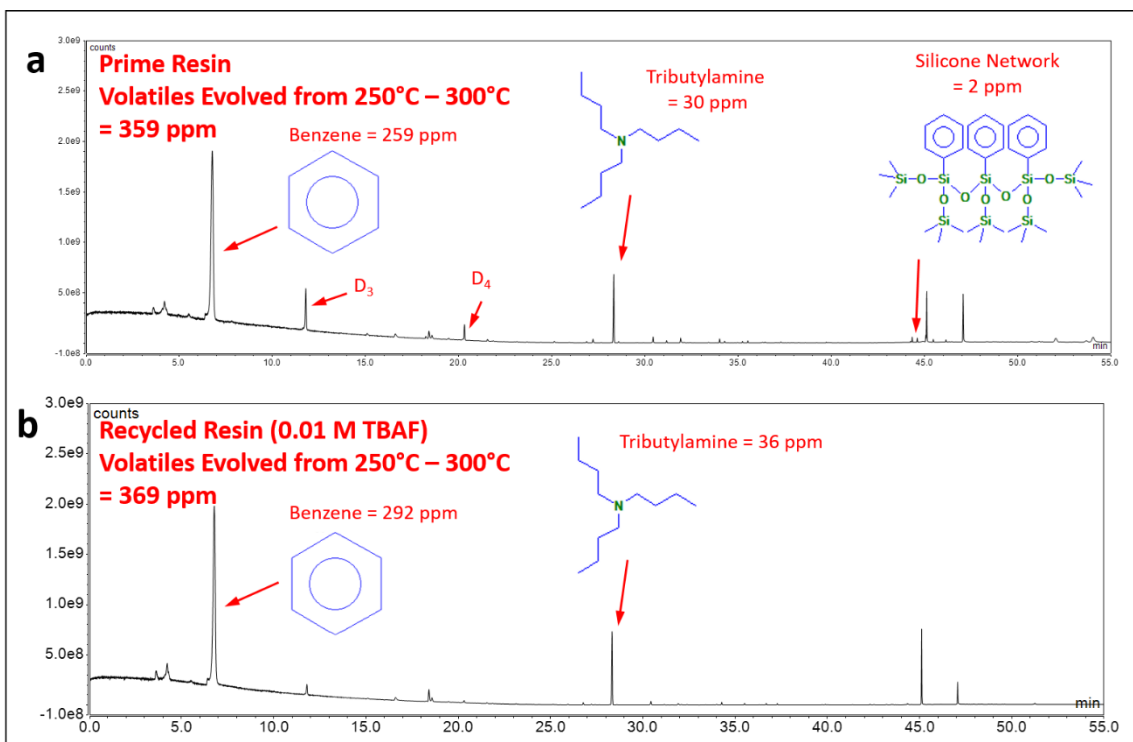


Figure 4.22 GC-MS of a) prime and b) recycled (0.01 M TBAF/THF) silicone resins cured at 250°C and tested at 250°C – 300°C to determine volatile content

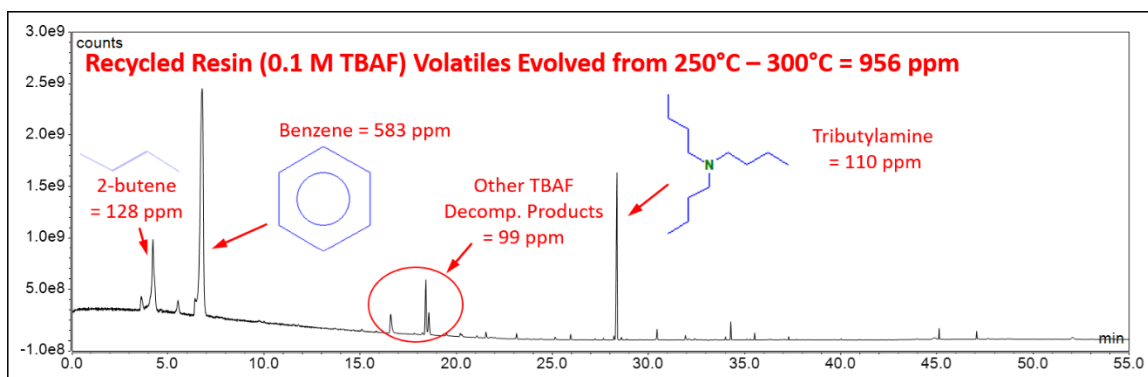


Figure 4.23 GC-MS of recycled (0.1 M TBAF/THF) silicone resins cured at 250°C and tested at 250°C – 300°C to determine volatile content

4.3.3 Recycling Commercial Silicones under Optimized Conditions

Optimized recycling conditions (0.01 M TBAF/THF at RT) were used to evaluate our technique on a commercial mixed phenyl/methyl silicone resin. A monolith of SILRES REN 50 (Wacker Chemie) was cured to 250°C in the same manner as the model phenyl/methyl silicone resin as described above. SILRES has a phenyl to methyl ratio of

0.82 : 1 and is typically used in heat and weather resistant coatings due to its combination of hydrophobicity, anti-corrosion, and thermal stability properties. The ratio of T : D (or Q or M) is unknown, but the DMA (Figure 4.24) indicates it is lower than the model phenyl/methyl silicone resin. This can be concluded by the lower T_g (104°C) and calculated cross-link density ($\gamma_e = 60 \text{ mol/m}^3$). Further confirmation was provided by the TMA (Figure B.2), which shows SILRES has a lower T_g and higher CLTE at both ambient and high temperature ranges compared to the model silicone. Similar to the model silicone resin, the T_g could not be detected by DSC (Figure B.3)

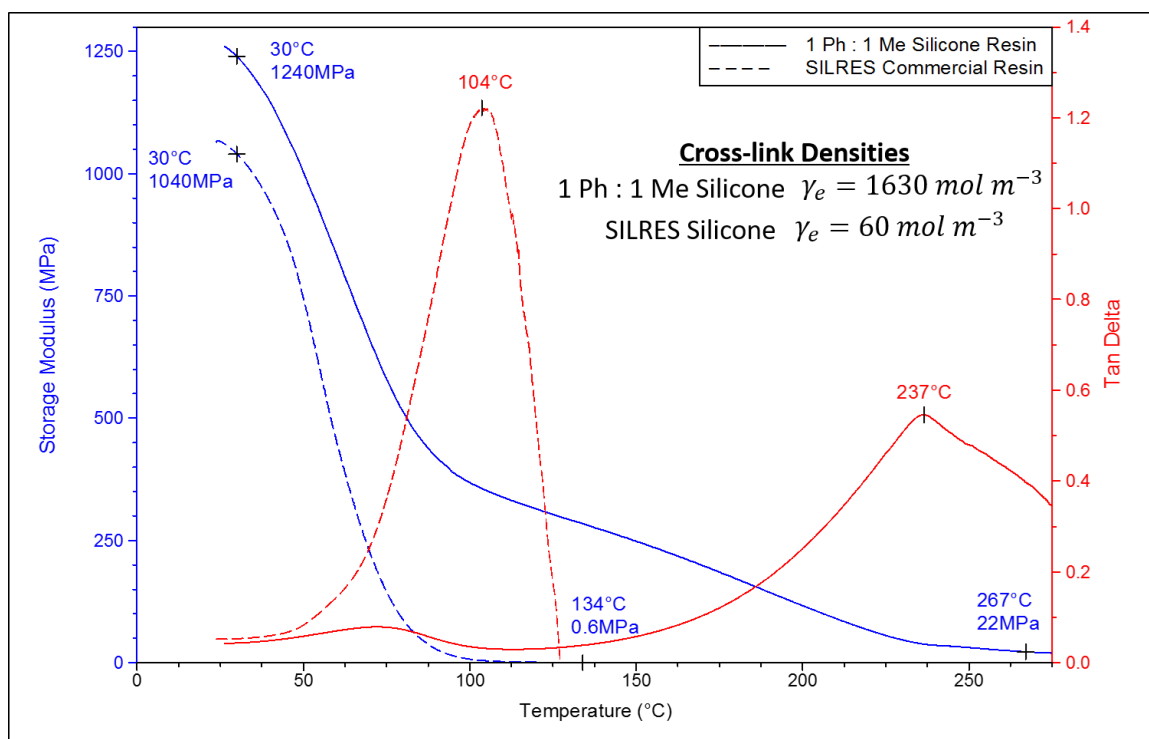


Figure 4.24 DMA of SILRES compared to the model mixed phenyl/methyl silicone resin

Pieces of SILRES cured at 250°C stirred at RT in 0.01 M TBAF/THF completely dissolved in 55 min (Figure 4.25). The cured resin is insoluble in THF alone as well as toluene and xylene. A 10 wt % solution of recycled SILRES was spray coated on clean Al coupons and cured at 250°C . Thin monoliths were cast for TGA and GC-MS. A coating and monolith of prime SILRES were also prepared for baseline properties and comparison.

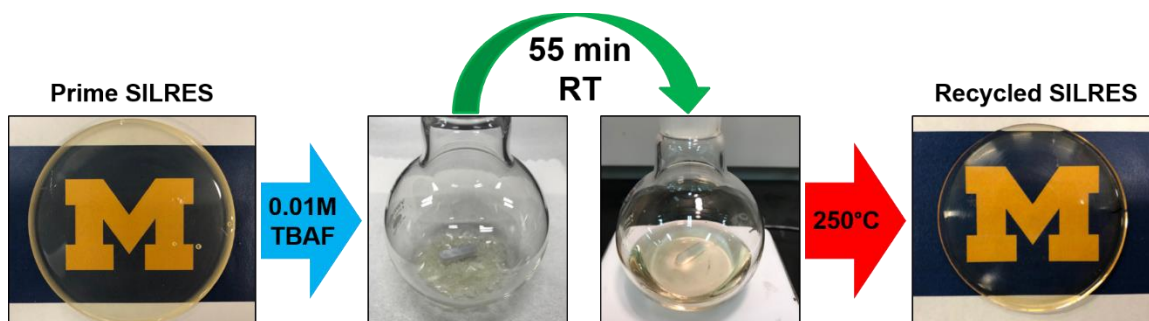


Figure 4.25 SILRES cured at 250°C dissolves in 55 min in presence of F⁻

The initial WCAs for both the prime and recycled coatings were 90° (Figure 4.26). After 50-200 wear cycles the prime coating was roughened and then significantly worn away as indicated by the abrupt increase in WCA to $116 \pm 4^\circ$ after 50 cycles followed a decline. The SEM analysis (Figure 4.27) confirms that much of the prime coating was worn away after 200 wear cycles. The SEM image of the initial prime coating also showed small areas of substrate indicating the coating is not uniform as applied.

The recycled SILRES coating showed little WCA change over 200 wear cycles varying only by $\leq 5^\circ$. SEM analysis confirmed the recycled coating had better retention of the coating after 200 wear cycles (Figure 4.28). After the recycling reaction, the reformed network was more wear resistant. The results of the tape adhesion test showed no significant difference between the prime and recycled SILRES coatings.

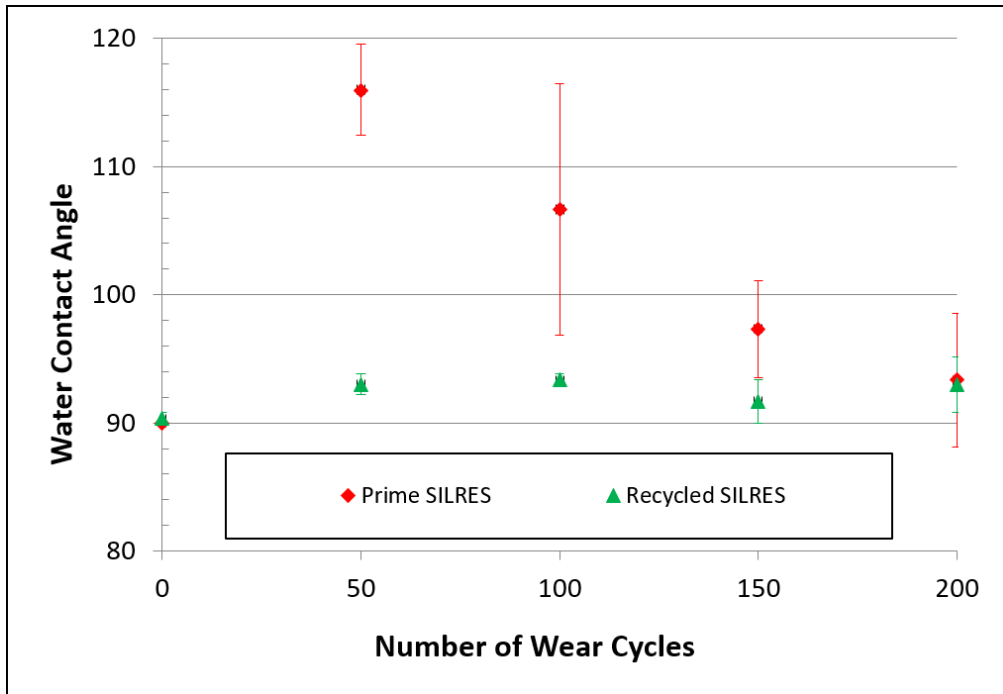


Figure 4.26 WCA versus number of wear cycles for prime and recycled SILRES

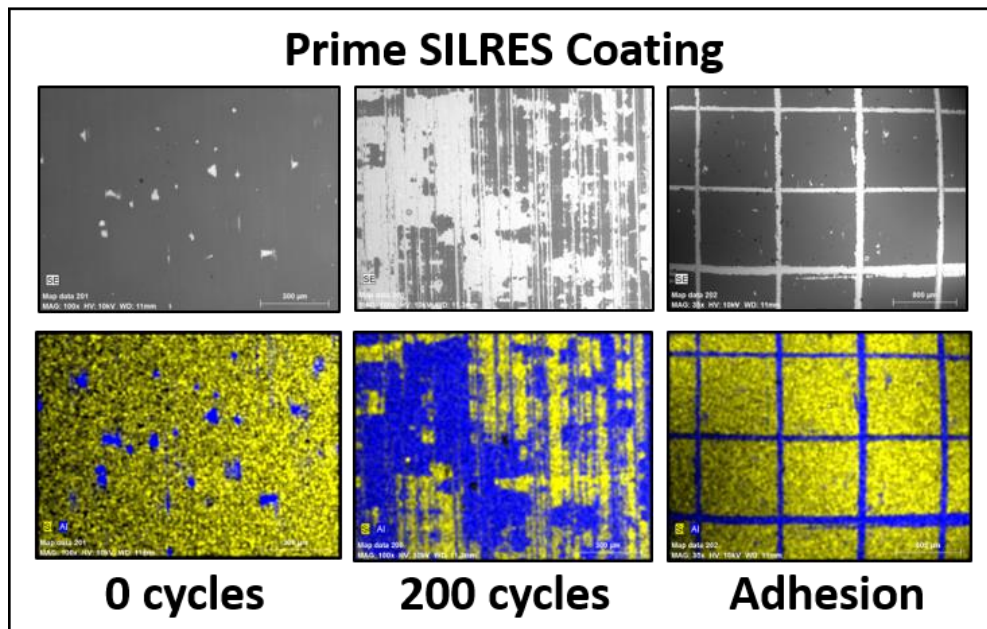


Figure 4.27 SEM-EDS images of prime SILRES coatings cured at 250°C before and after 200 wear cycles and cross-hatch tape adhesion test. Wear micrograph magnification 100x, scale bar 300 μm. Cross-hatch magnification 35x, scale bar 800 μm, EDS map: yellow = Si, blue = Al.

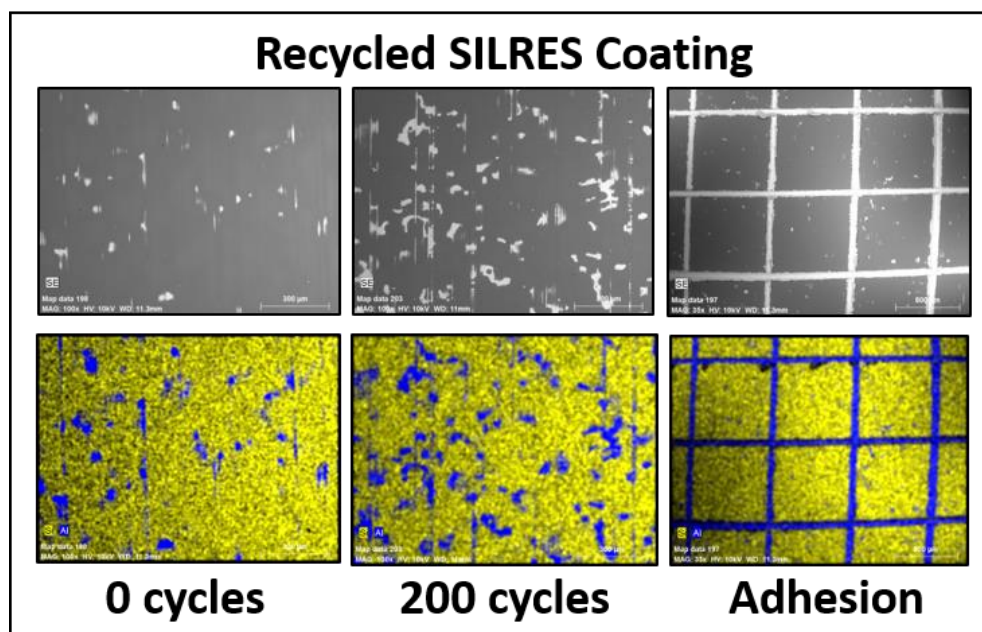


Figure 4.28 SEM-EDS images of recycled (0.01M TBAF/THF) SILRES coatings cured at 250°C before and after 200 wear cycles and cross-hatch tape adhesion test. Wear micrograph magnification 100x, scale bar 300 μm . Cross-hatch magnification 35x, scale bar 800 μm , EDS map: yellow = Si, blue = Al.

The thermal stability of the SILRES was also significantly improved after recycling via the optimized F^- rearrangement reaction. The $T_{d5\%}$ of the recycled SILRES was 73°C higher compared to the prime resin (Figure 4.29). The mechanical and thermal property improvement after recycling are attributed to the formation of a more cross-linked network as evidenced by GC-MS spectra (Figure 4.30) and DMA curves (Figure 4.31). The GC-MS spectrum showed 13x less silicone network degradation products evolved from the recycled SILRES compared to the prime resin between 250 and 300°C. The spectrum of the recycled SILRES also showed the evolution of benzene, which induces further cross-linking upon heating as described above. No benzene evolved from the prime SILRES, which also supports the concept that the presence of Si-F in the network promotes benzene evolution at lower temperatures as previously stated. The butanol detected in the prime SILRES comes from the solvent carrier and could act as a plasticizer contributing to lower wear and thermal resistance.

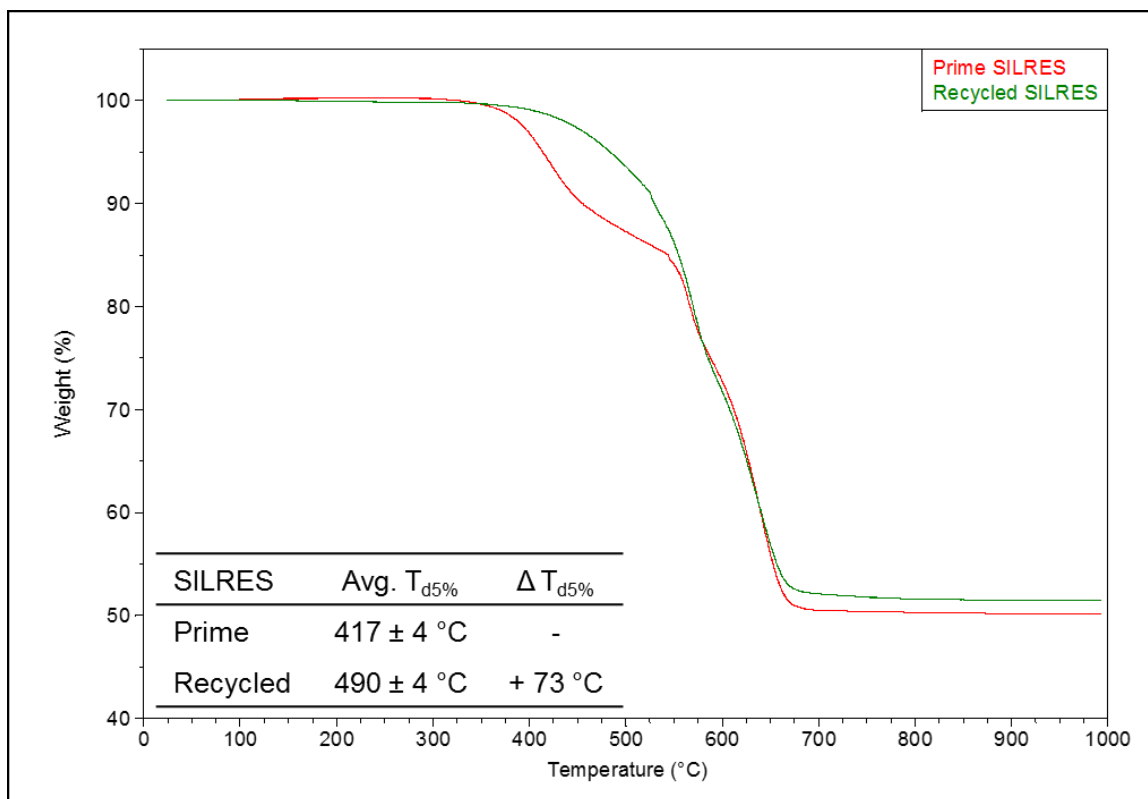


Figure 4.29 Typical TGAs of prime and recycled SILRES in air

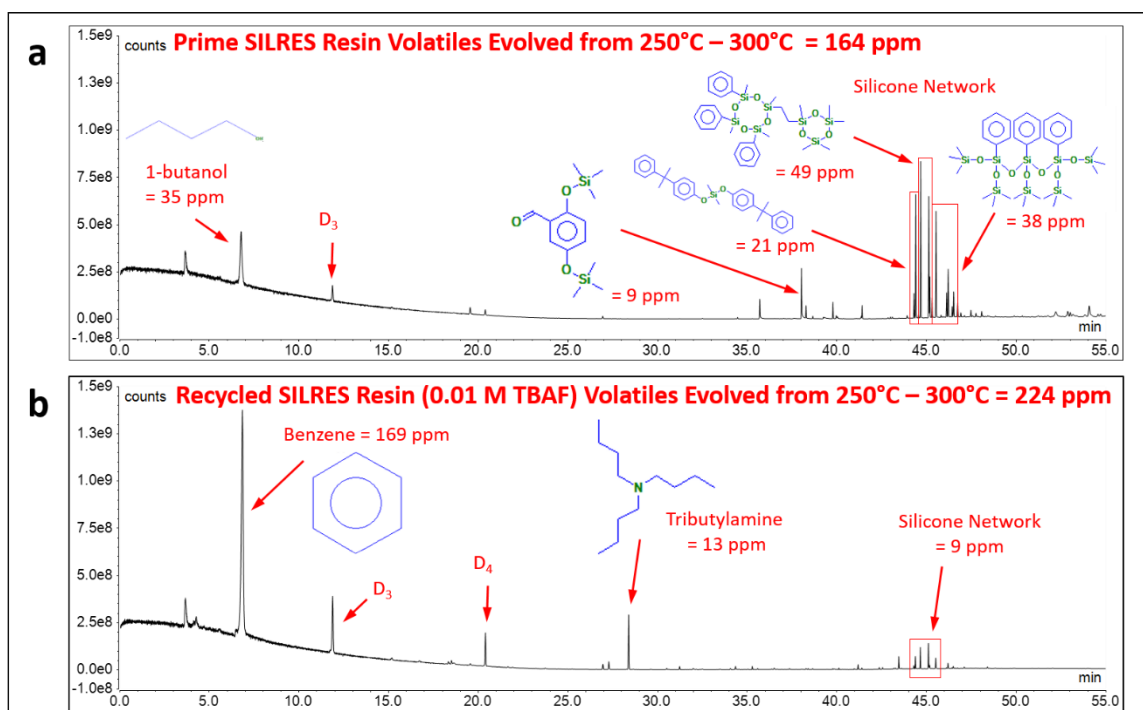


Figure 4.30 GC-MS of a) prime and b) recycled (0.01 M TBAF/THF) SILRES cured at 250°C and tested at 250°C – 300°C to determine volatile content

The storage modulus curve (solid blue, Figure 4.31) of the recycled SILRES is similar in shape versus temperature compared to the that of the model 1 Ph : 1 Me silicone resin shown above in Figure 4.24. This suggests that similar soluble species were formed during the F⁻ catalyzed rearrangement, which led to a similar network structure after the removal of solvent. The T_g of the recycled SILRES was not detected due to the gradual and continuous increase of the tan δ curve with temperature and therefore the cross-link density could not be calculated. However, the SILRES is clearly much stiffer after recycling. The storage modulus of the prime SILRES in the rubbery plateau is 0.6 MPa and at the same temperature, 134°C, the storage modulus of the recycled SILRES is three orders of magnitude higher. The storage modulus near room temperature is also higher after recycling by 22%.

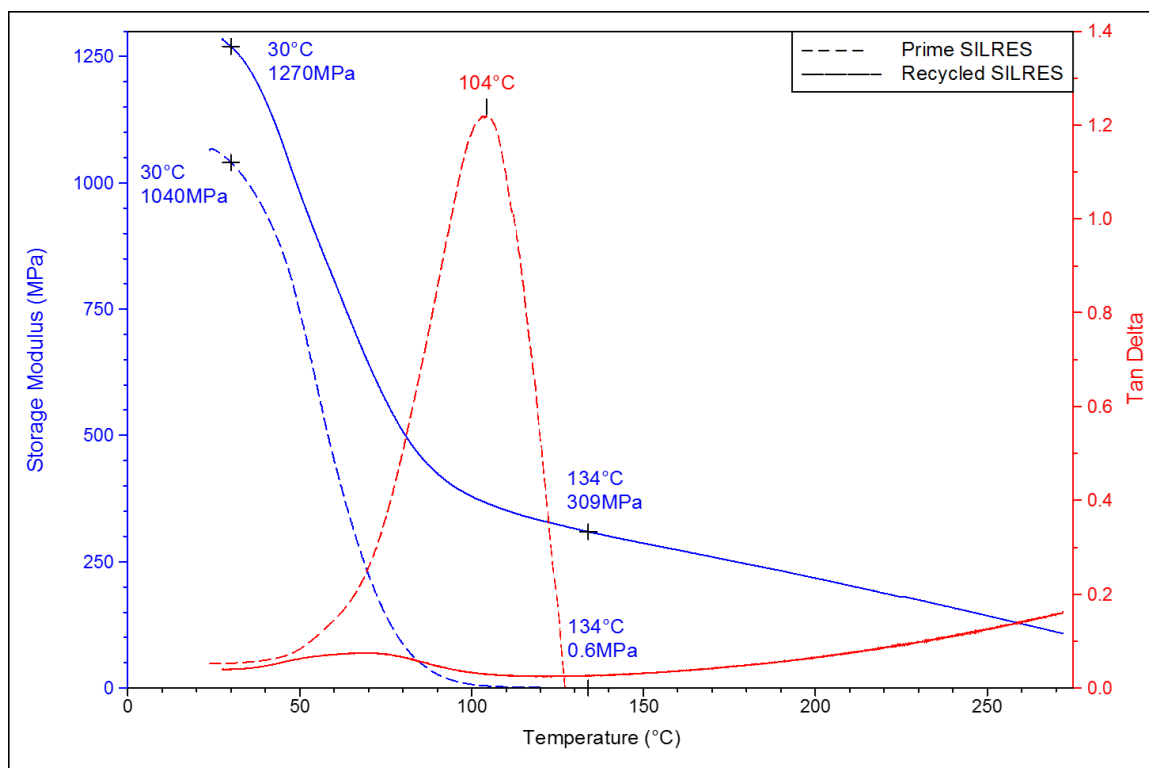


Figure 4.31 DMAs of prime and recycled SILRES silicone resins

Our technique also works for silicone rubbers, which is unsurprising since rubbers have lower cross-link densities than resins. A common, flexible room temperature cured silicone rubber, ELASTOSIL E10 (Wacker Chemie), dissolved in less than 15 minutes when stirred

in 0.01 M TBAF/THF at RT (Figure 4.32). Thus, our new technique for recycling silicones with a catalytic amount of F^- under ambient conditions not only works for the lab-made model phenyl/methyl silicone resin, but commercially relevant silicone resin and rubber as well.

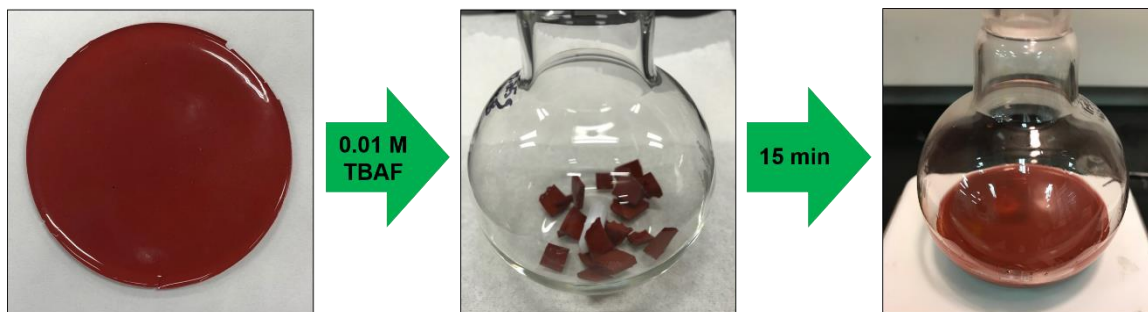


Figure 4.32 Dissolution of RTV silicone ELSATOSIL in the presence of F^- in 15 min

4.4 Conclusions

Wear resistance, adhesion, and thermal stability of the methyl/phenyl silicone resin were maximized after curing at 250°C. The cured resin was insoluble in THF and common silicone solvents (toluene, xylene), but in the presence of F^- all D and T units equilibrate to solubilize the resin in THF at room temperature. *This solubility equilibrium provides the opportunity to add new silicone structural units and functionality to the system if desired*, which will be explored in Chapter 5. The polymeric network then reforms after and only after solvent removal.

Under optimized recycling conditions (0.01 M TBAF) second generation coatings and monoliths retain pertinent mechanical and thermal properties. Room temperature chemical recycling techniques for thermosets are rare and non-existent for silicone resins with only catalytic amounts of reagent to the best of our knowledge. Furthermore, the process can be considered closed-loop because of the nearly 100% retention of wear and thermal properties making it more sustainable than mechanical/thermal recycling or landfilling.

Most importantly, we have shown our method also works for a widespread commercial silicone resin and rubber. Other silicone recycling techniques that do not rely on large

amounts of harmful reagents, high temperature, high pressure, etc. for depolymerization rely on the construction of niche silicones with reversible cross-links. These de-crosslinking techniques result in the loss of key properties such as thermal stability or mechanical properties. Here, we have demonstrated not only the retention of pertinent properties of a commercial silicone resin, but also the possibility of up-cycling due to improved wear and thermal resistance after recycling.

4.5 References

1. Moretto, H. H., Schulze, M., & Wagner, G. In *Ullmann's Encyclopedia of Industrial Chemistry*; Wiley-VCH: Weinheim, Germany, 2012; Chapter Silicones, pp 675-712.
2. Murphy, C. M.; Saunders, C. E.; Smith, D. C. Thermal and Oxidation Stability of Polymethylphenylsiloxanes. *Ind. Eng. Chem.* **1950**, *42*, 2462-2468.
3. Hanu, L. G.; Simon, G. P.; Cheng, Y. -B. Thermal Stability and Flammability of Silicone Polymer Composites. *Polym. Degrad. Stab.* **2006**, *91*, 1373-1379.
4. Hamdani, S.; Longuet, C.; Perrin, D.; Lopez-Cuesta, J. M.; Ganachaud, F. Flame Retardancy of Silicone-Based Materials. *Polym. Degrad. Stab.* **2009**, *94*, 465-495.
5. Abbasi, F.; Mirzadeh, H.; Katbab, A. A. Modification of Polysiloxane Polymers for Biomedical Applications: A Review. *Polym. Int.* **2001**, *50*, 1279-1287.
6. Lucas, P.; Robin, J. J. In *Advances in Polymer Science: Functional Materials and Biomaterials*; Springer-Verlag: Berlin, Germany 2007; Vol. 209, Chapter Silicone-Based Polymer Blends: An Overview of the Materials and Processes, pp 111-147.
7. Ma, M.; Hill, R.M.; Superhydrophobic Surfaces. *Curr. Opin. Colloid Interface Sci.* **2006**, *11*, 193-202.
8. Yilgor, E.; Yilgor, I. Silicone Containing Copolymers: Synthesis, Properties and Applications. *Prog. Polym. Sci.* **2014**, *39*, 1165-1195.
9. Gong, D.; Long, J.; Jiang, D.; Fan, P.; Zhang, H.; Li, L.; Zhong, M. Robust and Stable Transparent Superhydrophobic Polydimethylsiloxane Films by Duplicating via a Femtosecond Laser-Ablated Template. *ACS Appl. Mater. Interfaces* **2016**, *8*, 17511-17518.
10. Ghosh, A.; Antony, P.; Bhattacharya, A. K.; Bhowmick, A. K.; De, S. K. Replacement of Virgin Rubbers by Waste Ground Vulcanizates in Blends of Silicone Rubber and Fluororubber Based on Tetrafluoroethylene/Propylene/Vinylidene Fluoride Terpolymer. *J. Appl. Polym. Sci.* **2001**, *82*, 2326-2341.
11. Ghosh, A.; Rajeev, R. S.; Bhattacharya, A. K.; Bhowmick, A. K.; De, S. K. Recycling of Silicone Rubber Waste: Effect of Ground Silicone Rubber Vulcanizate Powder on the Properties of Silicone Rubber. *Polym. Eng. Sci.* **2003**, *43*, 279-296.
12. Salbidegoitia, J. A.; Fuentes, E. G.; Gonzalez-Marcos, M. P.; Gonzalez-Velasco, J. R. Recycle of Plastic Residues in Cellular Phones through Catalytic Hydrocracking to Liquid Fuels. *J. Mater. Cycles Waste Manag.* **2017**, *19*, 782-793.

13. Hsiao, Y. -C.; Hill, L. W.; Pappas, S. P. Reversible Amine Solubilization of Cured Siloxane Polymers. *J. Appl. Polym. Sci.* **1975**, *19*, 2817-2820.
14. Pappas, S. P.; Just, R. L. Aminolysis of Crosslinked Polysiloxanes: Tautomeric Catalysis by 2-Pyridone. *J. Polym. Sci., Polym. Chem. Ed.* **1980**, *18*, 527-531.
15. Okamoto, M.; Suzuki, S.; Suzuki, E. Polysiloxane Depolymerization with Dimethyl Carbonate Using Alkali Metal Halide Catalysts. *Appl. Catal., A* **2004**, *261*, 239-245.
16. Enthaler, S. Zinc-Catalyzed Depolymerization of End-of-Life Polysiloxanes. *Angew. Chem., Int. Ed.* **2014**, *53*, 2716-2721.
17. Enthaler, S.; Kretschmer, R. Low-Temperature Depolymerization of Polysiloxanes with Iron Catalysis. *ChemSusChem* **2014**, *7*, 2030-2036.
18. Enthaler, S. Iron-Catalyzed Depolymerization of Polysiloxanes to Produce Dichlorodimethylsilane, Diacetoxymethylsilane, or Dimethoxydimethylsilane. *J. Appl. Polym. Sci.* **2015**, 41287.
19. Weidauer, M.; Heyber, B.; Woelki, D.; Tschiersch, M.; Kohler-Krutzfeldt, A.; Enthaler, S. Iron-Catalyzed Depolymerizations of Silicones with Hexanoic Anhydride Provide a Potential Recycling Method for End-of-Life Polymers. *Eur. J. Lipid Sci. Technol.* **2015**, *117*, 778-785.
20. Dohlert, P.; Pfrommer, J.; Enthaler, S. Recycling Concept for End-of-Life Silicones: Boron Trifluoride Diethyl Etherate as Depolymerization Reagent to Produce Difluorodimethylsilane as Useful Commodity. *ACS Sustainable Chem. Eng.* **2015**, *3*, 163-169.
21. Dohlert, P.; Enthaler, S. Depolymerization Protocol for Linear, Branched, and Crosslinked End-of-Life Silicones with Boron Trifluoride Diethyl Etherate as the Depolymerization Reagent. *J. Appl. Polym. Sci.* **2015**, *132*, 42814.
22. Gou, Z.; Zuo, Y.; Feng, S. Thermally Self-Healing Silicone-Based Networks with Potential Application in Recycling Adhesives. *RSC Adv.* **2016**, *6*, 73140-73147.
23. Xiang, H. P.; Rong, M. Z.; Zhang, M. Q. A Facile Method for Imparting Sunlight Driven Catalyst-Free Self-Healability and Recyclability to Commercial Silicone Elastomer. *Polymer* **2017**, *108*, 339-347.
24. Asuncion, M. Z.; Laine, R. M. Fluoride Rearrangement Reactions of Polyphenyl- and Polyvinylsilsesquioxanes as a Facile Route to Mixed Functional Phenyl, Vinyl T₁₀ and T₁₂ Silsesquioxanes. *J. Am. Chem. Soc.* **2010**, *132*, 3723-3736.

25. Ronchi, M.; Sulaiman, S.; Boston, N. R.; Laine, R. M. Fluoride Catalyzed Rearrangements of Polysilsesquioxanes, Mixed Me, Vinyl T₈, Me, Vinyl T₁₀ and T₁₂ Cages. *Appl. Organometal. Chem.* **2010**, *24*, 551-557.
26. Jung, J. H.; Laine, R. M. Beads on a Chain (BOC) Polymers Formed from the Reaction of [NH₂PhSiO_{1.5}]_x[PhSiO_{1.5}]_{10-x} and [NH₂PhSiO_{1.5}]_x[PhSiO_{1.5}]_{12-x} Mixtures ($x=2-4$) with the Diglycidyl Ether of Bisphenol A. *Macromolecules* **2011**, *44*, 7263-7272.
27. Jung, J. H.; Furgal, J. C.; Goodson III, T.; Mizumo, T.; Schwartz, M.; Chou, K.; Vonet, J.-F.; Laine, R. M. 3-D Molecular Mixtures of Catalytically Functionalized [vinylSiO_{1.5}]₁₀/[vinylSiO_{1.5}]₁₂. Photophysical Characterization of Second Generation Derivatives. *Chem. Mater.* **2012**, *24*, 1883-1895.
28. Furgal, J. C.; Jung, J. H.; Goodson III, T.; Laine, R. M. Analyzing Structure-Photophysical Property Relationships for Isolated T₈, T₁₀, and T₁₂ Stilbenevinylsilsesquioxanes. *J. Am. Chem. Soc.* **2013**, *135*, 12259-12269.
29. Furgal, J. C.; Goodson III, T.; Laine, R. M. D_{5h} [PhSiO_{1.5}]₁₀ Synthesis via F⁻ Catalyzed Rearrangement of [PhSiO_{1.5}]_n. An Experimental/Computational Analysis of Likely Reaction Pathways. *Dalton Trans.* **2016**, *45*, 1025-1039
30. Krug, D. J.; Laine, R. M. Durable and Hydrophobic Organic-Inorganic Hybrid Coatings via Fluoride Rearrangement of Phenyl T₁₂ Silsesquioxane and Siloxanes. *ACS Appl. Mater. Interfaces* **2017**, *9*, 8378-8383.
31. Xue, F.; Jia, D.; Li, Y.; Jing, X. Facile Preparation of a Mechanically Robust Superhydrophobic Acrylic Polyurethane Coating. *J. Mater. Chem. A* **2015**, *3*, 13856-13863.
32. Wang, H.; Sun, F.; Wang, C.; Zhu, Y.; Wang, H. A Simple Drop-Casting Approach to Fabricate the Super-hydrophobic PMMA-PSF-CNFs Composite Coating with Heat-, Wear- and Corrosion-Resistant Properties. *Colloid Polym. Sci.* **2016**, *294*, 303-309.
33. Milionis, A.; Loth, E.; Bayer, I. Recent Advances in the Mechanical Durability of Superhydrophobic Materials. *Adv. Colloid Interface Sci.* **2016**, *229*, 57-79.
34. Sobolevskii, M. V.; Skorokhodov, I. I.; Ditsent, V. Ye.; Sobolevskaya, L. V.; Vovshin, E. I.; Blekk, L. M. Study of Thermal Transformations of Oligomethylphenylsiloxanes. *Vysokomol. Soedin., Ser. A* **1974** *16*, 729-734.
35. Grassie, N.; Macfarlane, I. G.; Francey, K. F. The Thermal Degradation of Polysiloxanes – II. Poly(methylphenylsiloxane). *Eur. Polym. J.* **1979**, *15*, 415-422.
36. Deshpande, G.; Rezac, M. E. The Effect of Phenyl Content on the Degradation of Poly(dimethyl diphenyl) Siloxane Copolymers. *Polym. Degrad. Stab.* **2001**, *74*, 363-370.

37. Menard, K. P. In *Dynamic Mechanical Analysis: A Practical Introduction*; CRC Press LLC: Boca Raton, FL, 1999; Chapter Time and Temperature Studies: Thermosets, pp. 103-135.

Chapter 5

In situ Modification of Recycled Silicone Resins

Fluoride ion (F^-) catalyzed rearrangement of highly cross-linked phenyl/methyl silicone resin provides an opportunity for *in situ* modification of the thermoset polymer. In the presence of F^- in THF all $RSiO_{3/2}$ and $R_2SiO_{2/2}$ units equilibrate to form soluble species. While the resin is in solution the ratio of starting materials can be altered to tailor target properties. Thermal stability was increased by $50^\circ C$ via the addition of phenyl- $SiO_{3/2}$ to increase cross-link density and phenyl content. In another *in situ* modification reaction, flexibility was increased via the addition of dimethyl- $SiO_{2/2}$. Entirely new functionalities can be introduced as well, for example, the addition of a perfluoroalkylsilane to silicone resin increased the hydrophobicity by 15° . This recycling and modification reaction offers a new technique for handling end-of-life silicone products with the potential for closed loop and even up-cycling. The adjustment or introduction of functionalities allows one to repurpose a low grade waste stream feedstock into second generation materials for more demanding applications.

5.1 Introduction

As described in Chapter 4, highly cross-linked thermoset silicone resins can be recycled in a THF solution containing catalytic amounts of fluoride ion.¹ The insoluble resin becomes soluble in solution by equilibrating all $\text{RSiO}_{3/2}$ and $\text{R}_2\text{SiO}_{2/2}$ units in the resin.¹⁻⁹ This recycling loop is represented by the green arrows in Figure 5.1. The solubilization of the resin presents a unique opportunity for *in situ* modification of a thermoset polymer. Once the silicone resin is dissolved new functionality can be introduced by the addition of functionalized silanes, siloxanes, or silsesquioxanes to the recycling solution (Figure 5.1).

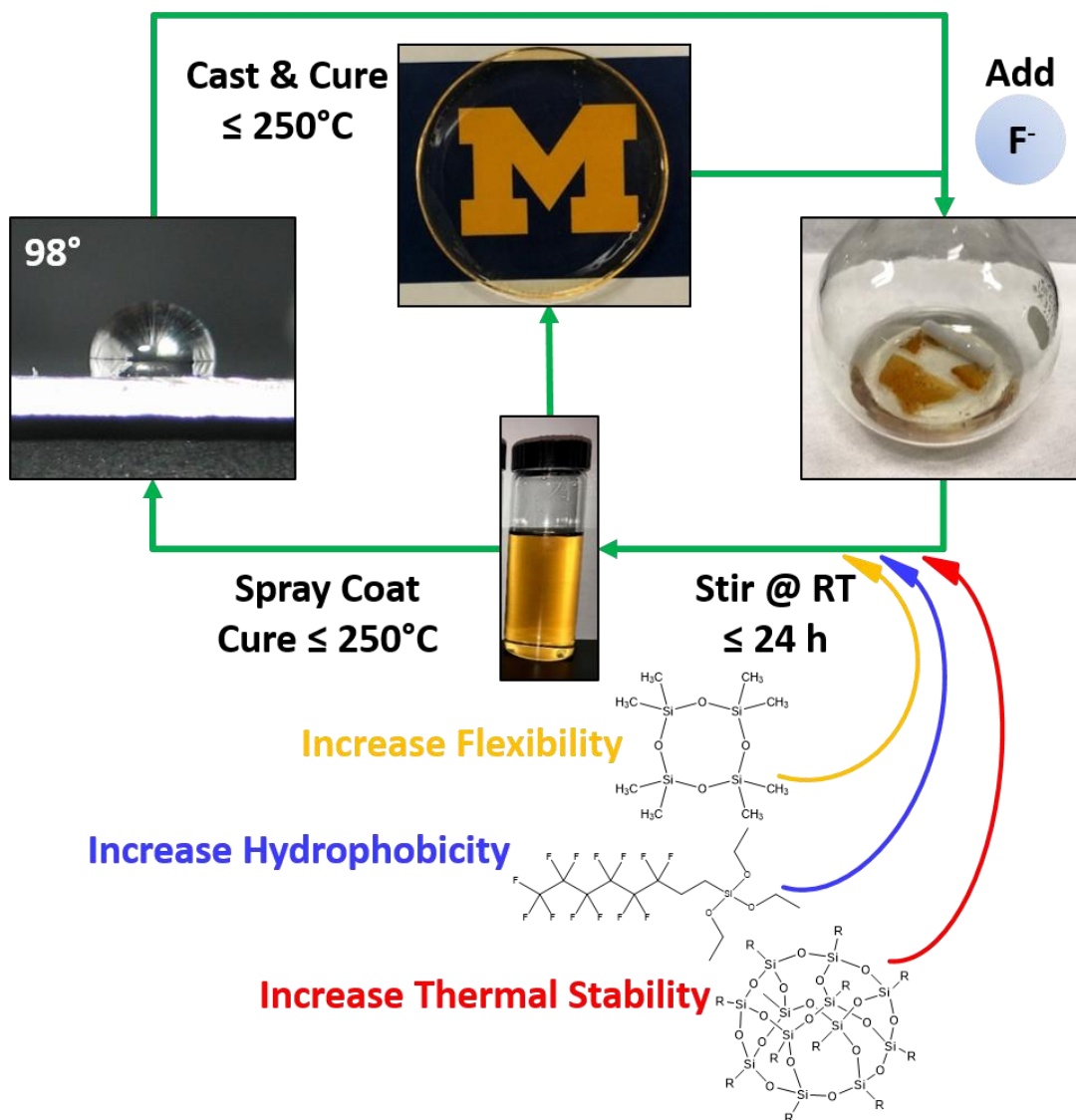
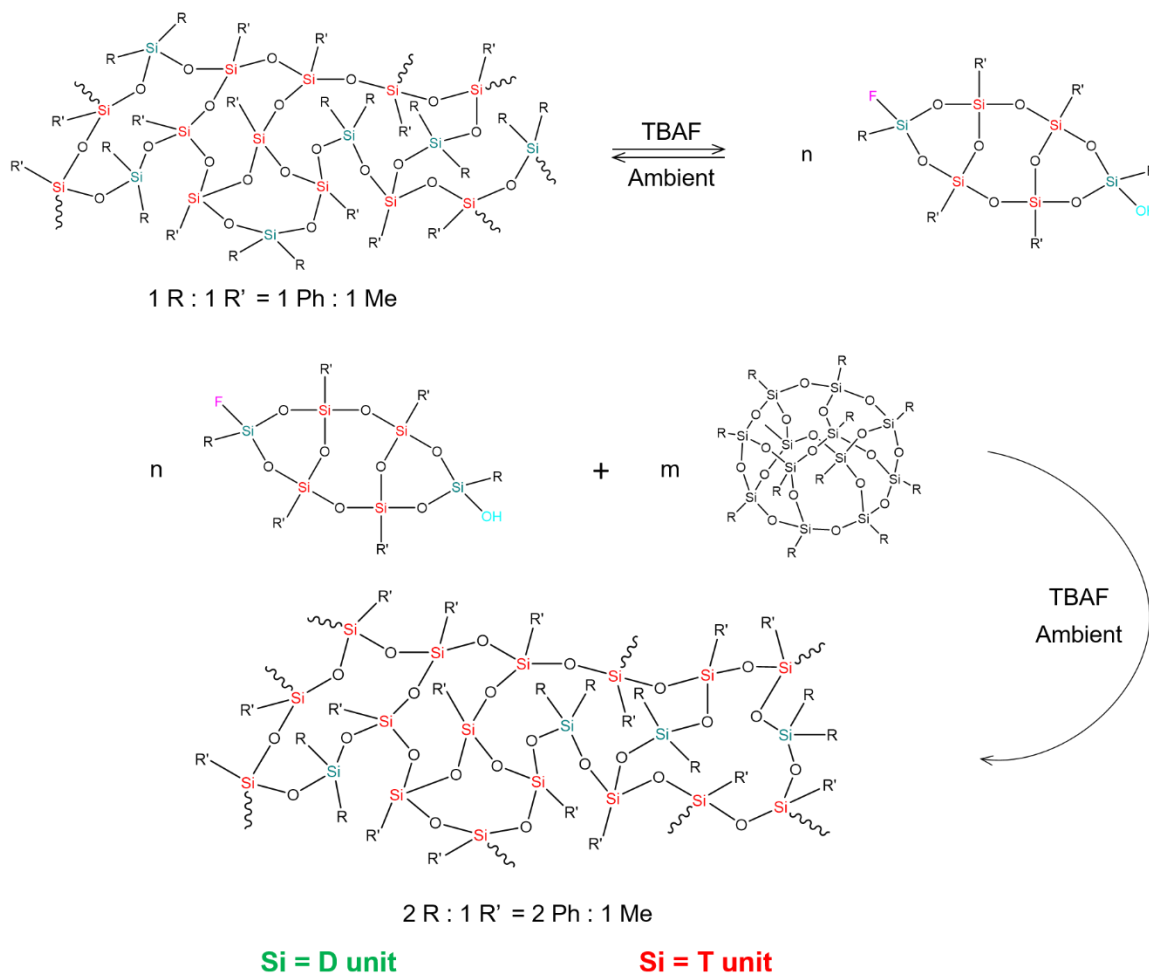


Figure 5.1 Silicone resin recycling loop and *in situ* modification after resin dissolution

In situ modification allows for adjustment of virgin materials based on their first use performance. For example, if the model mixed phenyl/methyl silicone resin (1 Ph : 1 Me) from Chapter 4 was first used in a high temperature application, but a new application required an increased use temperature, the thermal stability of the resin could be increased by increasing the phenyl to methyl ratio (Scheme 5.1). The first generation resin (1 Ph : 1 Me) could be recycled and modified (2 Ph : 1 Me) or unused resin solution could be modified directly.



Scheme 5.1 Modification of model 1 Ph : 1 Me silicone resin with DDPS to increase ratio phenyl/methyl ratio to 2 Ph : 1 Me and increase thermal stability

The flexibility of the resin, which is directly related to the D : T unit ratio, can also be modified *in situ* during recycling. The model phenyl/methyl silicone resin has a 2 T : 1 D unit ratio and is stiff and brittle after curing at 250°C. The addition of cyclic siloxane

tetramers like D₄ or Ph₈D₄ (octaphenylcyclotetrasiloxane) to the dissolved model compound will increase the number of D units and therefore the flexibility. Flexibility is ideal for many applications including tubing, medical prosthetics, catheters, and cookware.

Entirely new functionalities can also be incorporated during recycling. For example, a perfluoroalkylsilane, such as the PFS used in Chapter 3, can be incorporated to increase the hydrophobicity of a silicone resin for use in non-stick and anti-fouling applications. Multiple properties can be modified at once, which will also be shown below, to tailor the performance of the silicone for a wide variety of applications.

5.2 Experimental Procedures

The synthetic methods, processing techniques, and characterization procedures are described above in Chapter 2.

5.3 Results and Discussion

In the following sections we demonstrate the *in situ* modification of the model mixed phenyl/methyl silicone resin. First, the thermal and oxidative stability is increased by the addition of dodecaphenylsilsesquioxane (DDPS). Second, the flexibility of the resin is increased by the addition of D₄. Third, the hydrophobicity is increased by the addition of PFS. And lastly, we show an example for the *in situ* modification of the commercial silicone resin SILRES to increase stiffness and thermal stability.

5.3.1 *In situ* Modification of Recycled Silicone Resin for Increased Thermal Stability

The cured model compound, 1 Ph : 1 Me silicone resin, dissolves in 0.01 M TBAF/THF in approximately 18 h. However, the additional DDPS required to achieve the desired 2 Ph : 1 Me ratio for enhanced thermal and oxidative stability did not dissolve at the same TBAF molarity. Therefore, a study was conducted to find the [F⁻] necessary to dissolve DDPS in

a 10 wt % solution with D₄ at the concentrations required to attain the functional group ratio of 2 Ph : 1 Me. TBAF molarities in THF of 0.01, 0.02, 0.03, and 0.04 M were used to make prime coatings rather than expend cured recycled materials.

All DDPS dissolved after stirring at RT for 3 d in 0.04 M TBAF and thus was used for subsequent *in situ* modification reactions. Ultimately, the 0.01 M TBAF solution only dissolved 80% of the DDPS even after stirring for 112 d (Figure 5.2). For comparison, 89% of the DDPS dissolved in the 0.02 M TBAF solution after 91 d; and 96% of the DDPS dissolved in the 0.03 M TBAF solution after 76 d.

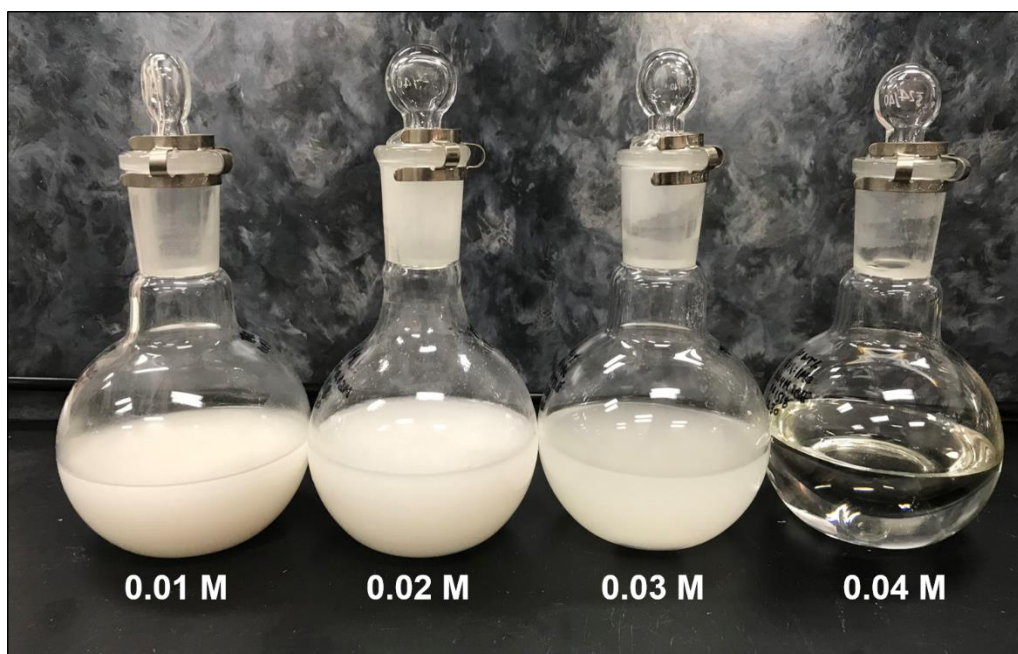


Figure 5.2 Increased [F⁻] (TBAF molarity) is necessary to dissolve extra DDPS required to produce a 2 Ph : 1 Me silicone resin

The [F⁻] necessary to fully dissolve the DDPS to produce a mixed phenyl/methyl silicone resin with a functional group ratio of 2 Ph : 1 Me required a TBAF/THF molarity of 0.04 M. For the *in situ* modification reaction cured (250°C) 1 Ph : 1 Me silicone resin and the additional DDPS were stirred in 0.04 M TBAF/THF at RT and dissolved in 2 d. The reaction was allowed to stir for a full 7 d like previous reaction solutions. Then, a coated Al coupon and thin monolith were prepared and cured to 250°C.

The thermal stability of the silicone resin increased significantly after recycling and increasing the phenyl content to 2 Ph : 1 Me. The average $T_{d5\%}$ measured by TGA in air increased by 50°C from $483 \pm 7^\circ\text{C}$ to $533 \pm 9^\circ\text{C}$ (Figure 5.3).

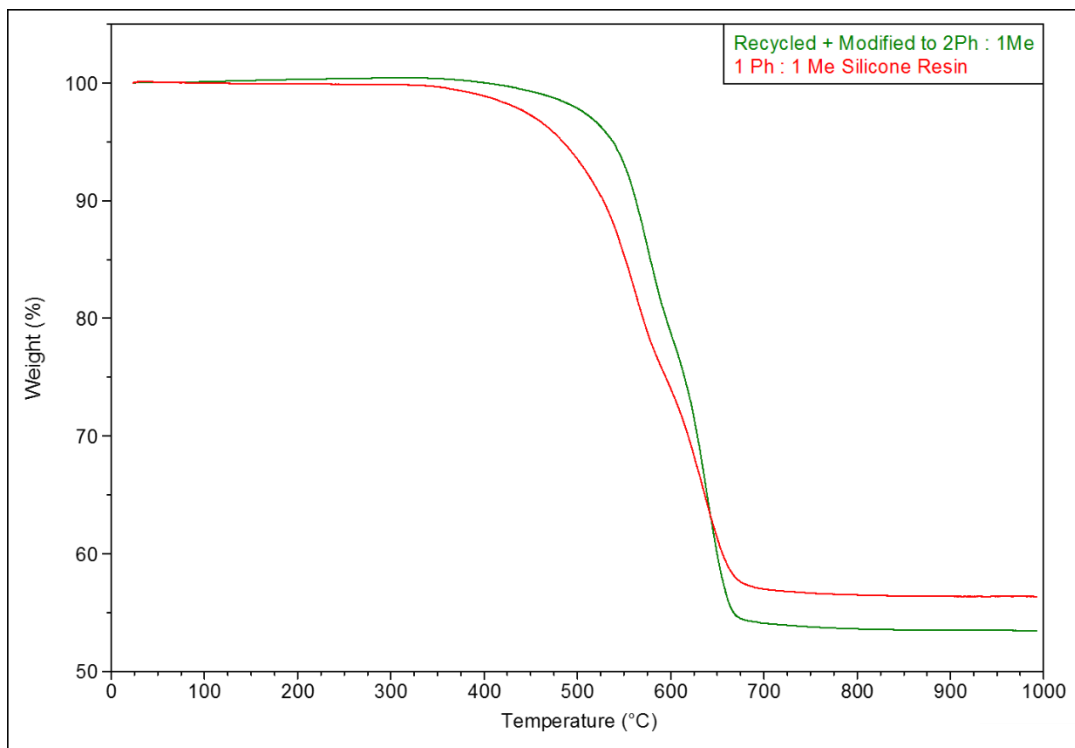


Figure 5.3 Typical TGAs in air of prime 1 Ph : 1 Me silicone resin and after recycling and *in situ* modification to 2 Ph : 1 Me silicone resin with higher thermal stability

This increase in thermal and oxidative stability is expected for several reasons. Since the phenyl groups come from a SQ the resin has an increased T:D unit ratio from 2:1 to 4:1. This increases the ratio of higher energy Si-O bonds to Si-C bonds, 452 and 318 kJ/mol, respectively, and thus more energy (heat) is required for disassociation of network bonds. The phenyl groups also strengthen Si-O bonds and their steric factors hinder chains from approaching each other, which suppresses exchange reactions.¹⁰ At high temperatures the increased phenyl content would also lead to more cross-linking via the mechanism described in Chapter 4 (Scheme 4.1) where the formation of a phenyl radical leaves a methylene group that attacks a Si atom to form another radical and a cross-link.

The high ratio of T:D also makes the modified silicone resin very brittle, which prevented casting a monolith large enough for DMA analysis. However, at low thicknesses,

i.e. a thin film, the silicone resin forms a uniform coating. The initial WCA (Figure 5.4) of the recycled and modified silicone resin (2 Ph : 1 Me) coating is slightly lower than the model compound (1 Ph : 1 Me). This decrease from 91° to 89° is slight and it is expected given that methyl groups are more hydrophobic than phenyl groups. Initial wearing of the modified coating with sandpaper showed a pronounced increase in WCA after 50 - 100 wear cycles accompanied by a higher variation in sample measurement, $97 \pm 5^\circ$ and $94 \pm 6^\circ$, respectively. This suggests that the increase in brittleness allowed for easier roughening or damage to the coating surface. After 200 wear cycles the WCAs of the two systems are similar indicating the overall wear resistance is similar.

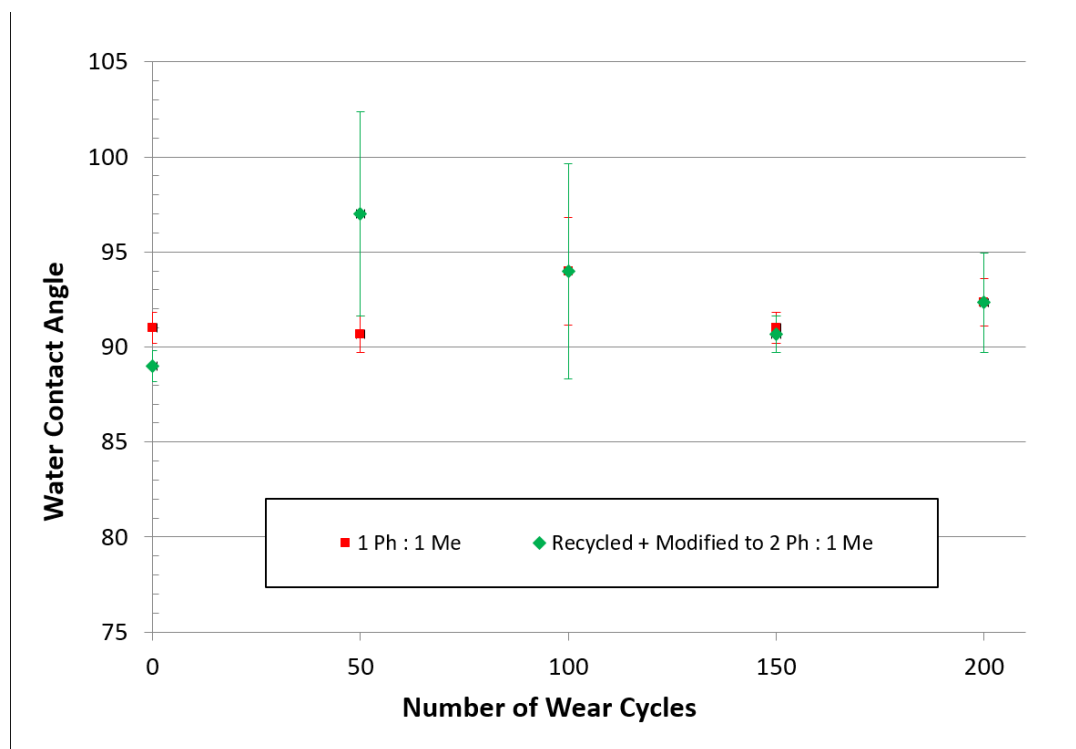


Figure 5.4 WCA vs number of wear cycles before and after recycling and *in situ* modification of a 1 Ph : 1 Me silicone resin to a 2 Ph : 1 Me silicone resin

The model mixed phenyl/methyl silicone resin already has a high thermal and oxidative stability. Nonetheless, if the thermal stability can be increased by 50°C without a significant loss in other key properties such as wear resistance, as shown above, the range of possible applications widens. Many automotive applications in or near engines have high temperature demands and aerospace environments can be even more severe. A

silicone resin with a thermal stability of near 500°C would be useful in both fields for protective or nonconductive coatings, sealants, adhesives, gaskets, lubricants, etc. High temperature silicones are also desirable as binders or vaporizable components in non-porous or porous ceramics, respectively.

5.3.2 *In situ* Modification of Recycled Silicone Resin for Increased Flexibility

Pure T-resins are seldom used because of their extreme brittleness due to high cross-link density. Such silicones have low energy absorption limiting their applications. Typically, the addition of D or M units are used to balance the stiffness of a silicone resin. As seen in the previous section, increasing the T:D from 2:1 to 4:1 resulted in a silicone resin that was too brittle to cast monoliths from solution. Here, the cured model compound (1 Ph : 1 Me) is recycled and modified with additional D₄ to adjust the T:D ratio from 2:1 to 1:2. The *in situ* modified silicone resin has a functional group ratio of 1 Ph : 4 Me and is flexible (Figure 5.5).



Figure 5.5 Recycled 1 Ph : 1 Me silicone resin after recycling and *in situ* modification to left) 1 Ph : 4 Me has right) increased flexibility

Lowering the T:D ratio also increases the molecular weight between cross-links, which lowers the cross-link density. More D units in the resin create longer linear sections in the random polymer network. This change in the network structure results in a significant decrease in the T_g (Figure 5.6) as measured by DSC. The T_g of the model compound (1 Ph : 1 Me) was not detectable by DSC (Figure B.1), which is often the case for highly cross-

linked polymers, but was detected by DMA at 237°C. DMA is 10-100 times more sensitive to the transition. However, the T_g of the recycled and *in situ* modified silicone resin (1 Ph : 4 Me) was detected by DSC at $-31 \pm 1^\circ\text{C}$. Decreasing the T:D from 2:1 to 1:2 resulted in a 200°C decrease in the T_g . Thus, our new *in situ* modification technique can be used to tailor the T_g and flexibility of a silicone resin over a very wide range.

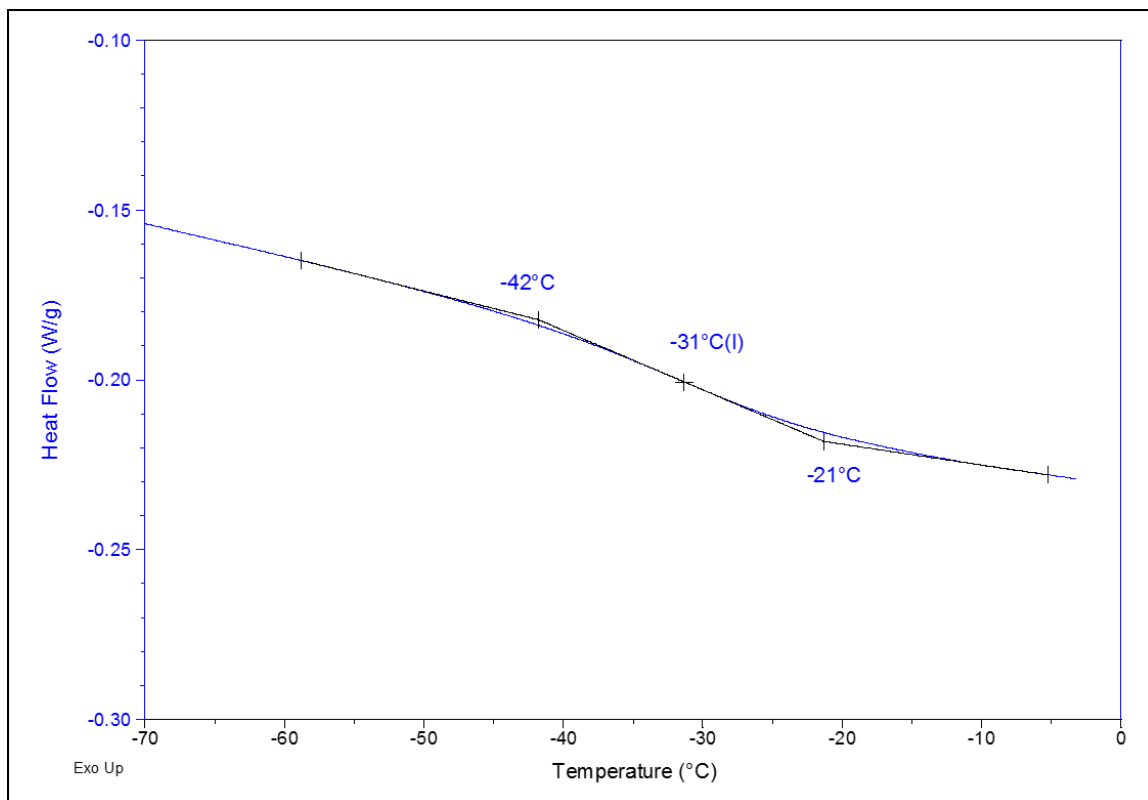


Figure 5.6 Typical DSC of recycled 1 Ph : 1 Me silicone resin modified to a 1 Ph : 4 Me silicone resin shows a T_g at -31°C

Lowering the cross-link density and phenyl content also has an obvious effect on the thermal stability of silicone resins. A TGA study showed that the 200°C decrease in T_g is accompanied by a 70°C decrease in the thermal stability to $411 \pm 4^\circ\text{C}$ (Figure 5.7). Nonetheless, the thermal stability is still relatively high compared to other common polymers and is similar to the commercial silicone resin, SILRES ($T_{d5\%} = 417 \pm 4^\circ\text{C}$), used throughout this dissertation, which is not flexible at RT.

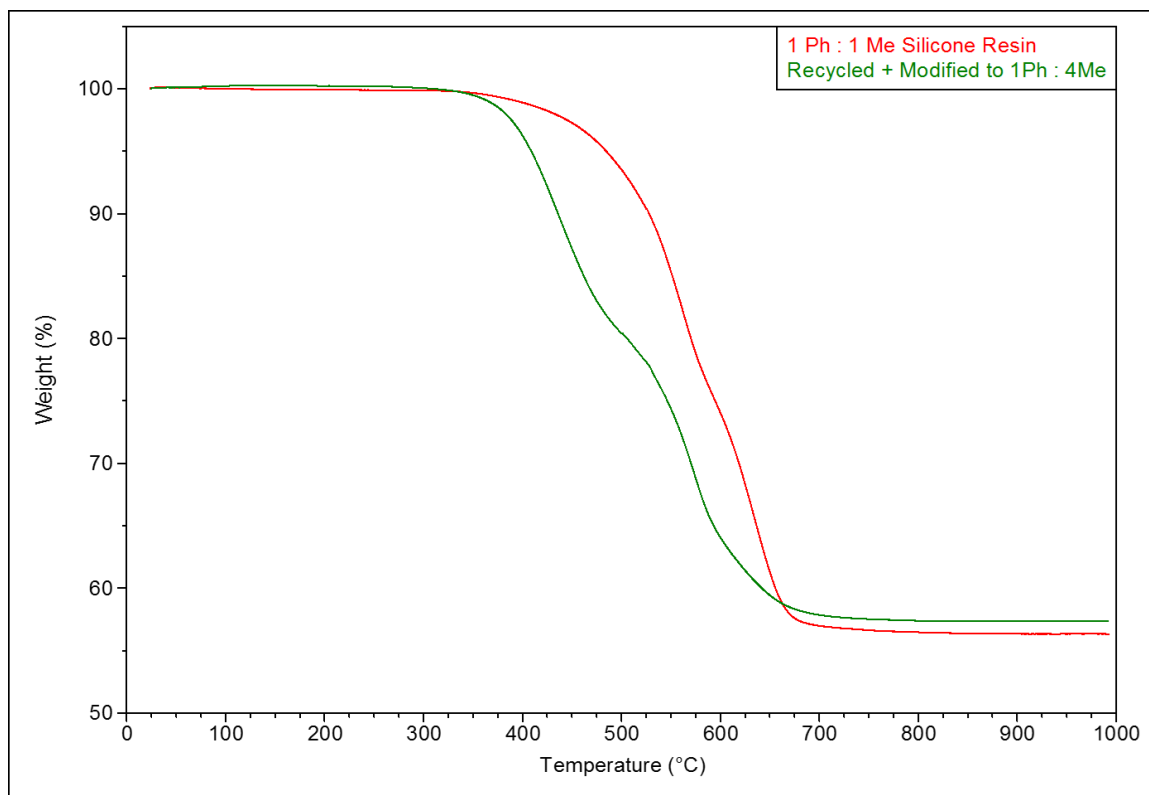


Figure 5.7 Typical TGA of prime 1 Ph : 1 Me silicone resin compared to after recycling and *in situ* modification to a 1 Ph : 4 Me silicone resin

5.3.3 *In situ* Modification of Recycled Silicone Resin for Increased Hydrophobicity

The previous two sections show how our new recycling and *in situ* modification technique can be used to easily tailor key thermal properties over a wide range to create new applications for second generation use. Here, we show how the addition of a new moiety can enhance hydrophobicity to make the system multi-functional. While recycling the model compound (1 Ph : 1 Me), a perfluoroalkylsilane was added to imbue the silicone resin with a low surface energy component. This silane, (tridecafluoro-1,1,2,2-tetrahydrooctyl)triethoxysilane, is essentially a T-unit building block and would increase the cross-link density of the overall system. Additional D₄ was added during *in situ* modification based on the previous observation (Chapter 3) that a spray coating with the ratio of 1 Ph : 1 Me : 1 PFS leads to the formation of islands upon spraying due to the low surface energy of PFS (Figure 3.11). Additional D₄ will also counteract any brittleness and potential steric hindrance between large phenyl rings and perfluoroalkyl chains.

The final ratio of functional groups in the recycled and modified silicone resin was 1 Ph : 4 Me : 1 PFS. The initial WCA of the modified silicone resin coating cured at 250°C increased by about 15° to $108 \pm 2^\circ$ (Figure 5.8). Only a slight increase in WCA, $110 \pm 4^\circ$, after 150 wear cycles indicates minimal surface roughening and that the polymer network can withstand a fair amount of wear. The standard deviation of the WCAs measured after 200 wear cycles is quite high, 10°, suggesting that the coating is beginning to wear and become non-uniform. Again, the combination of wear resistance and hydrophobicity is a difficult structure-property relationship to balance as discussed in detail in Chapter 3.

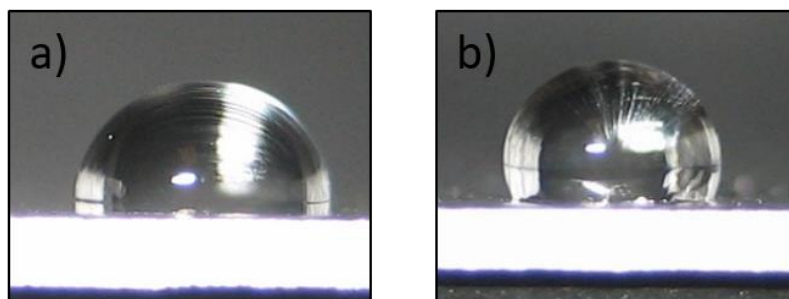


Figure 5.8 Typical initial WCA of 1 Ph : 1 Me silicone resin in a) prime condition and b) after recycling and *in situ* modification to 1 Ph : 4 Me : 1 PFS silicone resin

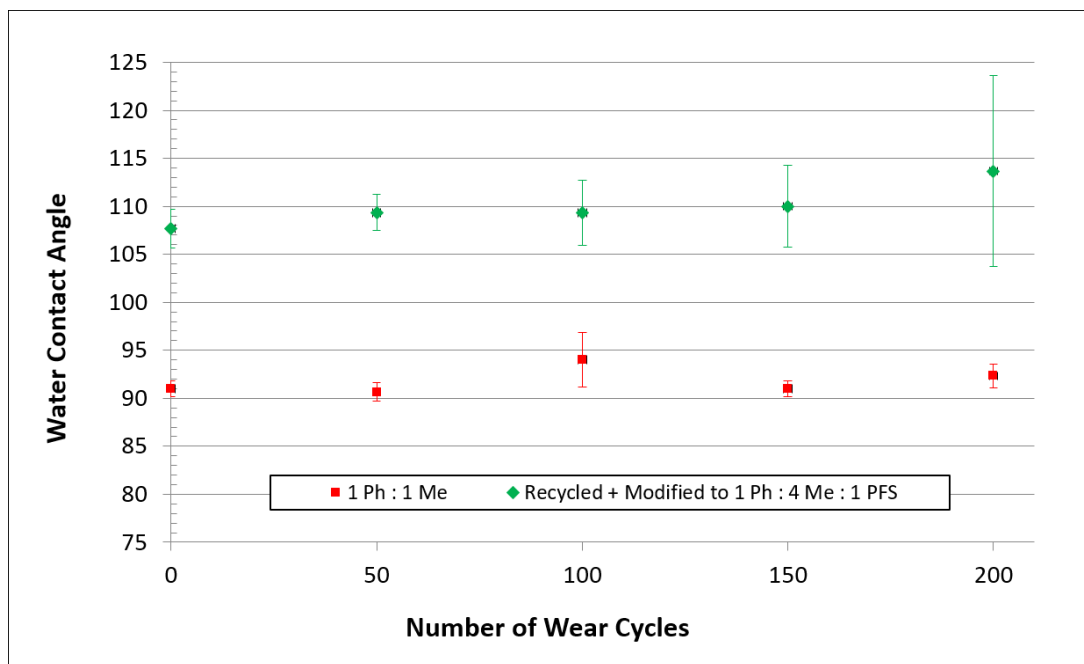


Figure 5.9 WCA vs number of wear cycles before and after recycling and *in situ* modification of a 1 Ph : 1 Me silicone resin to a 1 Ph : 4 Me : 1 PFS silicone resin

5.3.4 *In situ* Modification of Recycled Commercial Silicone Resin

As a final demonstration of our new *in situ* modification technique we show that a commercial silicone resin made via conventional synthesis, as opposed to F⁻ catalyzed rearrangement, can also be recycled and modified to target the enhancement of desired properties. The thermal properties of the SILRES have been shown to be inferior to the model compound (Table 5.1). SILRES has a lower T_g, thermal stability, and stiffness and a higher CLTE. The target and/or balance of these properties are dependent upon the application, but here we aim to increase the T_g, T_{d5%}, and stiffness as well as lower the CLTE.

Table 5.1 Thermal properties of SILRES and the model silicone resin (1 Ph : 1 Me)

Property	SILRES	Model Silicone
T _g	104 °C	237 °C
T _{d5%}	417 ± 4 °C	483 ± 7 °C
Storage Modulus (30°C)	1040 MPa	1240 MPa
Storage Modulus (150°C)	0.4 MPa	248 MPa
CLTE (15 - 35°C)	165 ppm/°C	131 ppm/°C
CLTE (150 - 200°C)	386 ppm/°C	208 ppm/°C

The ratio of phenyl to methyl in the SILRES is 0.82 Ph : 1 Me, hence some of the model compound's higher properties can be attributed to its higher phenyl content (1 Ph : 1 Me). The T:D structural unit ratio of the SILRES silicone network is unknown and could not be obtained from the manufacturer. Nonetheless, the strategy to improve the desired properties of SILRES was to simply increase the phenyl and T unit content by *in situ* modification with a small amount of DDPS (phenyl-T₁₂ SQ). Pieces of SILRES cured at 250°C readily dissolved in 0.01M TBAF/THF while stirring at RT. After the SILRES

dissolved, 10 wt % DDPS was added, which dissolved in approximately 36 h yielding a transparent solution.

Coatings and monoliths of the 10 wt % DDPS modified SILRES were prepared as detailed previously and cured at 250°C. TGA of the cured clear silicone resin showed an increase in thermal stability ($T_{d5\%}$) by about 30°C from $417 \pm 4^\circ \text{C}$ to $448 \pm 2^\circ \text{C}$ (Figure 5.10). The improvement is attributed to the increases in both the phenyl and T-unit contents.

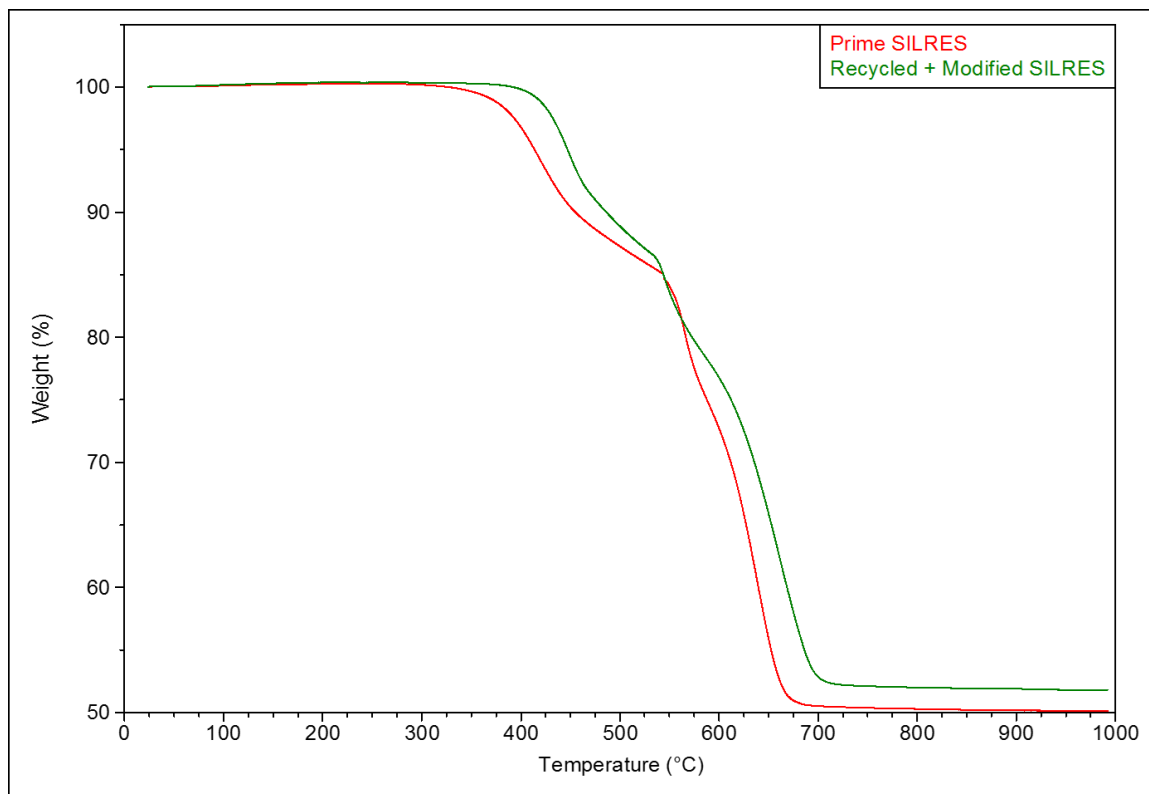


Figure 5.10 Typical TGAs in air of prime SILRES and after recycling and *in situ* modification to add 10 wt % DDPS for higher thermal stability

The CLTE of polymeric materials is an important property, especially in multi-material systems where CLTE mismatch can lead to delamination between layers. The CLTE may need to be minimized when joining to a low CLTE material like a metal or ceramic. Or the CLTE may need to be minimized at elevated temperatures to prevent loss of a low tolerance seal. The prime SILRES has a relatively high CLTE compared to the model silicone resin, which has a higher cross-link density due to the large number of T-units in the polymer

network. By increasing the number of cross-links with the 10 wt % addition of DDPS, the CLTE at elevated temperatures, 150-300°C, decreased by approximately 140-160 ppm/°C (Figure 5.11). The overall dimensional change across the temperature range of the modified silicone resin is less, which is useful for design considerations since the accommodation of large volume changes of a part (tubing, gasket, seal, etc.) could be problematic.

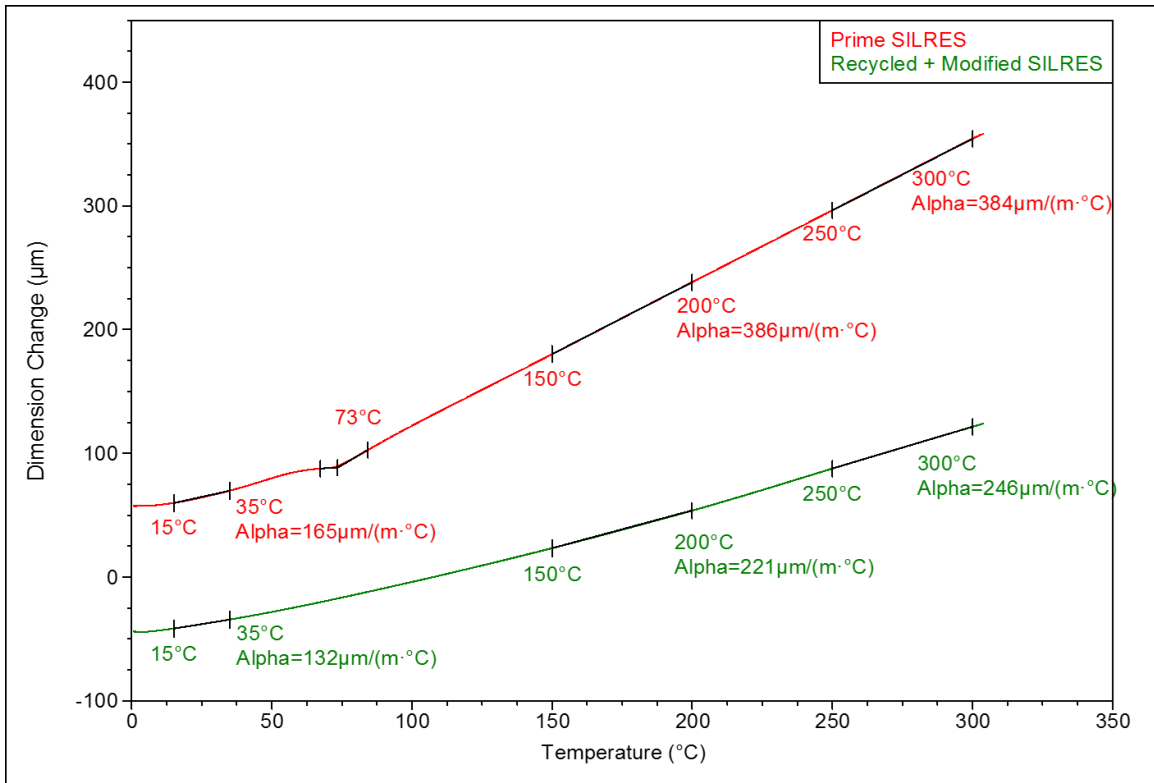


Figure 5.11 TMAs of prime SILRES and after recycling and *in situ* modification to add 10 wt % DDPS for lower CLTE

The mechanical properties of SILRES also benefit from a 10 wt % addition of DDPS as shown in Figure 5.12. The storage modulus at 30°C increased by 16% from 1040 MPa to 1211 MPa. This was expected due to the increase in T-units and therefore cross-link density. After the *in situ* addition of DDPS the shape of the storage modulus curve also changed, showing a more gradual decrease from 30-100°C. Around 100°C the storage modulus of prime SILRES plateaus at about 0.5 MPa, whereas the rate of decrease in the storage modulus of the recycled and modified SILRES becomes more gradual. The modified SILRES maintains a storage modulus above 100 MPa up to about 200°C.

This preservation of stiffness upon heating, by 3 orders of magnitude, is attributed to the increase in cross-link density from the increase in T-units during *in situ* modification with DDPS. The cross-link density was calculated from the storage modulus in the rubbery plateau (defined at $T_g + 30^\circ\text{C}$) as defined by the rubber elasticity theory, which was described in Chapter 4. The cross-link density increased by nearly 55x from 60 mol/m^3 to $3,290 \text{ mol/m}^3$.

The T_g after modification is also significantly higher due to the higher cross-link density. An increase of about 115°C from 104°C to 221°C was measured from the $\tan \delta$ peak. The second smaller peak at a lower temperature in the $\tan \delta$ curve of the modified SILRES is likely a β transition attributed to side chain movement and small localized movements in the backbone.¹¹

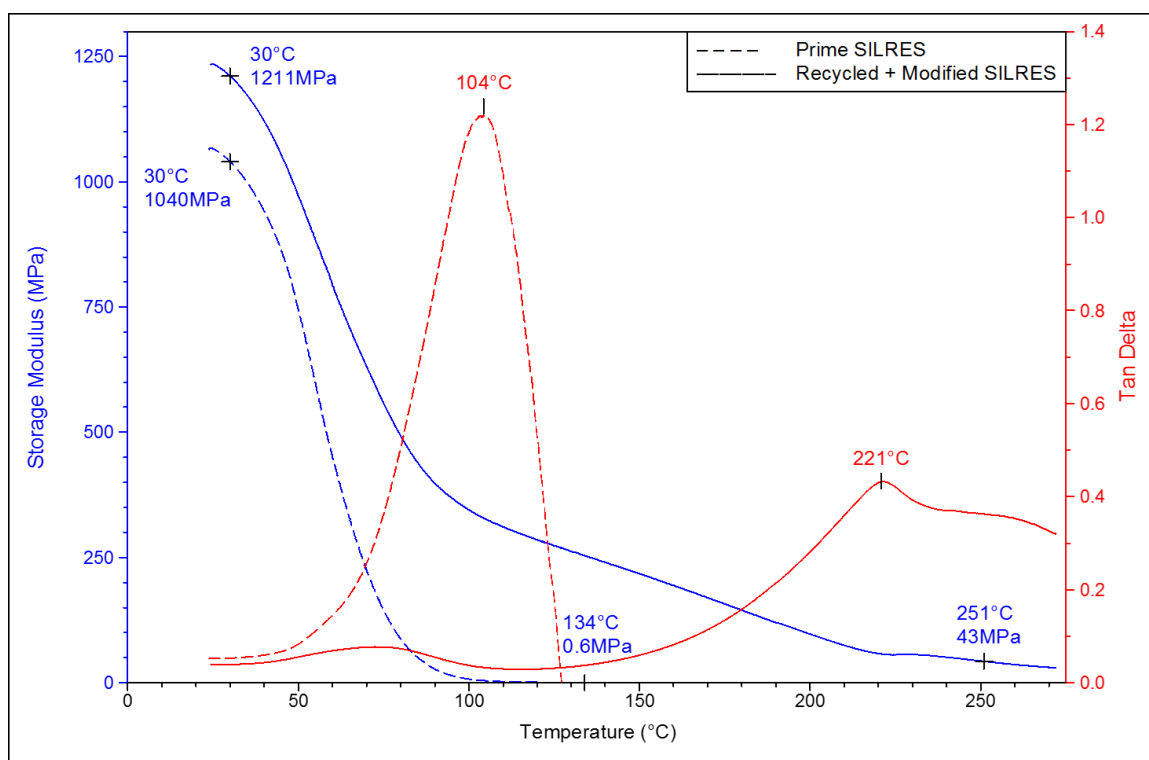


Figure 5.12 DMAs of prime SILRES and after recycling and *in situ* modification to add 10 wt % DDPS for higher stiffness

The increase in cross-link density and phenyl content also improves the wear resistance of this commercial silicone resin when applied as a coating on an Al substrate and cured at 250°C as evidence by the WCA versus wear cycle study (Figure 5.13). The prime SILRES

coating has an initial WCA of 90°, but after just 50 wear cycles with sandpaper the WCA increases abruptly to 116°. This is caused by roughening of the silicone due to the minimal polymer network integrity brought on by the low cross-link density. With continued wear the prime coating begins to wear away and the WCA decreases. The high standard deviation of WCA measurements also indicates non-uniformity of the diminishing thin film as it wears away.

The recycled and modified SILRES coating, however, maintains a relatively steady WCA, between 90-95°, throughout the entire wear test. This indicates, as has been shown throughout this dissertation, a more structurally robust silicone resin network, which is attributed to the increase in cross-link density.

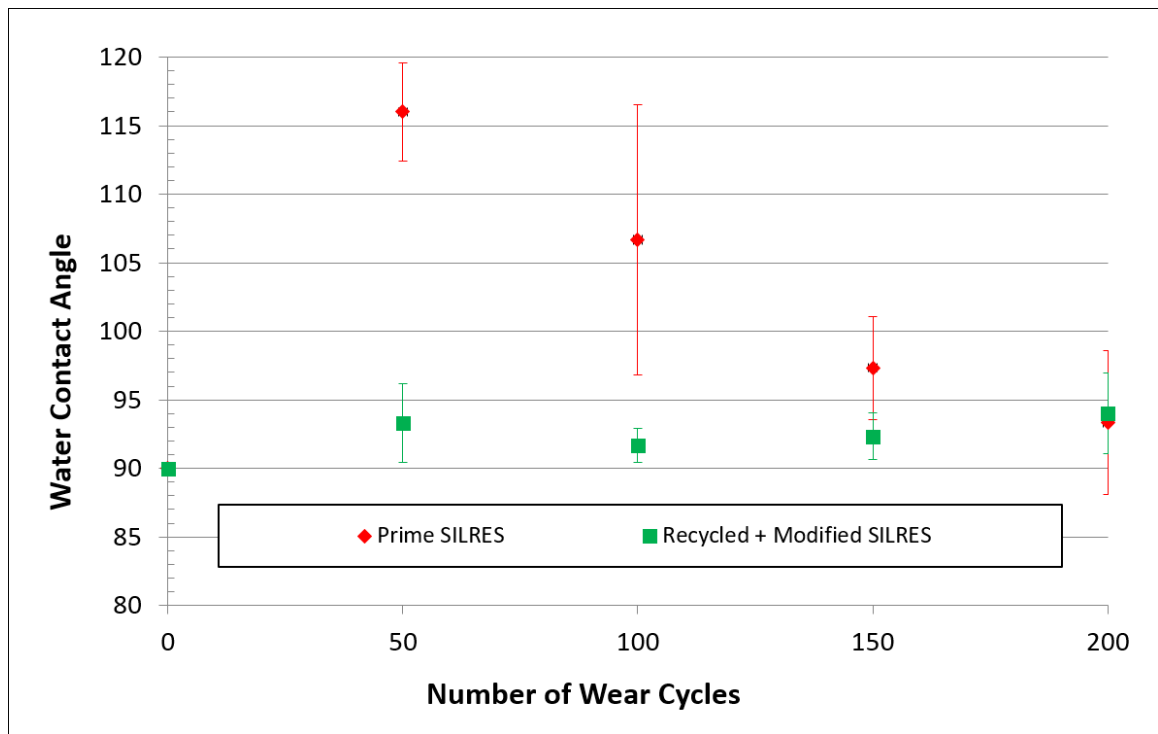


Figure 5.13 WCA vs number of wear cycles before and after recycling and *in situ* modification of SILRES to add 10 wt % DDPS

5.4 Conclusions

Highly cross-linked thermoset silicone resins cured at 250°C were easily modified *in situ* while recycling via an F⁻ catalyzed rearrangement reaction. The normally insoluble mixed phenyl/methyl model silicone resin was dissolved in the presence of catalytic amounts of F⁻ in THF while stirring at RT by equilibrating all D and T units into soluble intermediates. With the intermediate species of the prime resin in solution, an opportunity arises to change the ratio of starting materials or add new functionalities. The cross-linked silicone resin network then reforms on removal of the solvent with the adjusted or new properties.

Four examples of *in situ* modification were presented to demonstrate the ease and versatility of our new technique. The thermal stability of the model silicone resin was increased by 50°C by adding more of one of the starting material, DDPS, to increase the phenyl content and cross-link density. The flexibility was increased and the T_g was lowered 200°C by adding more of the other starting material, D₄. The hydrophobicity of the model silicone resin was increase by 15° by the addition of PFS, which introduced a new low surface energy functionality. Lastly, a widespread commercial silicone resin, SILRES, was modified with DDPS to increase cross-link density and phenyl content leading to better thermal stability and wear resistance.

The ability to use F⁻ catalyzed rearrangement to first synthesize a silicone resin upon solvent removal and then dissolve it by re-introduction of F⁻ in solution creates an opportunity for the inclusion of more of a starting silicone building block and/or entirely new functionalities. This type of *in situ* modification of a coating system is rare and especially unique for a highly cross-linked thermoset polymer.

End-of-life silicone products could not only be recycled with property retention (Chapter 4), but could be tailored (Chapter 5) for use in new applications with wholly different requirements. A silicone used in a low demand environment could be recycled and modified to be used as a high temperature hydrophobic protective coating. Or a stiff silicone gasket could be recycled and modified for a second generation use in flexible tubing.

5.5 References

1. Krug, D. J.; Asuncion, M. Z.; Laine, R. M. Facile Approach to Recycling Highly Cross-linked Thermoset Silicone Resins under Ambient Conditions. *ACS Omega* **2019**, *4*, 3782-3789.
2. Asuncion, M. Z.; Laine, R. M. Fluoride Rearrangement Reactions of Polyphenyl- and Polyvinylsilsesquioxanes as a Facile Route to Mixed Functional Phenyl, Vinyl T₁₀ and T₁₂ Silsesquioxanes. *J. Am. Chem. Soc.* **2010**, *132*, 3723-3736.
3. Ronchi, M.; Sulaiman, S.; Boston, N. R.; Laine, R. M. Fluoride Catalyzed Rearrangements of Polysilsesquioxanes, Mixed Me, Vinyl T₈, Me, Vinyl T₁₀ and T₁₂ Cages. *Appl. Organometal. Chem.* **2010**, *24*, 551-557.
4. Jung, J. H.; Laine, R. M. Beads on a Chain (BOC) Polymers Formed from the Reaction of [NH₂PhSiO_{1.5}]_x[PhSiO_{1.5}]_{10-x} and [NH₂PhSiO_{1.5}]_x[PhSiO_{1.5}]_{12-x} Mixtures ($x=2-4$) with the Diglycidyl Ether of Bisphenol A. *Macromolecules* **2011**, *44*, 7263-7272.
5. Jung, J. H.; Furgal, J. C.; Goodson III, T.; Mizumo, T.; Schwartz, M.; Chou, K.; Vonet, J. F.; Laine, R. M. 3-D Molecular Mixtures of Catalytically Functionalized [vinylSiO_{1.5}]₁₀/[vinylSiO_{1.5}]₁₂. Photophysical Characterization of Second Generation Derivatives. *Chem. Mater.* **2012**, *24*, 1883-1895.
6. Furgal, J. C.; Jung, J. H.; Goodson III, T.; Laine, R. M. Analyzing Structure-Photophysical Property Relationships for Isolated T₈, T₁₀, and T₁₂ Stilbenevinylsilsesquioxanes. *J. Am. Chem. Soc.* **2013**, *135*, 12259-12269.
7. Furgal, J. C.; Goodson III, T.; Laine, R. M. D_{5h} [PhSiO_{1.5}]₁₀ Synthesis via F⁻ Catalyzed Rearrangement of [PhSiO_{1.5}]_n. An Experimental/Computational Analysis of Likely Reaction Pathways. *Dalton Trans.* **2016**, *45*, 1025-1039
8. Laine, R. M.; Asuncion, M. Z.; Krug, D. J. Synthesis and Processing of New Silsesquioxane/Siloxane Systems. US20140120243
9. Krug, D. J.; Laine, R. M. Durable and Hydrophobic Organic-Inorganic Hybrid Coatings via Fluoride Rearrangement of Phenyl T₁₂ Silsesquioxane and Siloxanes. *ACS Appl. Mater. Interfaces* **2017**, *9*, 8378-8383.
10. Brooks, M. A. In *Silicon in Organic, Organometallic, and Polymer Chemistry*; Wiley-Interscience, New York, 2000; Chapter 9 Silicones, pp 256-308.

11. Menard, K. P. In *Dynamic Mechanical Analysis: A Practical Introduction*; CRC Press LLC: Boca Raton, FL, 1999; Chapter Time and Temperature Studies: Thermosets, pp. 103-135.

Chapter 6

Future Work

6.1 Discussion

In Chapter 3 we demonstrated the synthesis of silicone resins via the F^- catalyzed rearrangement of siloxane, silsesquioxane, and triethoxysilanes. A main objective was to combine hydrophobicity and wear resistance. The low surface energy perfluoroalkylsilane provided an increase in the initial WCA, but it was relatively small, 7° . This was attributed to non-uniform coating observed by SEM as the formation of islands due to the low surface energy of the perfluoroalkylsilane. Other ratios or lengths of perfluoroalkylsilane should be investigated for the optimization of initial WCA. Additional increases in WCA are possible with other siloxane building units, for example the replacement of D_4 with (3,3,3-trifluoropropyl)methylcyclotrisiloxane (CF_3-D_3) along with DDPS and PFS (functional group ratio 2 Ph : 1 Me : 1 CF_3 : 1 PFS, $250^\circ C$ cure on Al substrate) has an initial WCA of 110° (Figure 6.1), which is about 20° higher than the model compound. The $-CF_3$ group has been shown to have the lowest surface energy and pristine CF_3 surfaces are required for the theoretical maximum WCA, 120° , for a smooth surface.^{1,2}

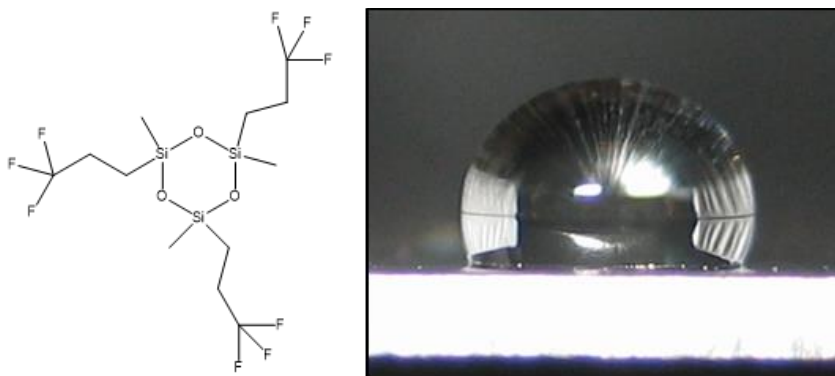


Figure 6.1 left) CF_3-D_3 structure, right) initial WCA of coating with CF_3-D_3

The wear resistance of the model silicone resin was found to be excellent with little change in the WCA over after 200 wear cycles and little to no wear observed via SEM. Other wear resistance testing should be conducted including taber abrasion for comparison to commercially available silicone coatings. The inclusion of adhesion promoting functionalities should be investigated to further increase the wear resistance of these coating systems. Hydrolyzable alkoxy silanes are used extensively for the functionalization of surfaces with oxides, but in the F^- catalyzed coating system Si-O bonds are rearranging in solution. An alternative would be to include an isocyanate functionalized silane such as 3-isocyanatopropyltriethoxysilane. The Si-O bonds in the silane facilitate integration to the silicone network and the isocyanate group can covalently bond with hydroxyl groups on oxide surfaces (Figure 6.2).³

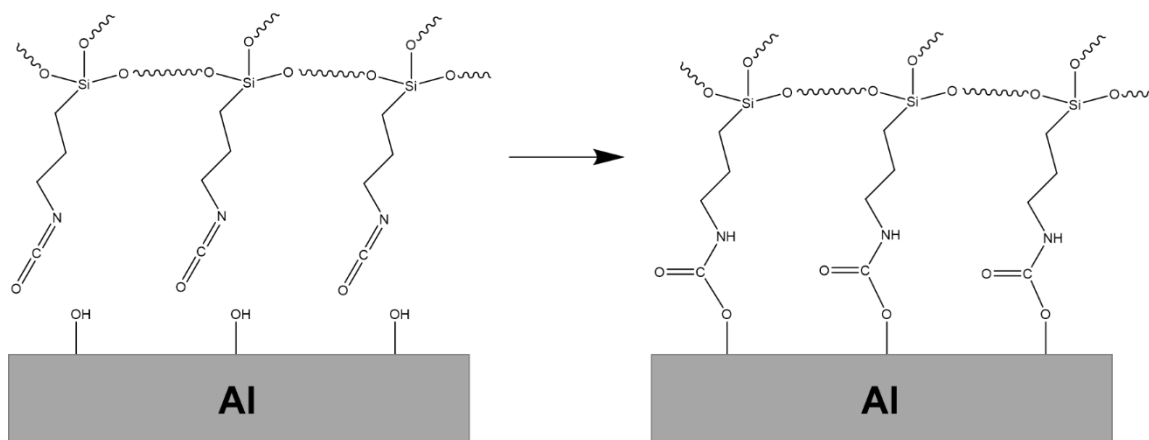


Figure 6.2 Schematic of isocyanate bonding to reactive aluminum oxide surface

Another approach to improving both the hydrophobicity and wear resistance is to build layered systems using these silicone resin coatings. Spray application of successive layers could be laid down on a substrate at RT or even after curing in between layers since the TBAF/THF solvent carrier of a new layer allows for some partial dissolution of the surface of the previous layer allowing for Si-O bond rearrangement between the two layers or networks. For proof of principle of the concept two layered systems were made and tested for wear resistance (Figure 6.3). The first system consisted of three layers. The base layer was the model silicone resin (DDPS + D₄), which exhibited good adhesion to an Al substrate. The coating from Chapter 3 with the highest WCA (143°) after 200 wear cycles

was used as the middle layer, which was DDPS + D₄ + PFS + MAS with 3 wt % silica nanoparticles. The top layer was a thin layer of the model compound. Basically, the concept was to sandwich a layer containing silica nanoparticles between two layers of the model silicone resin. As shown in Figure 6.3b, Layered System 1 showed less roughening with wear and a steady WCA of about 125° after the first 50 wear cycles indicating relatively good wear resistance.

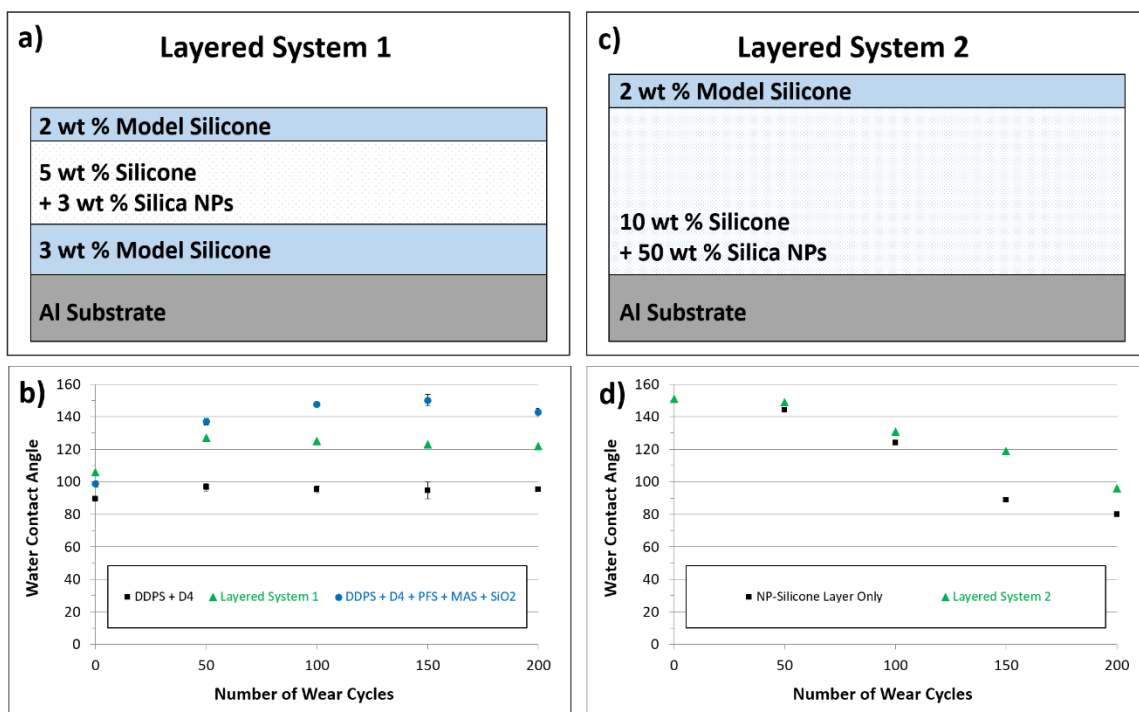


Figure 6.3 Schematics and WCA vs wear cycles with pertinent coatings for comparison of Layered System a-b) 1 and c-d) 2

The second layered system was designed to ascertain if a base layer of silicone highly filled with silica nanoparticles could be protected by a thin layer of the model silicone without sacrificing hydrophobicity. A purposely high loading of NPs, 50 wt %, was chosen to either exacerbate or highlight the wear resistance of Layered System 2. For comparison, the same silicone resin coating (DDPS + D₄ + PFS + MAS + 50 wt% SiO₂) was spray coated on an Al substrate without a protective top layer and cured at 250°C. As shown in Figure 6.3d, the addition of a 2 wt % layer of the model silicone resin provided some protection against wear resistance as indicated by the 15° higher WCA after 200 wear

cycles. Keeping the protective top layer thin (2 wt %) eliminated a decrease the initial WCA, which was 150°.

Other reaction parameters to consider for silicone resin synthesis, recycling, and *in situ* modification are the temperature, solvent, and fluoride ion source. All experiments were conducted at RT in THF with TBAF. The effects of temperature on the dissolution rate of insoluble starting materials like DDPS and perhaps more importantly the fully cured systems should be investigated. The balance between the costs of energy versus time would need to be determined for synthesis or recycling scale up. THF is relatively non-toxic, comparable to acetone, but other green solvent alternatives should be explored. Recycling difficult to recycle cross-linked thermosetting silicone resins has a positive environmental impact, but the endeavor is futile if it requires non-environmentally friendly reagents. Alternatives such as 2-methyltetrahydrofuran and cyclopentyl methyl ether should be investigated.

This dissertation and previous work by our group has shown that TBAF is a suitable F⁻ source for Si-O bond rearrangement reactions. When targeting discrete SQ cages the F⁻ must be captured as CaF₂ by treating with CaCl₂, then the remaining tetrabutylammonium chloride (depending on work up) can be washed off the product. When making or recycling silicone resins the opportunity to remove the TBAF is eliminated because the polymer only forms with removal of the solvent and capturing the TBAF first leads to formation of discrete SQ cages rather than polymers. The primary thermal decomposition product of TBAF was found to be tributylamine (Figures **4.13**, **4.22**, **4.23**, **D.1**). Trace amounts were found even after curing to 250°C, due to its high boiling point (214°C), and could act as a plasticizer. The tributylamine also imparts a yellow/brown color in prime and recycled silicone resins, which may be undesirable. Other F⁻ sources may prevent these issues. In particular, alkali-metal fluorides (NaF, KF) should be explored. NaF and KF have limited solubility in THF, but solvent blends could be considered and the presence of crown ethers have been shown to increase their solubility.⁴

The model silicone resin made from DDPS and D₄ had a high thermal stability, T_{d5%} > 480°C in air. The T_{d5%} increased by 50°C by adjusting the Ph:Me ratio from 1:1 to 2:1 (Figure **5.3**), however, the resulting resin was very brittle and difficult to process (other than as a thin film) because the T:D unit ratio increased from 2:1 to 4:1. The balance of

flexibility and thermal resistance should be explored by lowering or possibly eliminating all methyl groups by replacing D₄ with Ph₈D₄ (Figure 6.4). It should be possible to formulate a silicone resin with a thermal stability higher than reported here, > 530°C, with better processing/flexibility by adjustment of the cross-link density (i.e. T:D ratio).

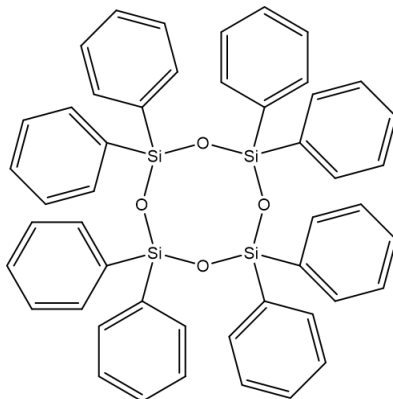


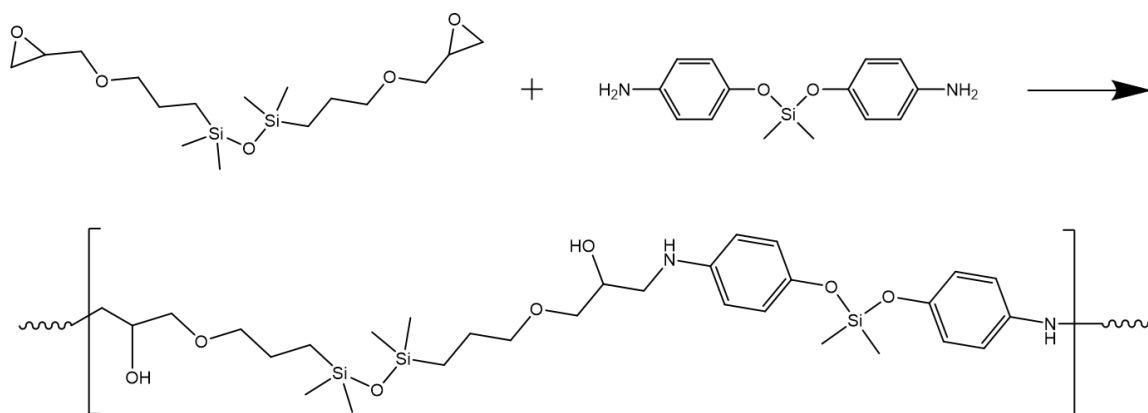
Figure 6.4 Structure of octaphenylcyclotetrasiloxane

Under optimized conditions, our novel technique worked well for recycling two commercial silicones. Dissolution time at RT for a mixed phenyl/methyl resin was about an hour and only 15 minutes for a RTV silicone rubber. These two materials suffice as the proof of principle that our method works for commercially relevant products, not just niche lab-made materials. However, other types of silicones should be trialed to demonstrate our method's full potential, such as high temperature vulcanized (HTV) silicone rubber. Real world silicone waste streams should be evaluated and perhaps the mixture of both rubber and resin end-of-life products to achieve a balance of properties such as stiffness. Our method should work for any silicone material because it attacks Si-O bonds.

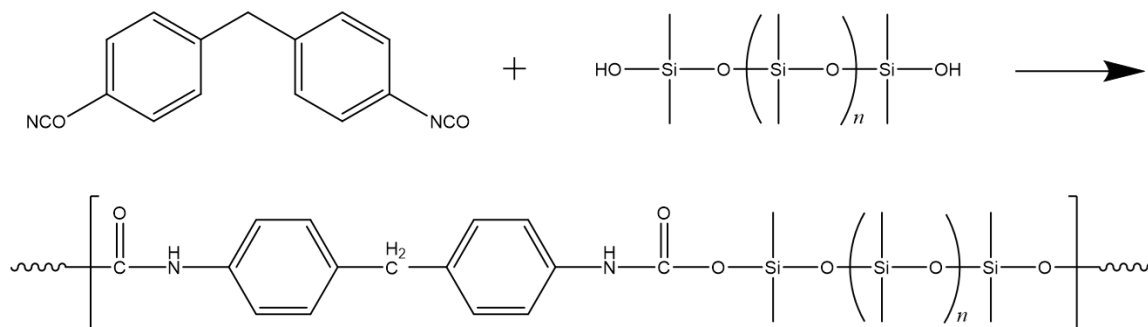
In a recent review⁵ on thermosets designed to be recyclable with labile bonds or linkages, Ma *et al.* noted that instead of designing thermosets with weak bonds, such as the di-sulfide⁶ silicone systems described in Chapter 4, that inherently lower the conventionally high properties of a thermoset, the use of catalysts that cleave common strong bonds is an attractive alternative. Since the F⁻ catalyzed rearrangement reaction attacks and cleaves siloxane bonds, our recycling technique could be extended to other difficult to recycle thermosets via incorporation of siloxane bonds in cross-links and/or monomer repeat units. The review by Ma *et al.* made no mention of siloxanes bonds being

considered for the route of catalyst driven cleavage of strong bonds suggesting this is an entirely unexplored sector of the field.

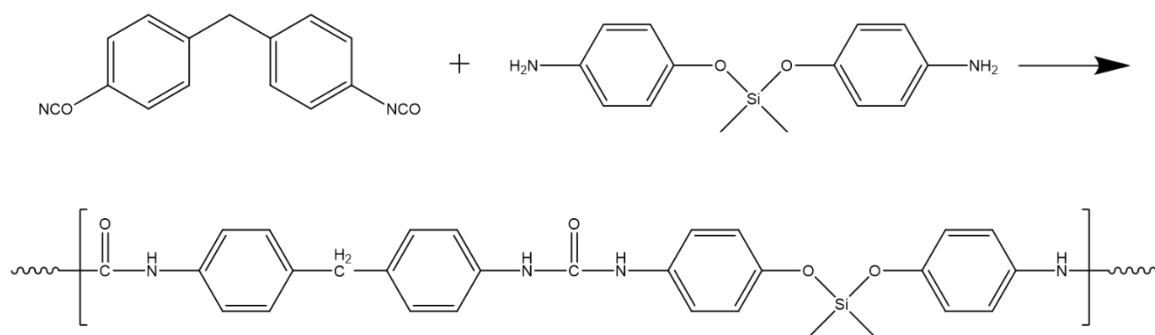
There are many di-functional siloxanes that could replace traditional thermoset building blocks to create recyclable epoxy-amines, polyurethanes, polyureas, cross-linked unsaturated polyesters and vinyl esters, etc. Introduction of the siloxane linkages to the polymer network should also increase thermal stability. Examples of such systems are shown in Schemes 6.1 - 6.4. The structures shown are all commercially available. In addition to exploring such siloxane based systems, appropriately functionalized SQs (Figure 6.5) could also be used to construct recyclable thermosets with even higher cross-link densities because of the T units.



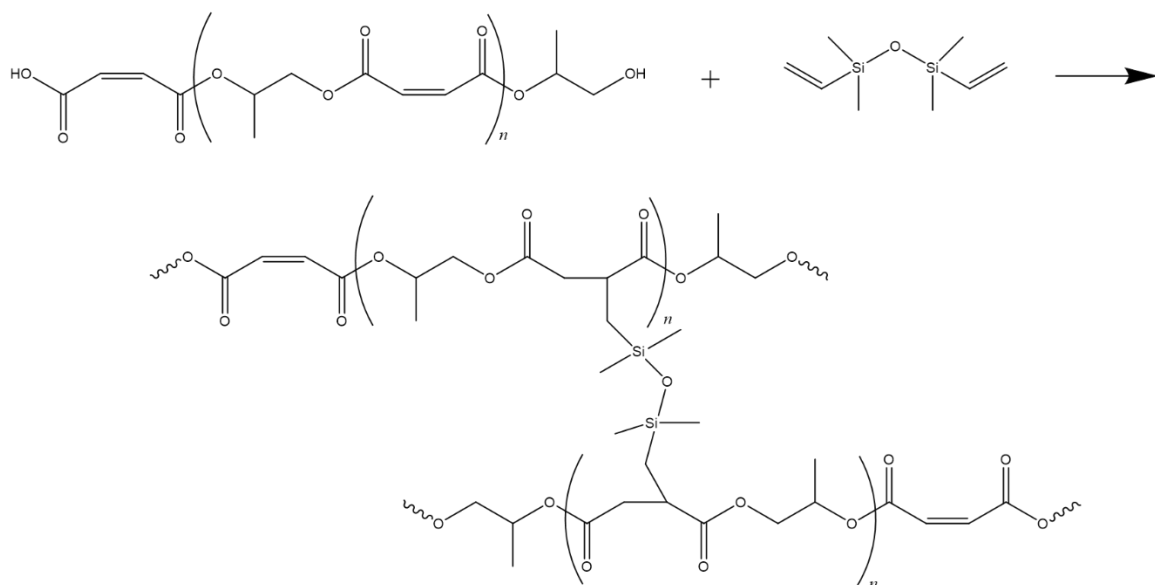
Scheme 6.1 Pathway to siloxane containing epoxy-amine thermoset susceptible to F^- catalyzed recycling



Scheme 6.2 Pathway to siloxane containing polyurethane thermoset susceptible to F^- catalyzed recycling



Scheme 6.3 Pathway to siloxane containing polyurea thermoset susceptible to F^- catalyzed recycling



Scheme 6.4 Pathway to siloxane containing cross-linked unsaturated polyester thermoset susceptible to F^- catalyzed recycling

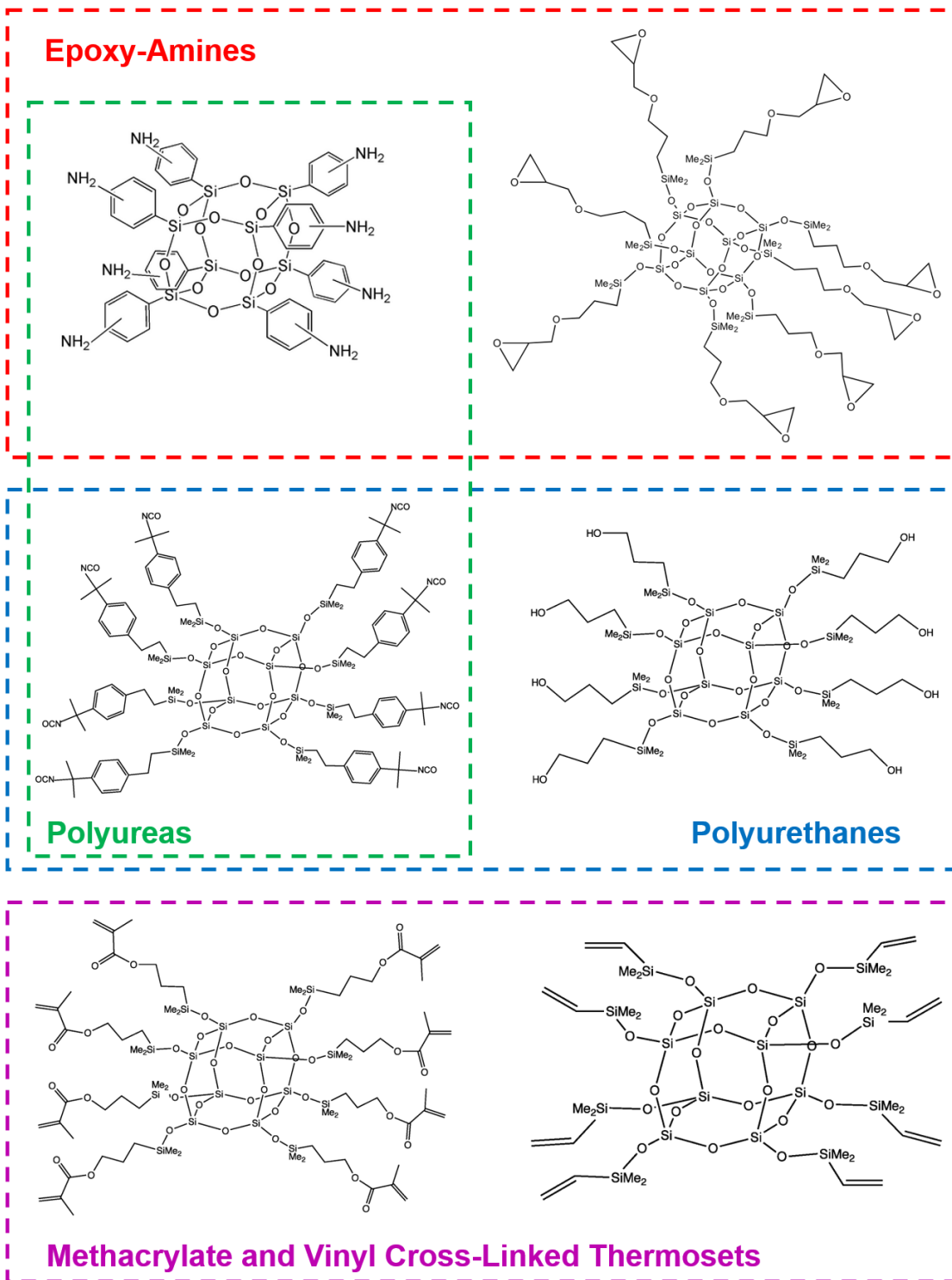


Figure 6.5 Examples of octafunctional SQ cages as building blocks for various thermoset polymers susceptible to F⁻ catalyzed recycling

Lastly, the short dissolution time for silicones like the commercially relevant SILRES presents an opportunity for easy repair, patterning, or modifying of cured coatings. As a demonstration, a cotton swab soaked with 0.01M TBAF was used to selectively remove a portion of prime SILRES cured at 250°C (Figure 6.6). Thus, a damaged area could be removed and then sprayed over with new silicone resin (Figures A.5 and A.6). Adhesion between the base-layer and repair-layer is expected to be good since the base-layer will be partially solubilized by the F/solvent of the repair-layer as mentioned above regarding layered systems.

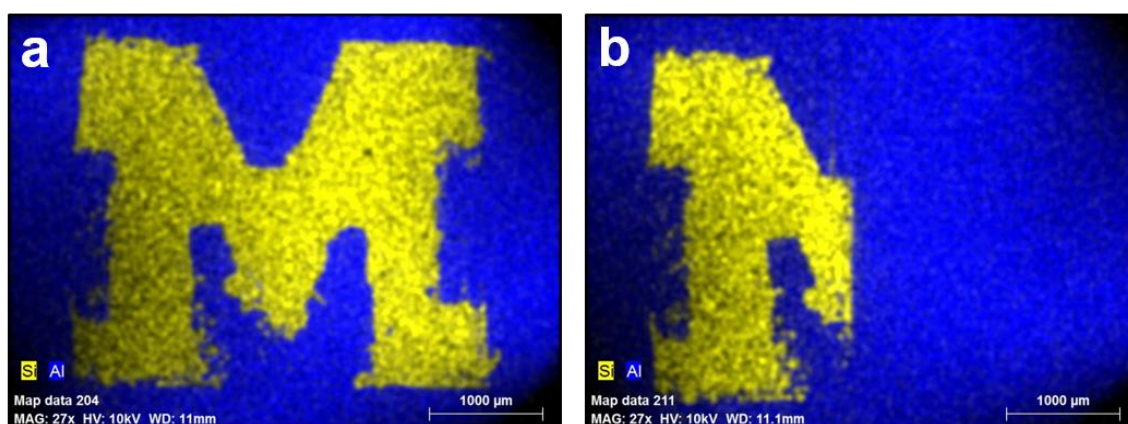


Figure 6.6 Cured (250°C) SILRES pattern a) before and b) after selective removal with 0.01M THF/TBAF; magnification 27x, scale bar 1000 µm

6.2 References

1. Hare, E.; Shafrin, E.; Zisman, W. Properties of Films of Adsorbed Fluorinated Acids. *J. Phys. Chem.* **1954**, *58*, 236-239.
2. Nishino, T.; Meguro, M.; Nakamae, K.; Matsushita, M.; Ueda, Y. The Lowest Surface Free Energy Based on -CF₃ Alignment. *Langmuir* **1999**, *15*, 4321-4323.
3. Hozumi, A.; Kim, B.; McCarthy, T. J. Hydrophobicity of Perfluoroalkyl Isocyanate Monolayers on Oxidized Aluminum Surfaces. *Langmuir* **2009**, *25*, 6834-6840.
4. Wynn, D. A.; Roth, M. M.; Pollard, B. D. The Solubility of Alkali-Metal Fluorides in Non-Aqueous Solvents with and without Crown Ethers, as Determined by Flame Emission Spectrometry. *Talanta* **1984**, *31*, 1036-1040.
5. Ma, S.; Webster, D. C. Degradable Thermosets Based on Labile Bonds or Linkages: A Review. *Prog. Polym. Sci.* **2018**, *76*, 65-110.
6. Xiang, H. P.; Rong, M. Z.; Zhang, M. Q. A Facile Method for Imparting Sunlight Driven Catalyst-Free Self-Healability and Recyclability to Commercial Silicone Elastomer. *Polymer* **2017**, *108*, 339-347.

Appendix A

Supplemental SEM Images

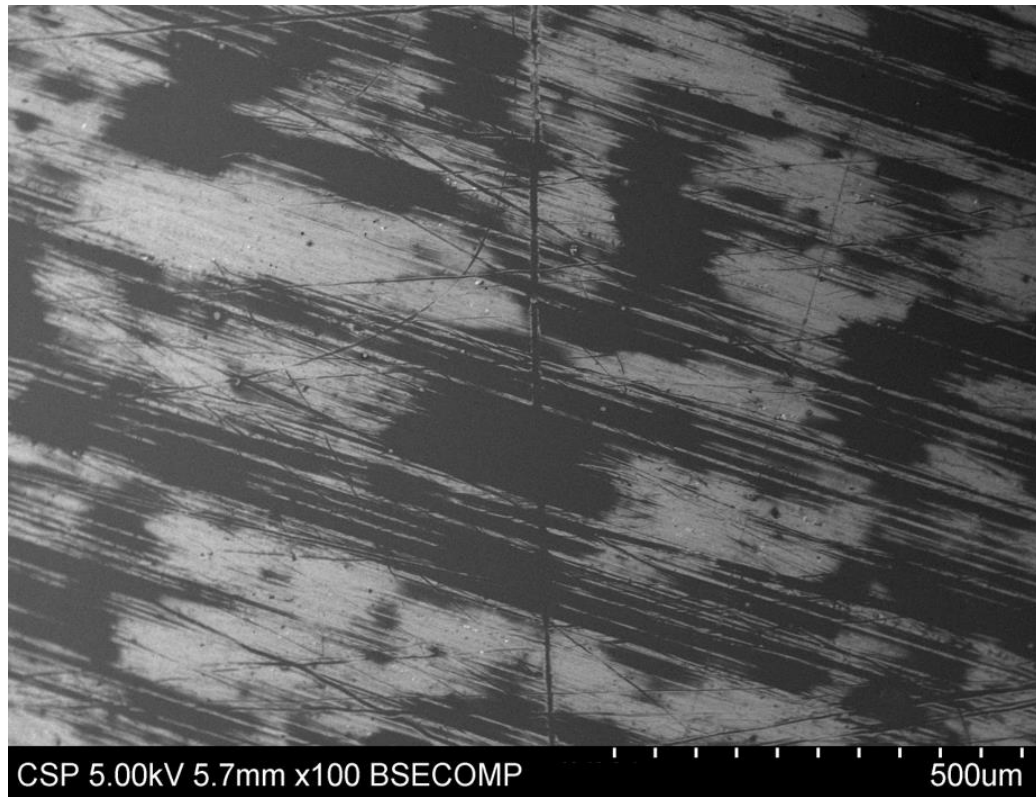


Figure A.1 SEM of 5 wt % silicone resin coating; magnification 100x, scale bar 500 μm

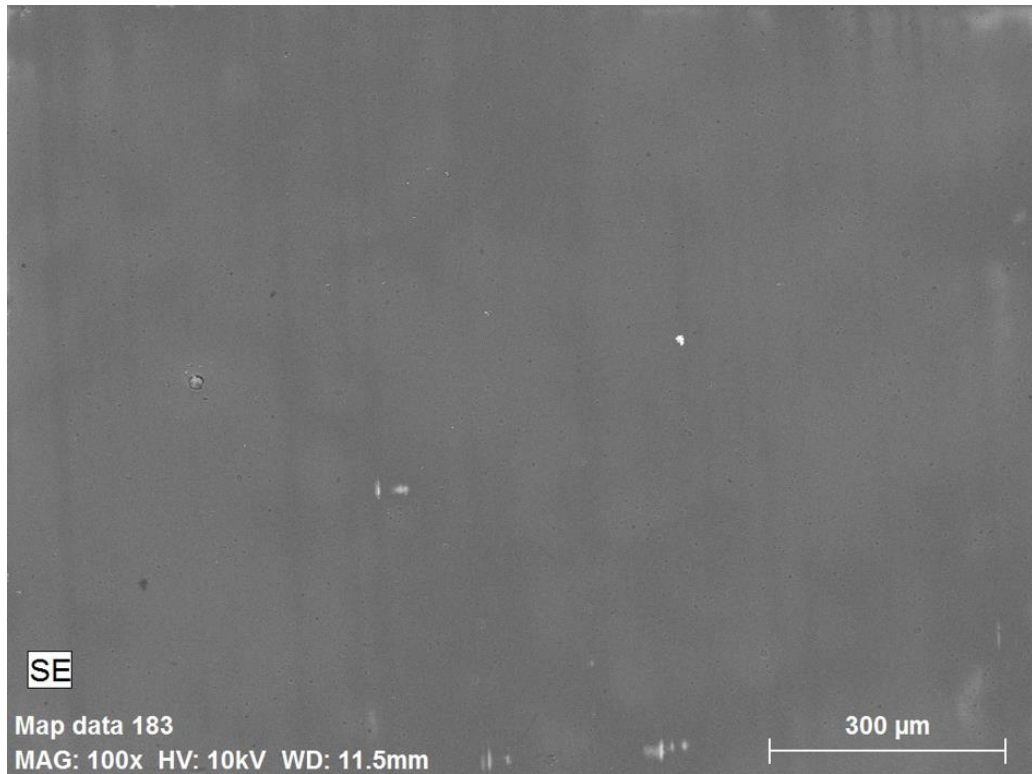


Figure A.2 SEM of 10 wt % silicone resin coating; magnification 100x, scale bar 300 μm

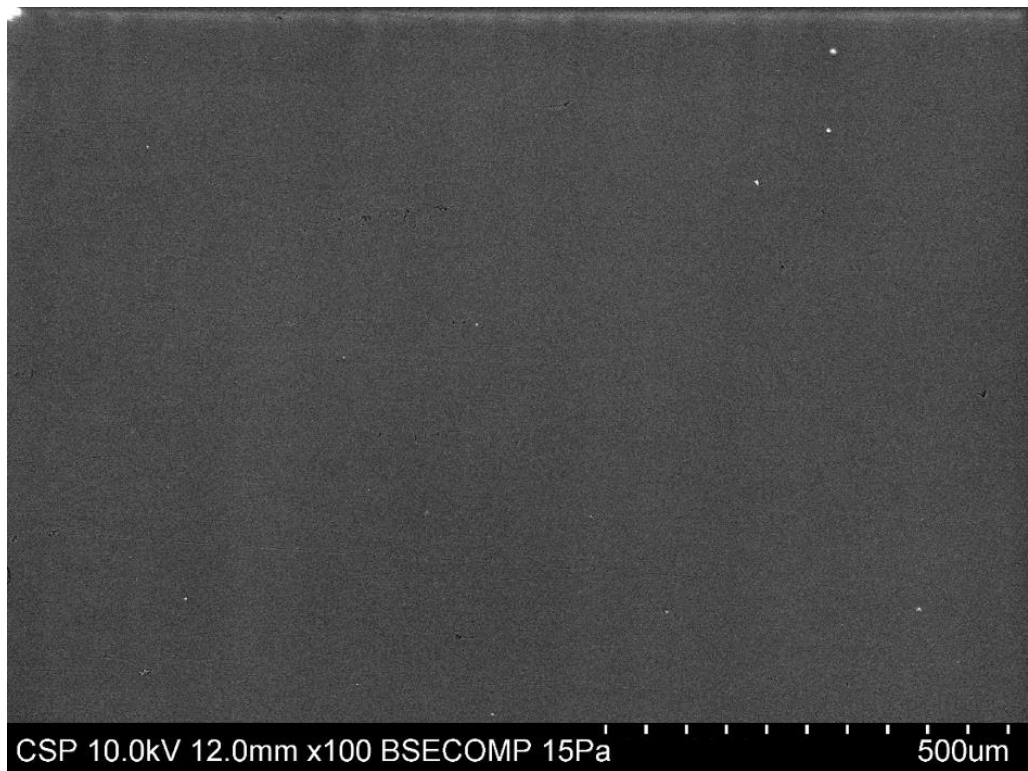


Figure A.3 SEM of 15 wt % silicone resin coating; magnification 100x, scale bar 500 μm

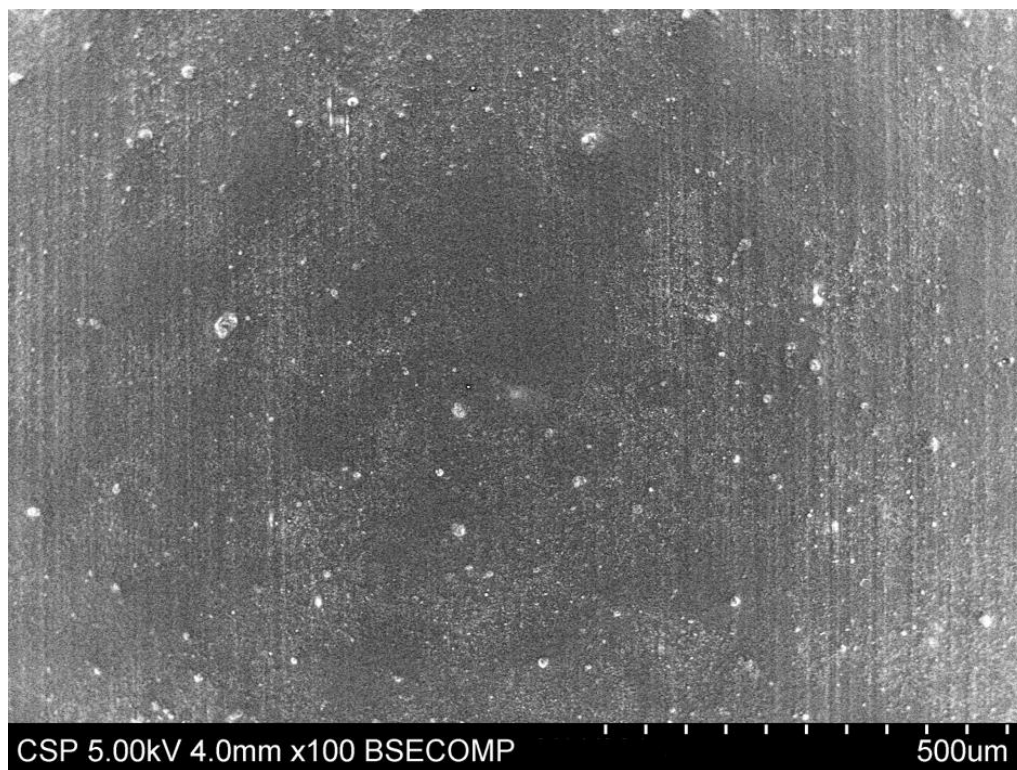


Figure A.4 SEM of 25 wt % silicone resin coating; magnification 100x, scale bar 500 μm

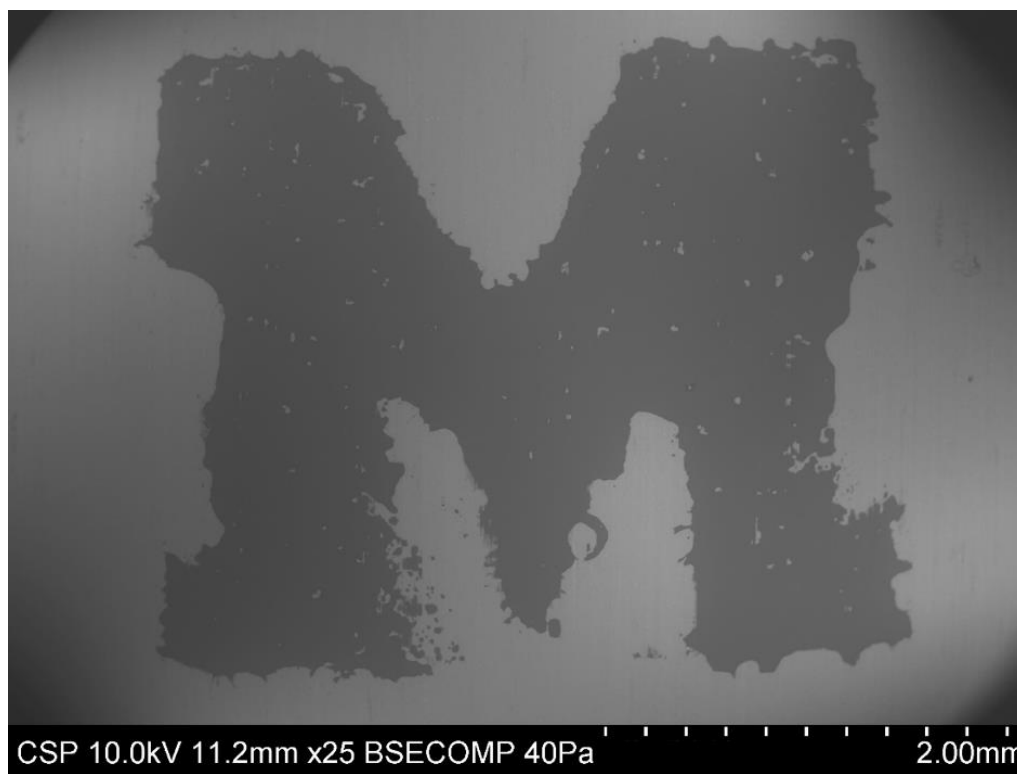


Figure A.5 SEM of patterned SILRES coating; magnification 25x, scale bar 2 mm

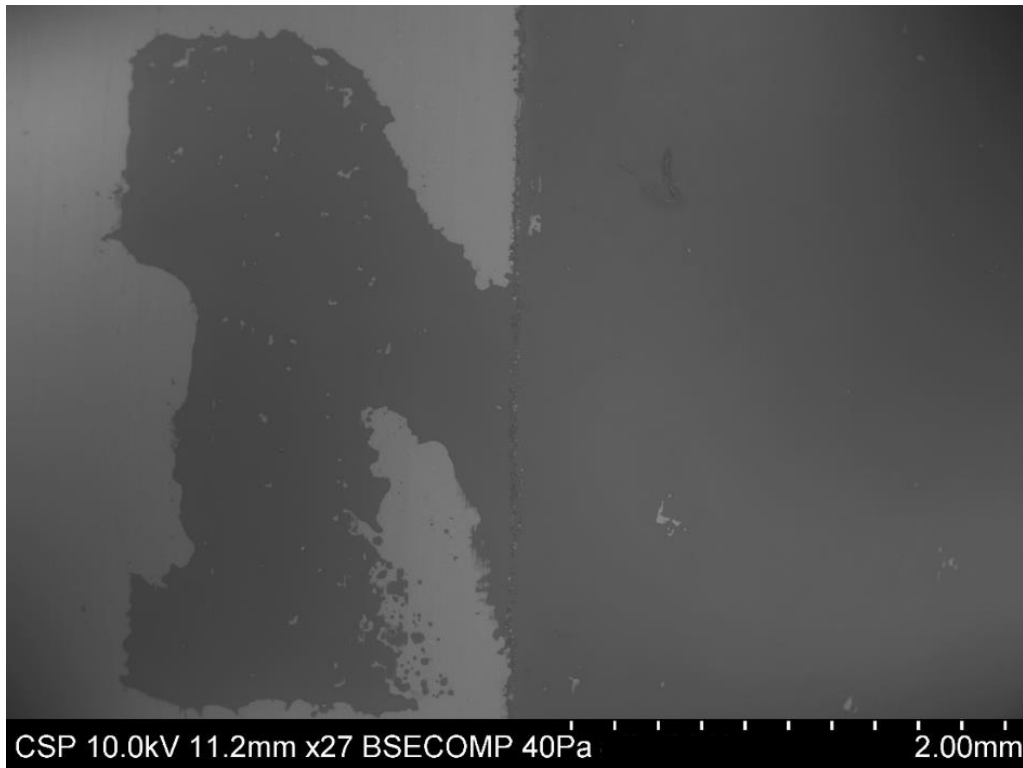


Figure A.6 SEM of reapplication of SILRES coating over patterned (or “damaged”) coating; magnification 27x, scale bar 2 mm

Appendix B

Supplemental Thermal Analyses

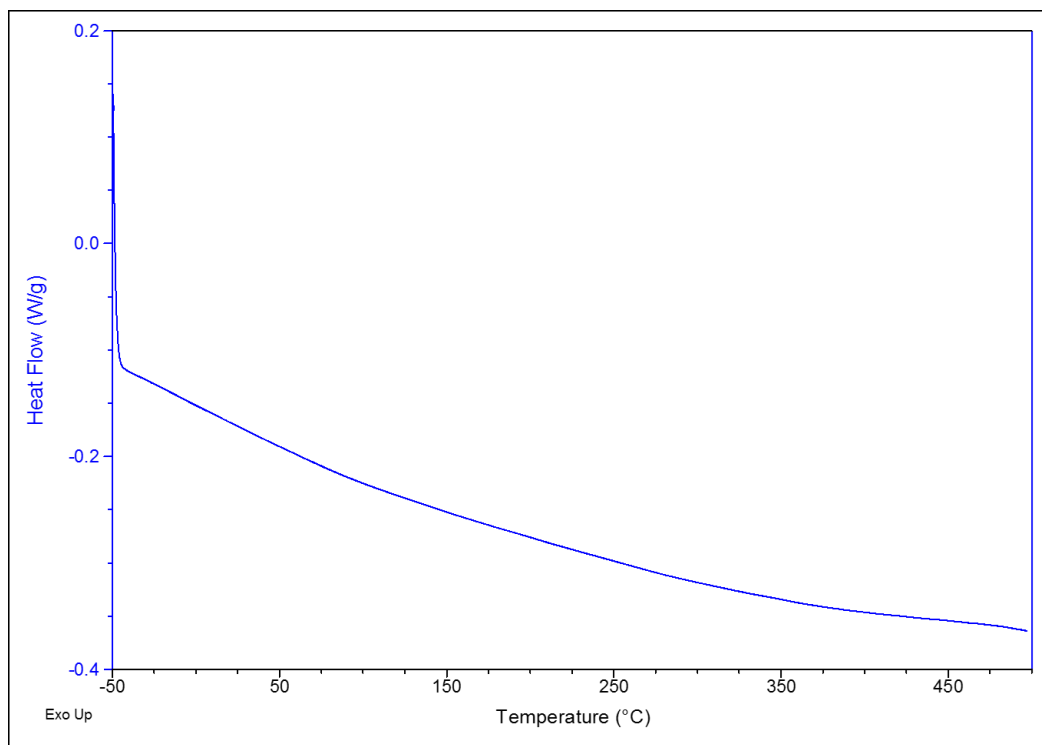


Figure B.1 DSC of model mixed phenyl/methyl silicone resin (1 Ph : 1 Me)

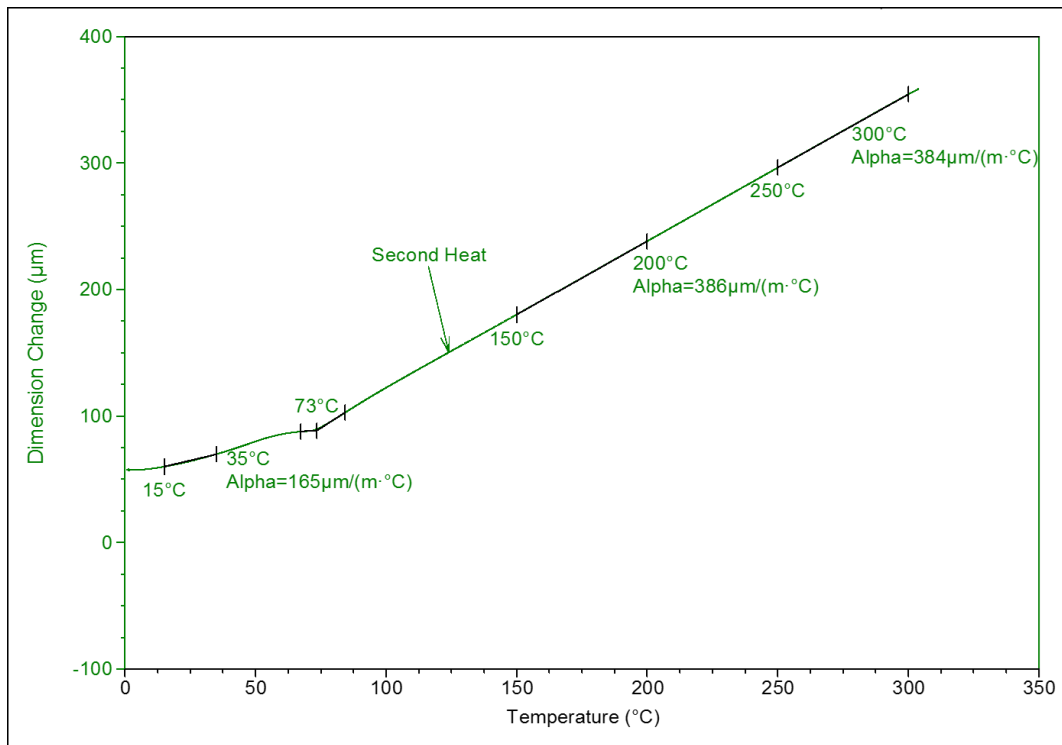


Figure B.2 TMA of commercial SILRES silicone resin

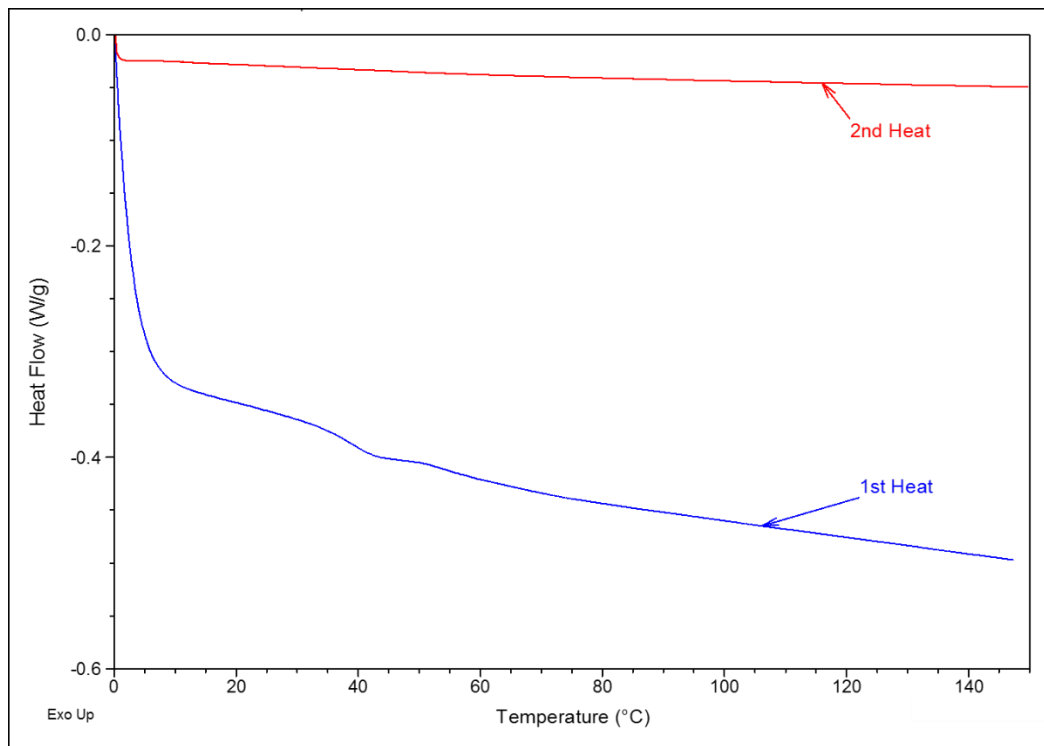


Figure B.3 DSC of commercial SILRES silicone resin

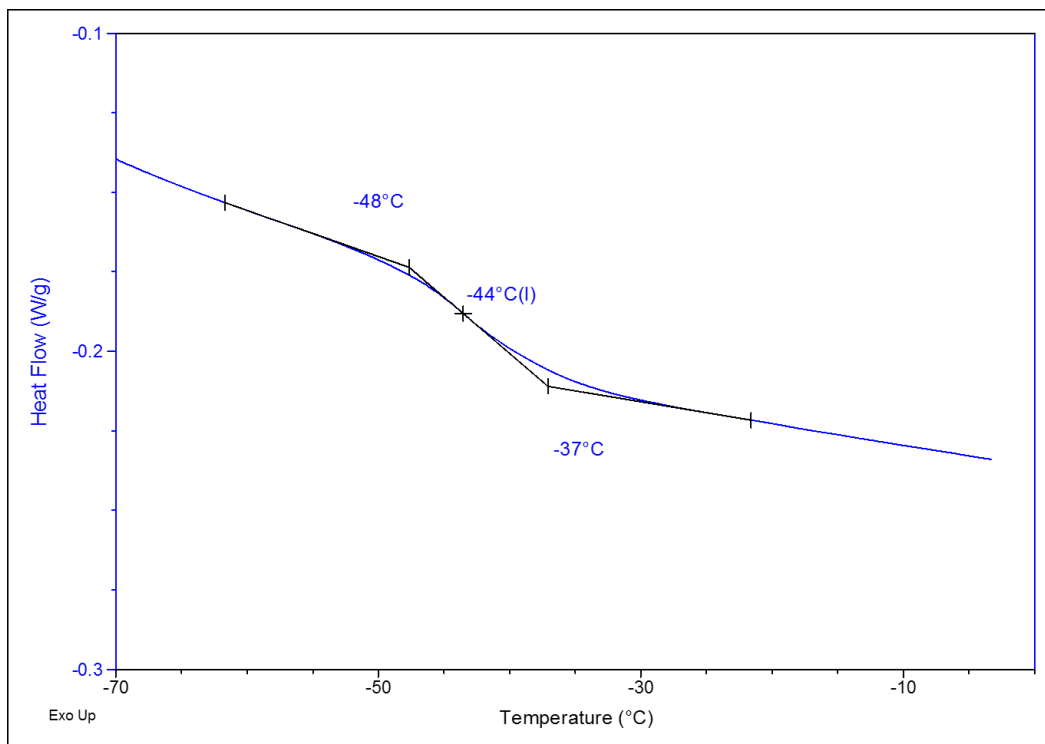


Figure B.4 DSC of 1 Ph : 4 Me silicone resin

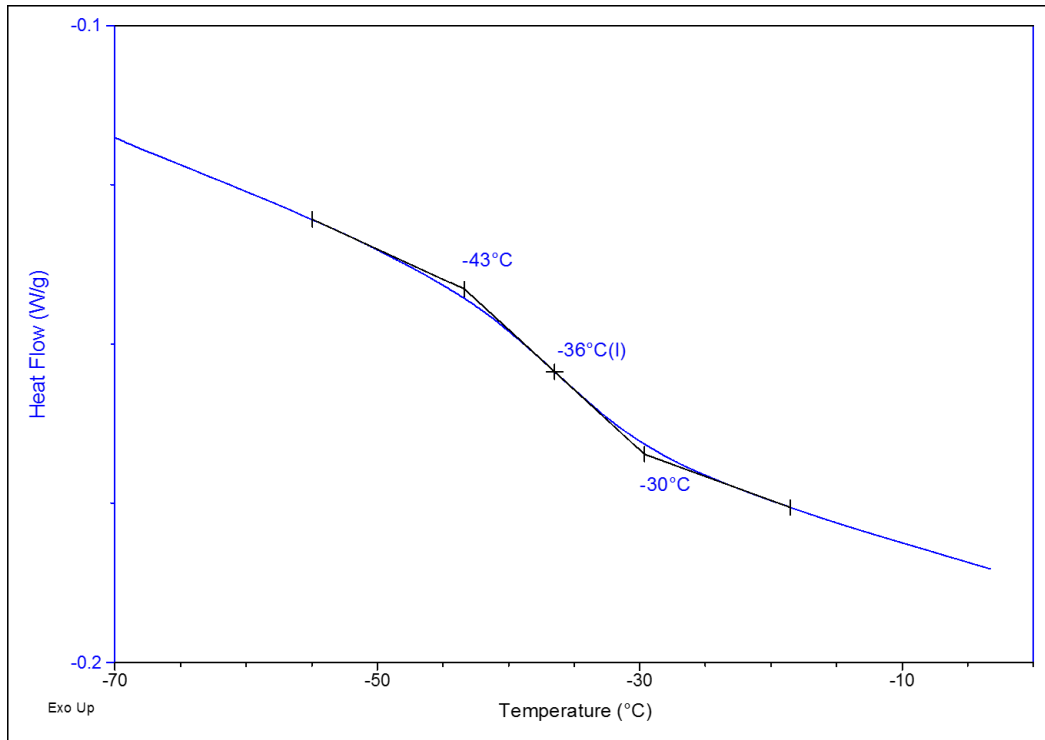


Figure B.5 DSC of 1 Ph : 4 Me : 0.2 PFS silicone resin

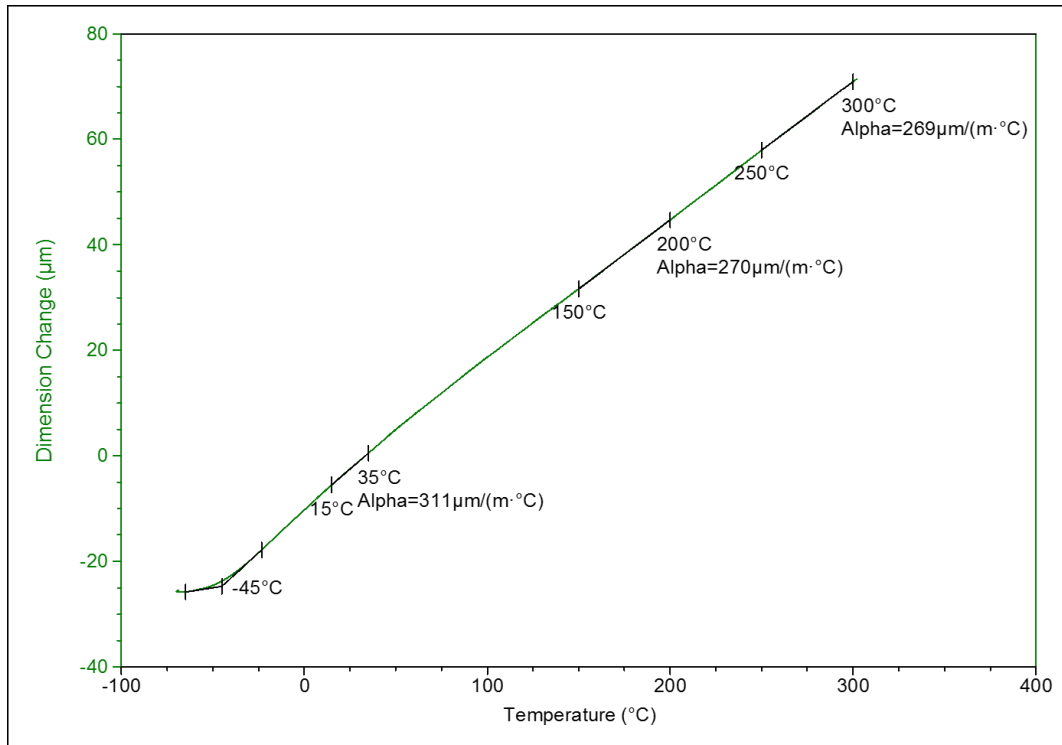


Figure B.6 TMA of 1 Ph : 4 Me silicone resin

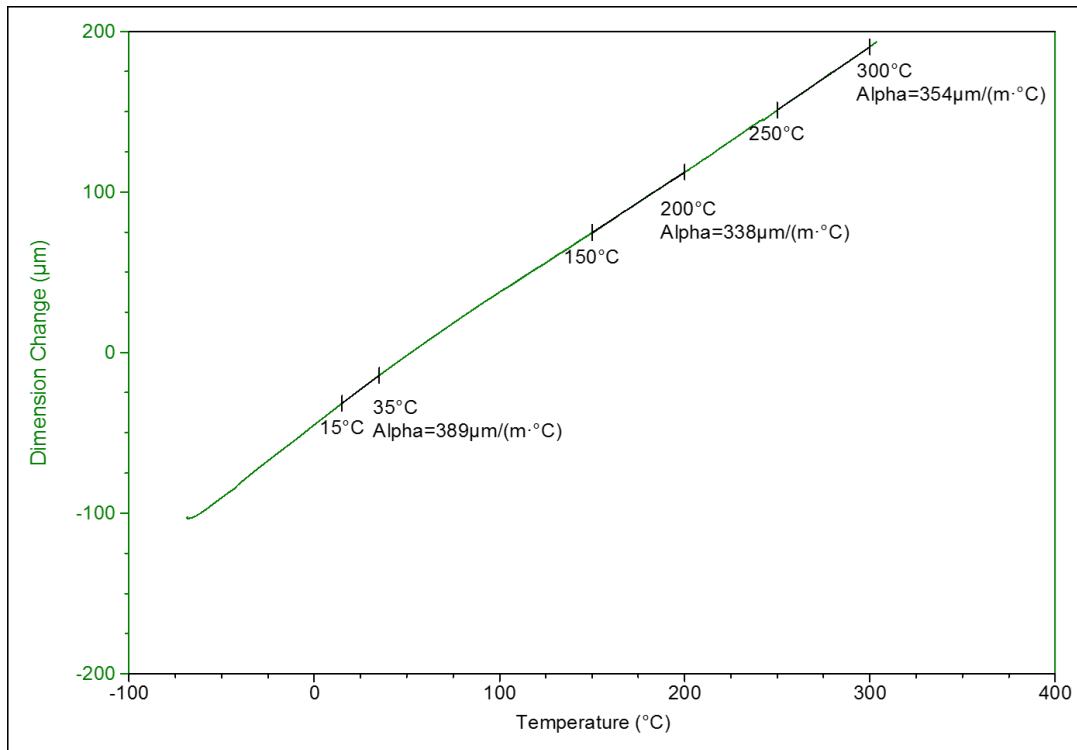


Figure B.7 TMA of ELASTOSIL E10 commercial RTV silicone rubber

Appendix C

Cure Temperature Effect on Recycled Silicone Resin Properties

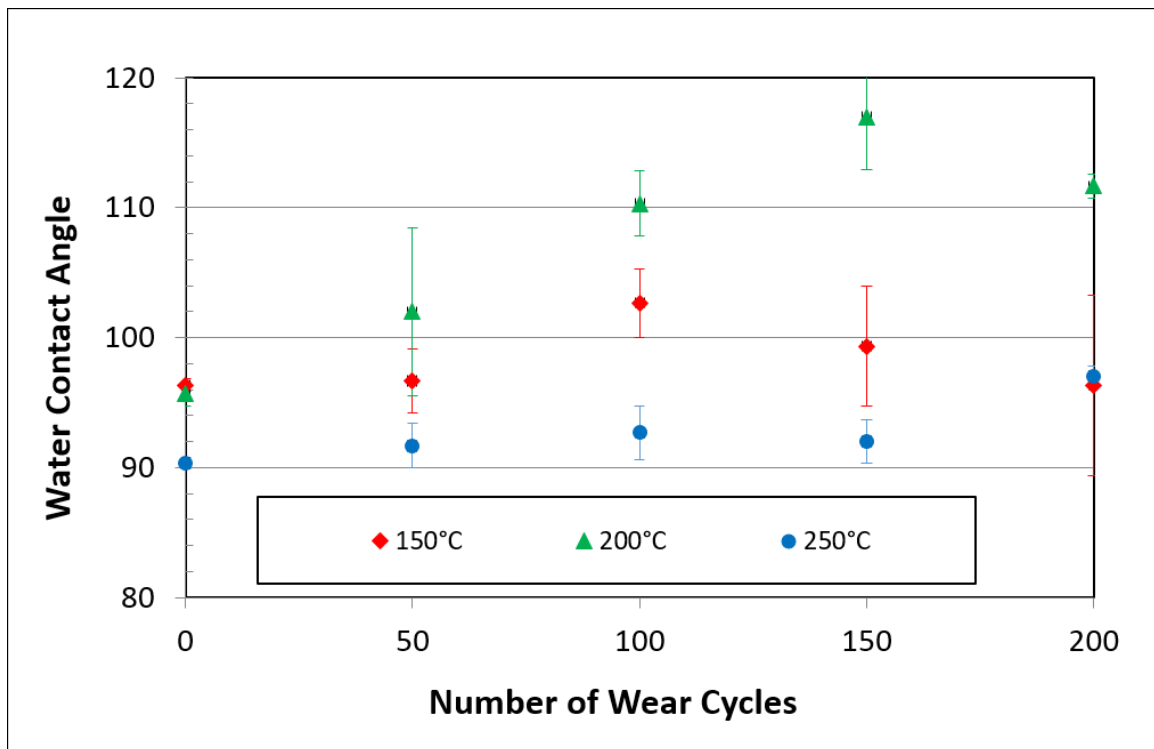


Figure C.1 WCA vs wear cycles on recycled model silicone resin (1 Ph : 1 Me) cured at increasing temperatures

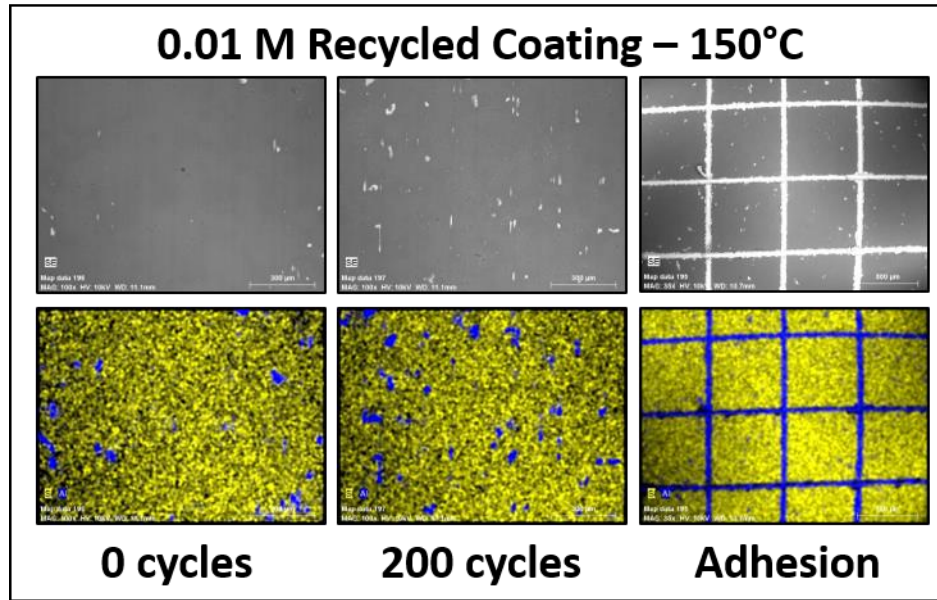


Figure C.2 SEM-EDS images of recycled (0.01M TBAF/THF) model silicone resin coatings cured at 150°C before and after 200 wear cycles and cross-hatch tape adhesion test. Wear micrograph magnification 100x, scale bar 300 μm . Cross-hatch magnification 35x, scale bar 800 μm , EDS map: yellow = Si, blue = Al.

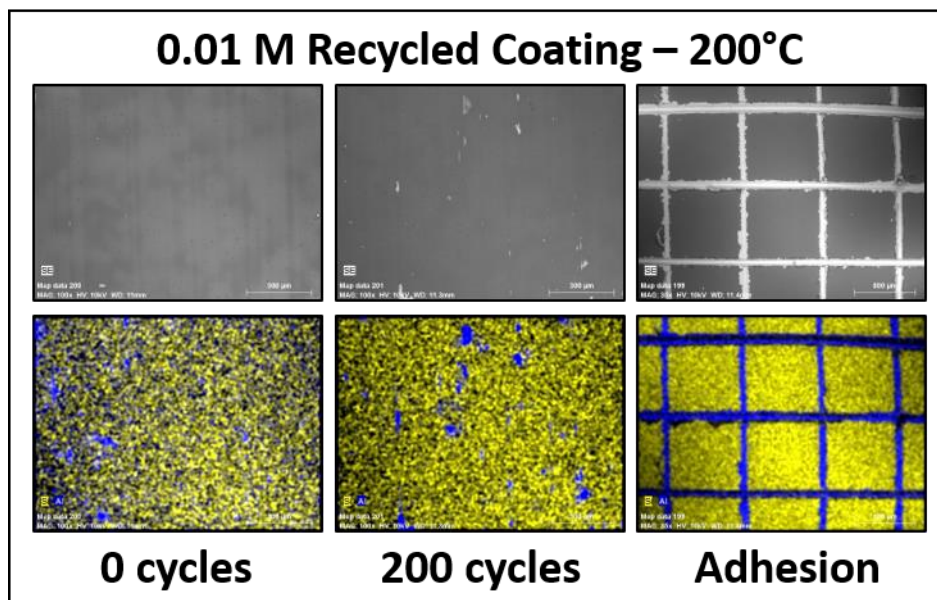


Figure C.3 SEM-EDS images of recycled (0.01M TBAF/THF) model silicone resin coatings cured at 200°C before and after 200 wear cycles and cross-hatch tape adhesion test. Wear micrograph magnification 100x, scale bar 300 μm . Cross-hatch magnification 35x, scale bar 800 μm , EDS map: yellow = Si, blue = Al.

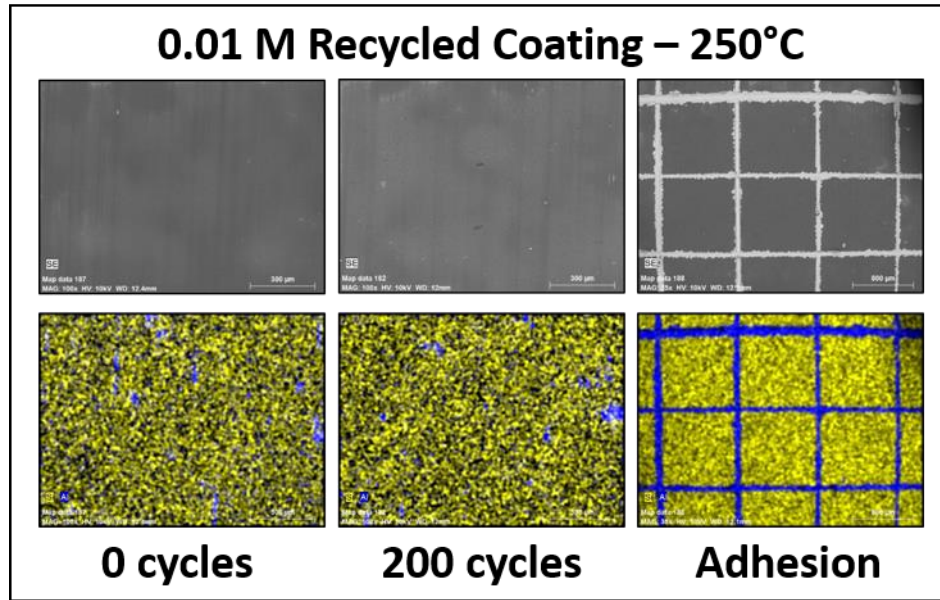


Figure C.4 SEM-EDS images of recycled (0.01M TBAF/THF) model silicone resin coatings cured at 250°C before and after 200 wear cycles and cross-hatch tape adhesion test. Wear micrograph magnification 100x, scale bar 300 µm. Cross-hatch magnification 35x, scale bar 800 µm, EDS map: yellow = Si, blue = Al.

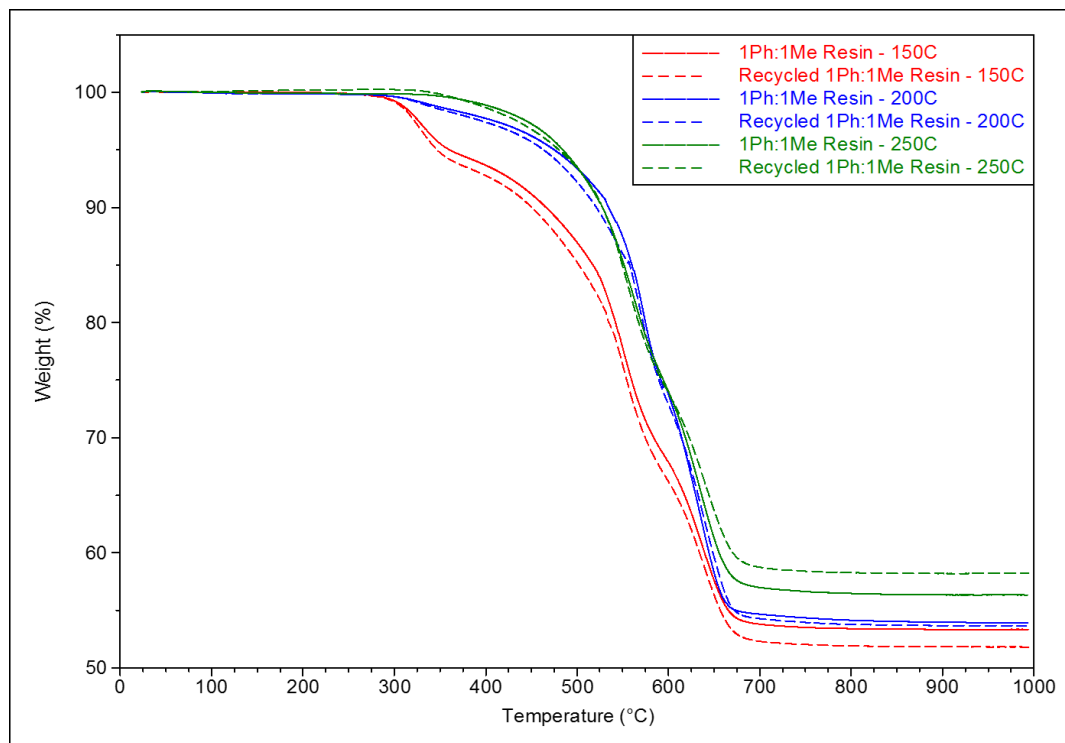


Figure C.5 Typical TGAs in air of prime and recycled model silicone resin with increasing cure temperature

Table C.1 Thermal stability of prime and recycled model silicone resin (1 Ph : 1 Me) with increasing cure temperature

Cure Temp.	Prime Resin	Recycled Resin	Δ Avg.
	$T_{d5\%}$	$T_{d5\%}$	$T_{d5\%}$
150°C	353 ± 5 °C	349 ± 4 °C	- 5 °C
200°C	470 ± 6 °C	467 ± 3 °C	- 3 °C
250°C	483 ± 7 °C	478 ± 2 °C	- 5 °C

Appendix D

Supplemental GC-MS

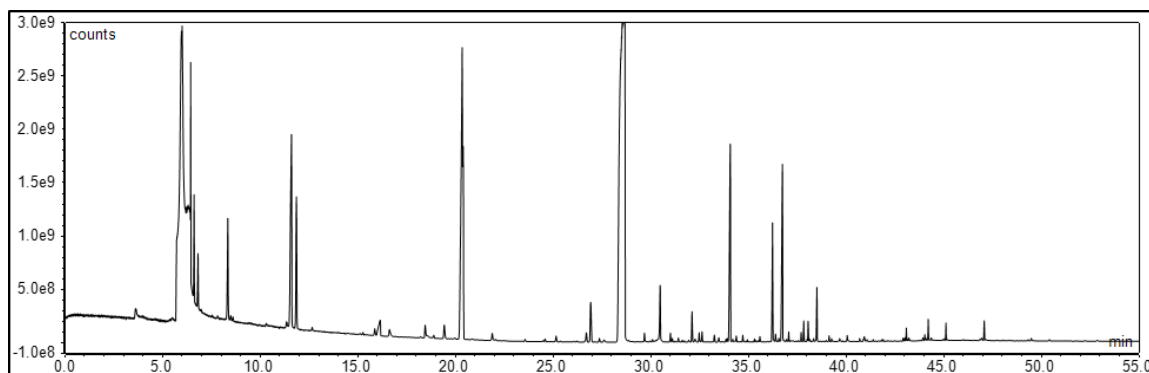


Figure D.1 GC-MS of 0.01M TBAF in BHT stabilized THF accounts for decomposition products found in silicone resin systems synthesized via F^- catalyzed rearrangement

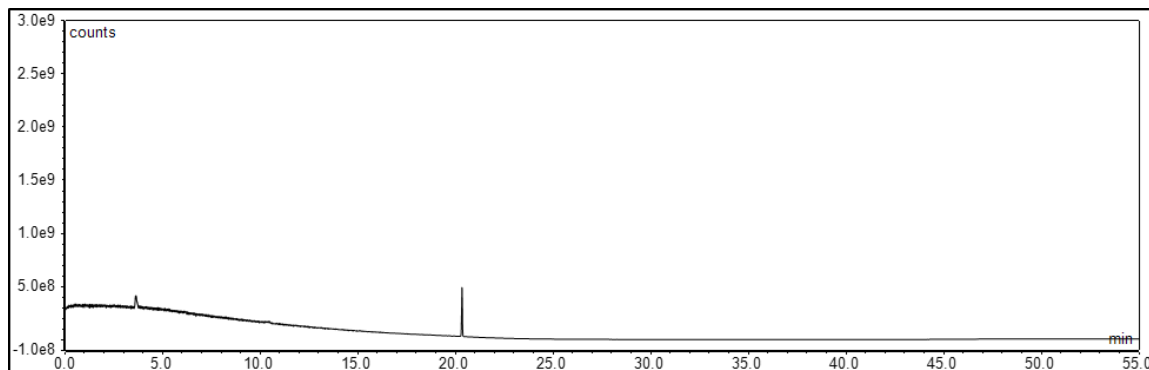


Figure D.2 GC-MS of D_4

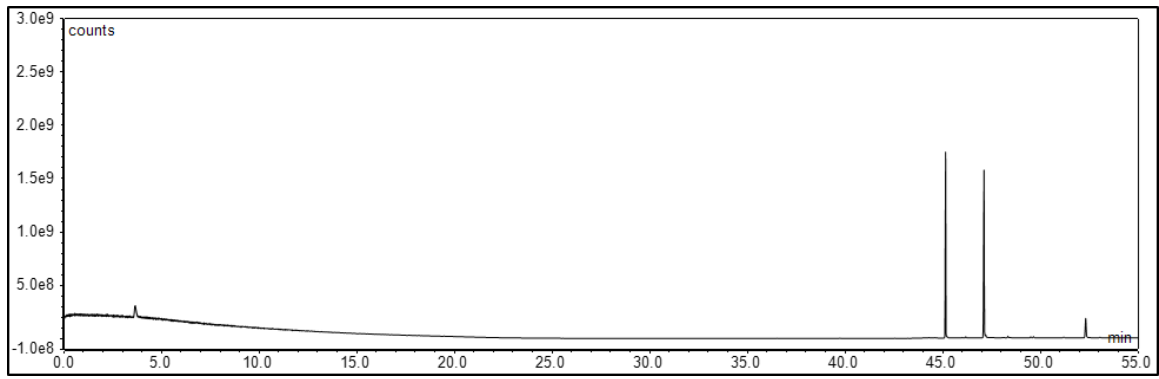


Figure D.3 GC-MS of Al dishes used for casting some samples shows dish coated with grease release agent as a source of potential contamination